



PONTIFICIA UNIVERSIDAD CATOLICA DE CHILE  
SCHOOL OF ENGINEERING

# **DESIGN OPTIMIZATION OF A REINFORCED CONCRETE FRAME BUILDING TO MINIMIZE THE DRIFT**

**ORLANDO DANIEL ARROYO AMELL**

Thesis submitted to the Office of Research and Graduate Studies in  
partial fulfillment of the requirements for the Degree of Master of  
Science in Engineering (or Doctor in Engineering Sciences)

Advisor:

**SERGIO GUTIÉRREZ CID**

Santiago de Chile, november, 2016

© 2016, Orlando Daniel Arroyo Amell



PONTIFICIA UNIVERSIDAD CATOLICA DE CHILE  
SCHOOL OF ENGINEERING

# **DESIGN OPTIMIZATION OF A REINFORCED CONCRETE FRAME BUILDING TO MINIMIZE THE DRIFT**

**ORLANDO DANIEL ARROYO AMELL**

Members of the Committee:

**SERGIO GUTIÉRREZ CID**

**MATÍAS HUBE GINESTAR**

**DIEGO LÓPEZ-GARCÍA**

**JUAN FELIPE BELTRÁN**

**CRISTIAN VIAL EDWARDS**

Thesis submitted to the Office of Graduate Studies in partial fulfillment of  
the requirements for the Degree of Doctor in Engineering Science

Santiago de Chile, november, 2016

A Dios, mis padres y amigos, por su apoyo en el camino.

## **AGRADECIMIENTOS**

Al Padre Universal por su provisión de sabiduría, discernimiento y comprensión. Gracias por haber puesto en el camino las personas maravillosas que contribuyeron a llevar a cabo este trabajo.

A Emilce, mi madre por su apoyo incondicional y por animarme en cada momento para cumplir esta meta en mi vida. A mi familia por creer en mí en todo momento. A mi mejor amiga, Lilibeth, por su confianza y su apoyo constante durante estos años. A mis amigos de la Legión, mil gracias por toda la camaradería y hermandad.

A mi asesor, Sergio por haberme dado la oportunidad de emprender este proyecto, por sus consejos académicos y humanos. A mi asesora Abbie, por su apoyo constante, su voluntad de ayuda y sus valiosas contribuciones a este proyecto. A los Profesores Matías, Diego, Juan Felipe y Christian, por sus aportes como parte de mi comisión doctoral.

A Jennifer, Josefina, Carlos y todas las personas cuyos nombres no alcanzaría a escribir, quienes hacen posible nuestras labores académicas, mil gracias por sus esfuerzos.

## TABLE OF CONTENTS

	Pág.
AGRADECIMIENTOS .....	iii
TABLE OF CONTENTS .....	iv
INDEX OF TABLES .....	vi
INDEX OF FIGURES.....	vii
RESUMEN.....	viii
ABSTRACT .....	ix
EXECUTIVE RESUME .....	x
1. INTRODUCTION .....	1
1.1 Context .....	1
1.2 Objective and Hypothesis.....	3
1.3 Summary of theoretical principles .....	3
1.3.1 Eigenfrequency Optimization .....	4
1.3.2 Problem formulation based on partial differential equations.....	5
1.4 Results and scientific contribution .....	6
1.4.1 Eigenfrequency optimization as a framework for RCF seismic optimization. ....	6
1.4.2 Eigenfrequency optimization with full homogenization .....	10
1.4.3 Investigation of the method's extension of benefits using performance based earthquake engineering .....	13
1.5 Conclusions and future work.....	21
2. EIGEFREQUENCY OPTIMIZATION WITH GEOMETRIC OPTIMIZATION FOR REINFORCED CONCRETE FRAMES .....	24
3. EIGENFREQUENCY OPTIMIZATION WITH FULL HOMOGENIZATION FOR REINFORCED CONCRETE FRAMES .....	488

4.	EVALUATION OF THE IMPACT OF EIGENFREQUENCY OPTIMIZATION USING PERFORMANCE BASED EARTHQUAKE ENGINEERING .....	88
----	---	----

## INDEX OF TABLES

Pág.

Table 1-1: Dimensions for 10-story buildings .....	11
Table 1-2. Comparison of first-mode periods $T_n$ .....	14

## INDEX OF FIGURES

	Pág.
Figure 1-1: Design process for a reinforced concrete moment resisting frames.....	1
Figure 1-2: Two dimensional model of a membrane .....	7
Figure 1-3: Ten story regular building .....	8
Figure 1-4: Optimized and rounded dimensions for the 10 story building .....	8
Figure 1-5: Pushover results for the 10 story building .....	9
Figure 1-6: Pushover results for the 10 story building .....	11
Figure 1-7: Displacement and drift responses for a scale factor of 1.0 .....	12
Figure 1-8: Impact of optimization on different structural parameters .....	15
Figure 1-9: Pushover comparison of 15 story buildings .....	16
Figure 1-10: Pushover story drift distribution for the 15 story buildings .....	17
Figure 1-11: Median of maximum story drift response for the 15 story buildings ..	18
Figure 1-12: Comparison of collapse fragility functions for the 15 story buildings..	19
Figure 1-13: Deaggregation of losses for the 15 story buildings .....	21

## RESUMEN

Los marcos de hormigón armado son un sistema estructural utilizado en todo el mundo, especialmente en los países en desarrollo, debido al costo relativamente bajo del sistema en comparación con otras alternativas. Como reflejo de esta ubicuidad, los investigadores han propuesto métodos de optimización basados en diferentes marcos de optimización, que son capaces de proporcionar buenas soluciones para el problema de optimización, sin embargo, su uso en la práctica por parte de los ingenieros estructurales ha sido escaso. Esta situación se ha producido debido a que estos métodos utilizan modelos estructurales no lineales para evaluar el desempeño sísmico y que son difíciles de implementar para el ingeniero estructural promedio. Además, éstos no pueden proporcionar resultados dentro de los plazos utilizados en la práctica de la ingeniería. Esta investigación presenta un método de optimización para mejorar el rendimiento sísmico de edificios de marcos de hormigón que utiliza la optimización de frecuencias propias para formular el problema y optimización geométrica y el método de homogenización de proponer algoritmos de solución eficientes. El método se aplicó para optimizar edificios con varias configuraciones de altura y planta. Los beneficios de optimización se evaluaron mediante análisis tiempo historia no lineales los análisis aplicados a modelos de fibras de los edificios, cuyos resultados se utilizan para llevar a cabo evaluaciones basadas en la ingeniería sísmica basada en desempeño. Los resultados muestran que la aplicación del método reduce las derivas y desplazamientos de entrepiso en los pisos inferiores y que la fragilidad a colapso de los edificios se reduce. Además, los edificios optimizados tienen una distribución más uniforme de la deriva a lo largo de la altura de los edificios, como consecuencia de la distribución de resistencia que resulta de la aplicación del método. El trabajo futuro en este tema puede llevarse a cabo investigando la aplicación de la optimización de frecuencias propias para marcos de acero, así como evaluar si la formulación del problema se puede extender para incluir más variables de diseño sin comprometer la simplicidad en la formulación y el rendimiento computacional.

Palabras Claves: Marcos de hormigón armado, Optimización de frecuencias propias, ingeniería sísmica basada en desempeño, homogenización, optimización geométrica.

## ABSTRACT

Reinforced concrete frames (RCF) are a widely used structural system around the world, especially in developing countries, due to the system's relatively low cost compared to other alternatives. Reflecting this ubiquity, researchers have proposed optimization methods for RCF based on different optimization frameworks, which are capable of providing good solutions to the optimization problem, however, their usage by practicing structural engineers has been scarce. This situation has occurred because these methods use nonlinear structural models to evaluate the seismic performance and they are difficult to implement for the average structural engineer. Besides, they cannot provide results within the time frames used in engineering practice. This research presents an optimization method to improve the seismic performance of RCF buildings that uses eigenfrequency optimization to formulate the problem and geometric optimization and the homogenization method to propose efficient solution algorithms. The method is applied to optimize buildings with several height and plan configurations. The optimization benefits are assessed using nonlinear time history analyses applied to fiber models of the buildings, whose results are used to conduct evaluations based on performance based earthquake engineering. The results show that the method application reduces the story drifts and displacements in the bottom stories and that the buildings collapse fragility is reduced. Furthermore, optimized buildings have a more uniform distribution of the drift along the buildings' height as a consequence of the strength distribution that results from the application of the method. Future work in this topic can be pursued investigating the application of eigenfrequency optimization for steel frames and evaluate if the problem formulation can be extended to involve more design variables without compromising the simplicity in the formulation and the computational performance.

Keywords: Reinforced concrete frames, Eigenfrequency optimization, Performance based earthquake engineering (PBEE), homogenization, geometric optimization

## EXECUTIVE RESUME

This thesis proposes a method to minimize the drift of reinforced concrete frames (RCF) based on eigenfrequency optimization. This work has two major scientific contributions: first, it demonstrated that eigenfrequency optimization can be used as a framework to formulate the seismic optimization problem for reinforced concrete frames. Second, it proposed an efficient algorithm to solve the optimization problem based on geometric optimization and on the homogenization method.

This document is structured in four chapters. The first one corresponds to an introductory chapter, describing the problem, its objectives, hypothesis, methodology and results.

Chapters 2 to 4 correspond to three ISI papers that present the results of this work to the scientific community. The first paper was published in the Journal of Computing in Civil Engineering and it describes the eigenfrequency optimization as a framework, proposing a simplified solution method based on geometric optimization. The second paper is accepted for publication in Engineering Optimization and it presents the eigenfrequency optimization based on homogenization for optimizing the seismic design of RCF. The third paper presents an in-depth investigation based on performance based earthquake engineering, of the seismic improvements obtained by using the method proposed in the second paper. It is the result of the collaboration with Dr. Abbie Liel during the author's research internship at the University of Colorado Boulder. At the time of presenting this document, this paper is under review. A fourth, practical paper is being elaborated based on design recommendations extracted from the third paper, which will be submitted to a suitable journal.

## 1. INTRODUCTION

### 1.1 Context

Reinforced concrete frames (RCF) are a widely used structural system around the world, especially in developing countries, due to the system's relatively low cost compared to other alternatives. Reports from the World Housing Encyclopedia indicate that RCF account for about 75% of the building stock in Turkey (WHE Report 64), 60% in Colombia (WHE Report 11) and 80% in Mexico (WHE Report 115).

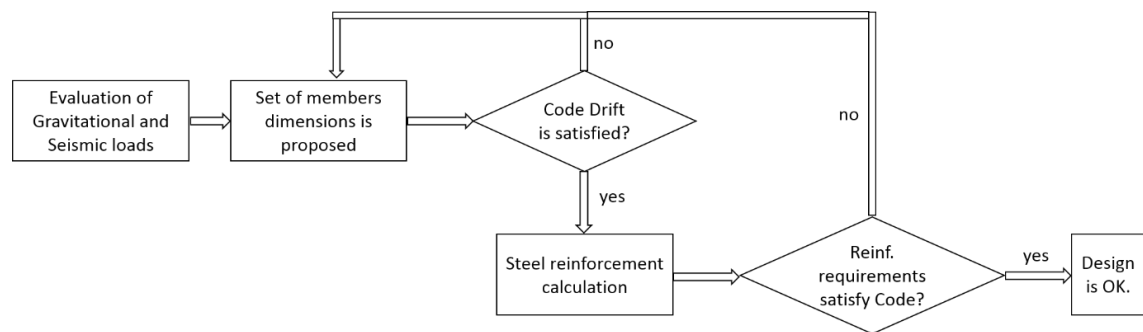


Figure 1-1. The typical design process for a reinforced concrete moment resisting frame uses an iterative process to calculate the column and beam (members) dimensions and steel reinforcement that satisfy the code provisions.

Traditionally, these buildings are designed by structural engineers following an iterative process that involves three steps (Figure 1-1). First, gravitational and seismic loads are evaluated following the procedures stated by design codes. Then, they calculate a set of columns and beams dimensions that satisfy the elastic drift limit imposed by the code. Finally, steel reinforcement is calculated to satisfy the codes' strength and ductility requirements. In few cases, when elements dimensions are small and they exceed the maximum allowable steel, it is necessary to adjust the columns and beams dimensions to meet these requirements. A design is said to satisfy the code when it fulfills the drift limit

and the strength and ductility requirements. Due to the rapid pace of structural design offices, the customary practice is that a design is considered as final when it satisfies the code and conforms to what previous experience has taught. Because of this practice, most RCF buildings have suboptimal seismic performance.

To address this issue, researchers have proposed optimization methods (e.g. Zou, et al. 2007; Li & Liu, 2010; Li et al. 2010; Khatibinia et al. 2013; Bai et al. 2016; Hajirasouliha et al. 2012) for RCF based on different optimization frameworks (Fragiadakis & Lagaros, 2011), such as deterministic based optimization (DBO) and reliability based optimization (RBO), where the cost of the structure is considered as the objective function and the code requirements are considered as constraints. These methods have demonstrated being effective to solve the optimization problem; however, their usage among engineers have been scarce because they do not have enough computational performance and feasibility of implementation in a practical environment.

The fact that engineers demand seismic optimization methods that are easy to implement and computationally efficient have been acknowledged by researchers, who have introduced methods with improved solution techniques (Hoffman & Richards, 2014), simplified methods for seismic evaluation (Zacharenaki et al, 2013) and where they explicitly consider code constraints (Zou et al., 2007). Although these efforts have yielded improvements in the computational cost, solving RCF seismic optimization problems still takes several hours or even days in consumer-level computers (Zacharenaki et al., 2013). More importantly, these methods still demand the development of complex nonlinear structural models and therefore, they have not captured the attention of engineers. A more detailed discussion about the need to develop seismic optimization methods with an

orientation to being useful in practice is presented at the end of this chapter, corresponding to an opinion paper written during the development of this thesis.

## **1.2 Objective and Hypothesis**

This thesis is developed with the objective to propose a seismic optimization method that finds the dimensions of columns and beams that minimize the drift in a RCF building, subjected to a constraint in the total volume of the building. The method must have the following characteristics:

1. Optimized buildings must have better seismic performance than traditionally designed buildings, both in the elastic and inelastic regimes.
2. Buildings must be within the scope of existing seismic design codes.
3. High computational performance and feasibility of implementation.
4. The construction complexity of resulting building designs should not increase significantly, nor its analysis and design.

To meet these goals, this work develops an optimization procedure to improve the seismic performance of RCF buildings that uses an eigenfrequency optimization framework for the problem statement and which can be solved using the homogenization method. The hypothesis of this thesis is that eigenfrequency optimization can provide a solid framework to optimize the seismic design of RCF buildings.

## **1.3 Summary of theoretical principles**

This section presents a short description of the theoretical background in this thesis. A more detailed discussion is given in Arroyo and Gutiérrez (2017) and in the third chapter of this document.

### 1.3.1 Eigenfrequency Optimization

Topology optimization describes a class of optimization that addresses the problem of determining the optimum distribution of material within a domain. The two most common objectives for topology optimization are the minimum compliance and the eigenfrequency optimization. In eigenfrequency optimization, one or more structural frequencies are optimized. Eigenfrequency optimization has seen several applications in structural engineering, such as stiffness maximization of beam-column connections (Lee et al. 2012) vibration reduction in truss structures (Senba et al. 2013) and the maximization of the fundamental eigenfrequency of geometrically nonlinear beams (Yoon, 2010).

Several solution methods have been proposed for topology optimization problems, including the solid isotropic material with penalization (SIMP) method (Bendsoe and Sigmund, 2003) evolutionary algorithms, and the full homogenization method (Bendsoe and Kikuchi, 1988). The nature of the topology optimization problem can lend itself to solution methods that start with a single initial solution that is gradually improved (*e.g.* SIMP and full homogenization), offering outstanding computational performance that can be programmed to solve 3D problems even on devices with modest computational power such as smartphones and tablets (Nobel-Jørgensen et al. 2014).

The method proposed in this work uses eigenfrequency optimization for the problem formulation and the homogenization method as solution technique. The application of eigenfrequency optimization for RCF makes sense, because during an earthquake the response of a building is heavily dependent on the smallest natural frequencies of the structure, thus, it is reasonable to optimize these structural properties. This dominating

nature of the smallest natural frequencies in the structural response has been used to develop efficient analyses procedures, such as the modal pushover analysis (Chopra et al., 2004; A. K. Chopra & Goel, 2002); moreover, several standards (ASCE 7-10; ASCE 41-06) acknowledge that the seismic behavior in structures without important torsional irregularities, is controlled by the first natural frequency, allowing the use of the equivalent lateral force procedure to evaluate the seismic demands on structural members.

In addition to optimizing a property that has a direct influence on the seismic performance of the structure, eigenfrequency optimization offers several advantages. First, the objective function is calculated based on the elastic model of the building, resulting in low computational costs. Second, it provides easiness and flexibility in terms of the problem formulation, as it allows for a discrete statement in terms of classical structural analysis (SA), and it can also be stated in a continuous formulation based on partial differential equations (PDEs), which is used here to solve the problem with the homogenization method.

### 1.3.2 Problem formulation based on partial differential equations

Eigenfrequency optimization is formulated using PDEs as follows:

$$\begin{array}{ll}
 \text{Max} & \omega_n(\boldsymbol{\rho}) \\
 \text{subject to} & \boldsymbol{\rho} \geq \boldsymbol{\rho}_{\min} \\
 & V(\boldsymbol{\rho}) = V_0 \\
 & -\text{div}(Ce(u)) = \omega_n^2 \boldsymbol{\rho} u \quad \text{in } \Omega \\
 & Ce(u)n = 0 \quad \text{on } \Gamma_N \\
 & u = 0 \quad \text{on } \Gamma_D
 \end{array}$$

Here,  $\rho$  represents density of material, which should be greater than a function  $\rho_{\min}$  in the domain  $\Omega$ , and  $V(\rho) = V_0$  means that the total amount of material must be equal to a predefined volume  $V_0$ . The last three constraints mean that  $\omega_n$  is an eigenfrequency of the structure.

As a result of using the material density  $\rho$  as the optimization variable, this formulation requires  $\rho_{\min}$  and  $\Omega$  to be defined in terms of the lower and upper bounds of the dimensions of the structural members. Once the optimal density of material  $\rho_{opt}$  has been obtained, it needs to be expressed as column and beam dimensions. The steel reinforcement to be used is calculated after the optimization.

The main advantage of the PDE formulation is that it lends itself to solution methods that work with a single initial solution that is gradually improved, like the SIMP (Bendsoe & Sigmund, 2003) and the full homogenization (Tartar, 2009) methods, offering higher computational efficiency and the associated possibility of having a larger search space.

Details about the solution method used in this work, as well as the proposed computational algorithm are presented in Chapter 3.

## **1.4 Results and scientific contribution**

### **1.4.1 Eigenfrequency optimization as a framework for RCF seismic optimization.**

The first scientific contribution of this work is the demonstration that eigenfrequency optimization can be used as a framework to formulate the seismic optimization problem for reinforced concrete frames. This is the result of the first stage of the research and it is

covered in the second chapter of this document, which is published in the ASCE Journal of Computing in Civil Engineering.

In this publication, the eigenfrequency optimization is proposed for optimizing the column dimensions of RCF buildings. A surrogate model for the buildings based on a membrane is considered (Figure 1-2). The surrogate model to use consists in viewing the building in elevation as a membrane of variable thickness, then optimizing on the thickness to maximize the first eigenfrequency of the membrane and then translating this thickness into depths of the columns of the frames to be used in the building. If the building is either not regular or not slender, the proposed surrogate model is not appropriate for eigenfrequency optimization.

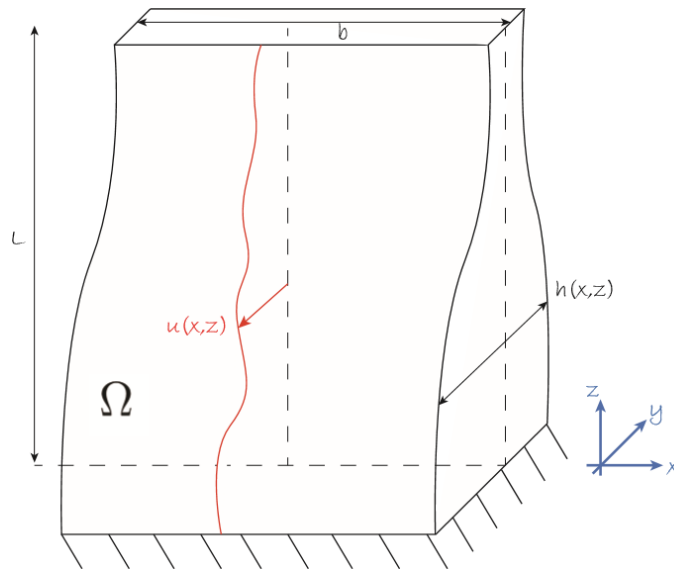


Figure 1-2. Two dimensional model of a membrane

The simplicity of the surrogate model allowed to use geometric optimization to solve the problem (more details in Chapter 2), which was applied to a 10 story building (Figure 1-3).

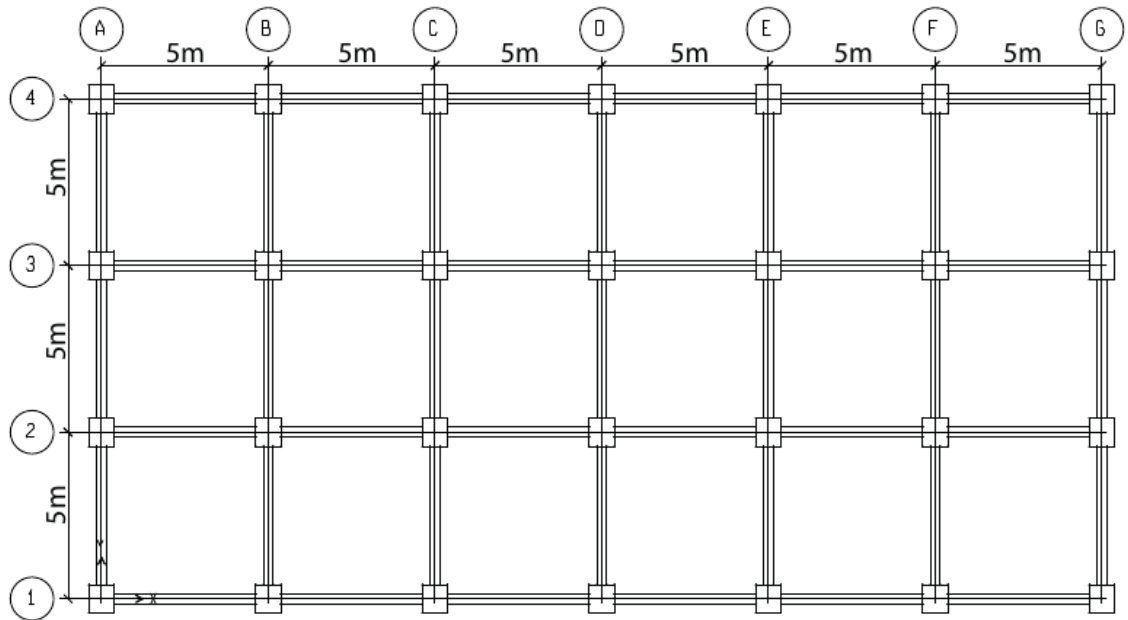


Figure 1-3. Ten story regular building used for demonstrating the applicability of eigenfrequency optimization

The optimization of dimensions gave the results shown in the blue line of figure 1-4, which were rounded to the closest multiple of 5cm in order to accommodate with construction practices. The total time invested for the optimization is 27s running on a desktop computer with an Intel Core i5 3570K (3.4GHz) with 8GB of RAM.

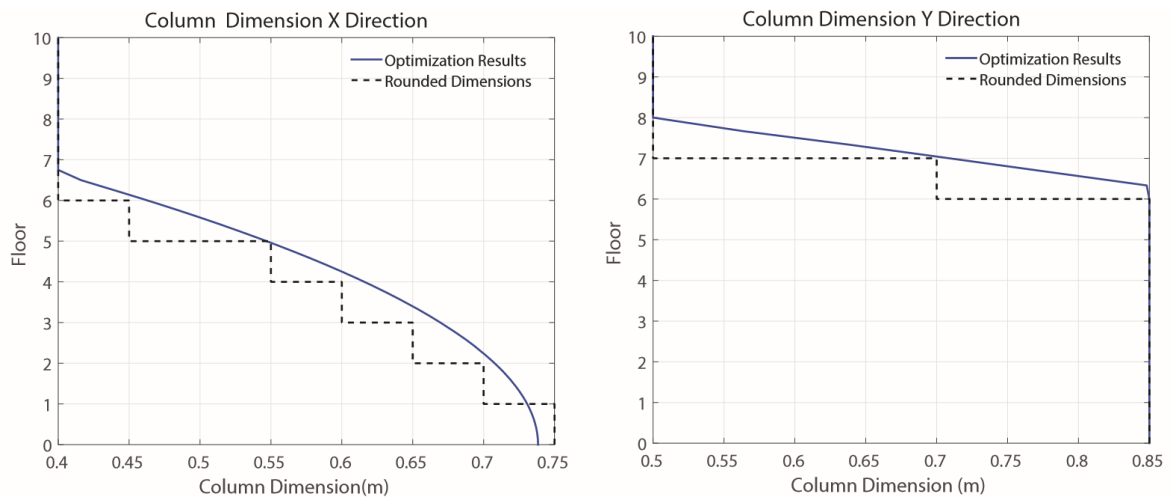


Figure 1-4. Optimized and rounded dimensions for the 10 story building.

The seismic performance of the optimized building is compared using a pushover analysis with a traditional building designed following the procedure described in figure 1-1. The details of the nonlinear models are presented in Chapter 2, and the results of this comparison is shown in figure 1-5, where it can be observed that the optimized building has an overstrength that is 22.3 and 22.4% higher than the baseline structure for the x- and y-directions, respectively. Similarly, the ductility factor is 31.2% greater in the x-direction and 10.2% in the y-direction.

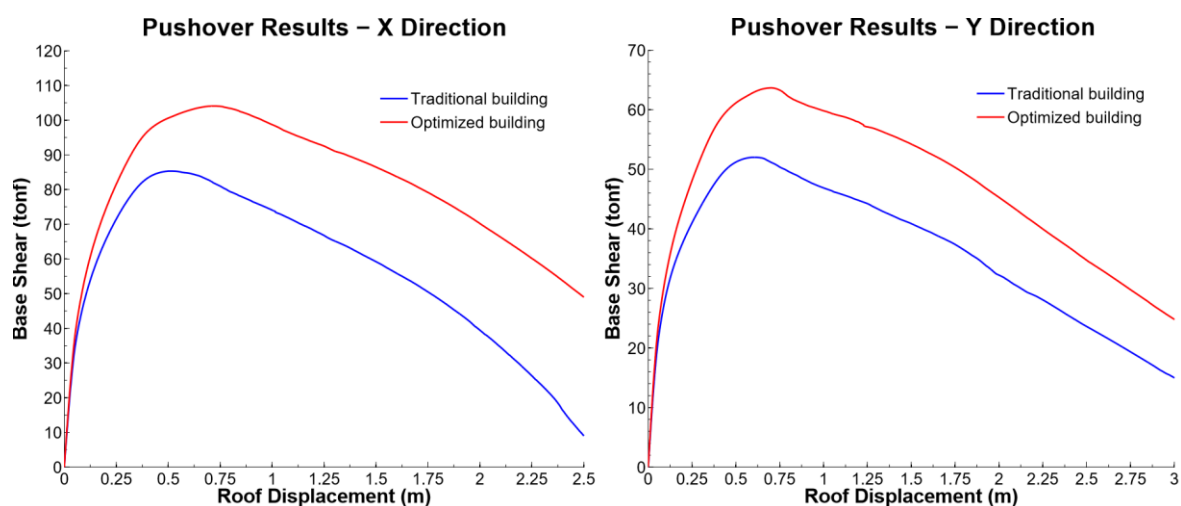


Figure 1-5. Pushover results for the 10 story building.

Further details about these results can be found in Chapter 2 of this document, but to sum them up, it can be stated that the optimized building shows an improved behavior with respect to the baseline in three key areas: elastic drift, overstrength, and ductility. What is more, all these improvements come with no additional expenses associated with material costs, because the volume of the optimized building is almost the same as that of the traditional one.

### 1.4.2 Eigenfrequency optimization with full homogenization

The second contribution of this work is proposing an optimization method that uses eigenfrequency optimization with the full homogenization method to determine the optimum member dimensions of reinforced concrete frames.

In this stage, eigenfrequency optimization is formulated as described in section 1.3.2, which requires solving the problem using the finite element method. In this formulation, an optimization domain  $\Omega$  must be defined based on the maximum desired dimensions for beams and columns. In this domain, the columns and beams dimensions are expressed as a material density  $\rho$ , therefore, the minimum dimensions are expressed as  $\rho_{\min}$ . As previously discussed, this formulation allows to use efficient optimization techniques.

In this work, the full homogenization (FH) method is used as a solution technique for this approach. A description of the mathematical basis of the FH method for a two dimensional case and a computational algorithm to solve the problem are presented in Chapter 3. A more complete description of the method can be found in (Allaire, 2002) and, more specifically, for eigenfrequency optimization in (Allaire et al., 2001). Being this a first study on eigenfrequency optimization for RCF based on full homogenization, this work focuses only on the first eigenfrequency.

The proposed method is used to determine the column and beam dimensions that optimize the seismic performance of the building in figure 1.3. The building was first designed following the traditional procedure according to the ASCE 7 and the ACI 318 for the state of California (37.38°N, 121.88°W) using ETABS v13.1.2 (Habibullah, 1997). After that, it was optimized using the method proposed in this thesis, with the results shown in the following table:

Table 1-1. Dimensions for 10-story buildings (all dimensions are given in cm)

Story	<u>Optimized building</u>				<u>Traditional building</u>	
	<u>Columns</u>		<u>Beams</u>		<u>Columns</u>	<u>Beams</u>
	Inner	Outer	X Dir	Y Dir	Both	Both
10	50x60	50x60	35x35	35x35	55x75	35x40
9	55x65	55x65	35x35	35x35	55x75	35x40
8	55x70	55x70	35x40	35x40	55x75	35x40
7	60x70	55x70	35x40	35x40	55x75	35x40
6	60x75	55x75	35x40	35x40	55x75	35x40
5	60x75	55x75	35x40	35x40	55x75	35x40
4	65x80	60x80	35x45	35x45	55x75	35x40
3	70x80	65x80	35x45	35x50	55x75	35x40
2	70x80	70x80	35x45	35x50	55x75	35x40
1	70x85	70x80	35x45	35x45	55x75	35x40

The seismic performance of the buildings is compared using OpenSees by means of a pushover analysis and an incremental dynamic analysis of the record set of the FEMA P-695.

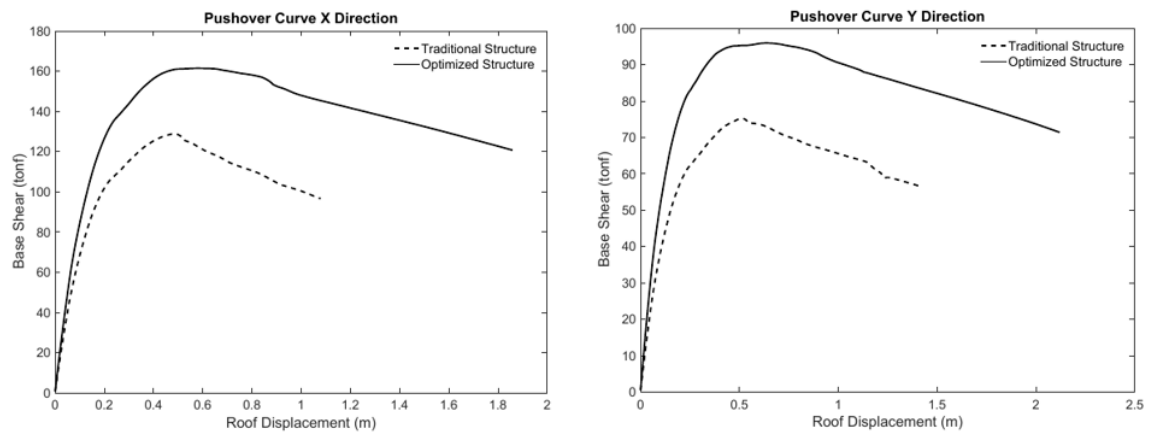


Figure 1-6. Pushover results for the 10 story building.

The pushover results (figure 1-6) show that the optimized building has an overstrength that is 23.8% and 27.9% higher than the baseline building for the X and Y direction, respectively. On the other hand, the ductility factor sees a notable improvement, as it is 81.9% greater in the X direction and 98.2% in the Y direction.

The performance improvement shown in the Pushover is verified using Nonlinear Time History Analysis. We start by looking at the displacement response for a scale factor of 1.0 in figure 6, where it can be appreciated that the median displacement of the optimized building is smaller than the baseline, in a range that varies from 45% for the first floor in the X direction, down to 10% for the tenth floor in the Y direction.

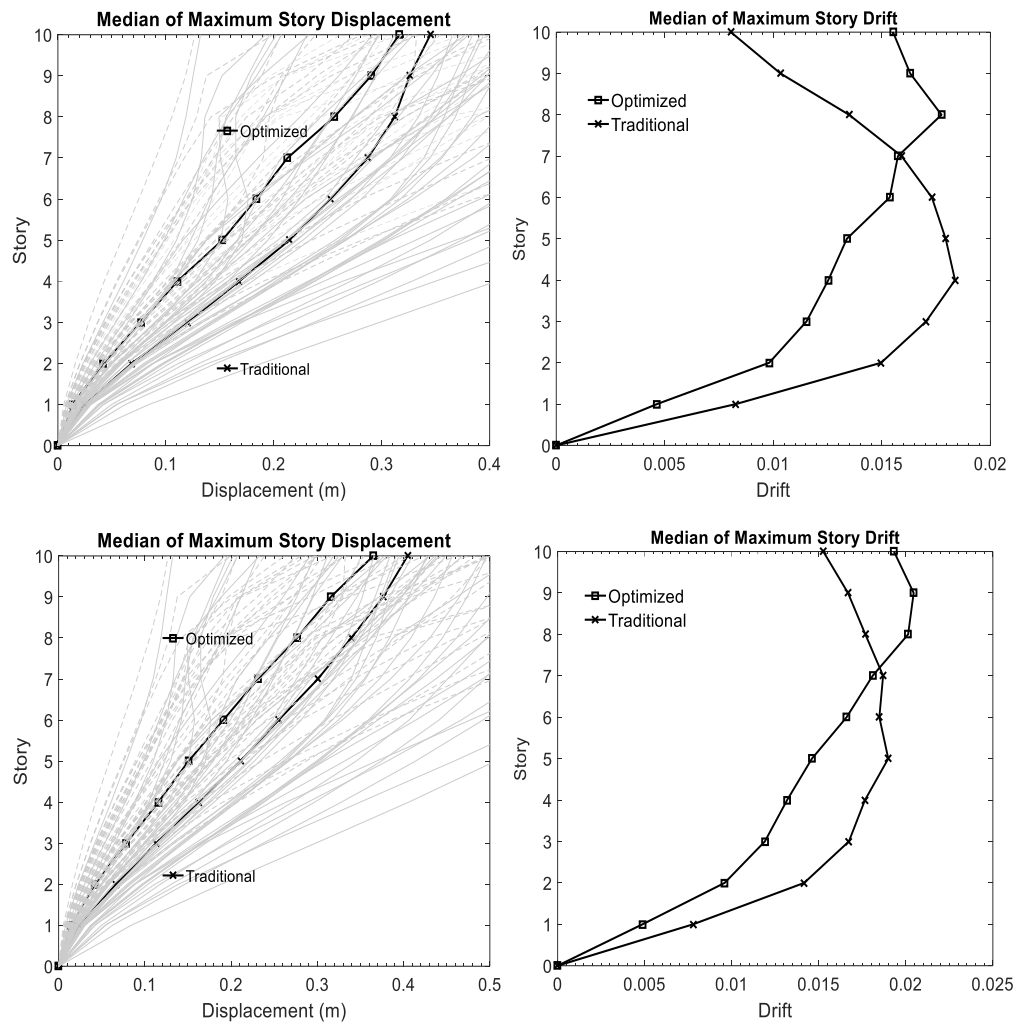


Figure 1-7. The displacement and drift responses for a scale factor of 1.0 are smaller for the optimized building, especially in the bottom stories. Top: X direction. Bottom: Y direction. Dotted and continuous gray lines represent individual ground motion results for the optimized and traditional buildings, respectively.

The behavior of the structures is further clarified by examining the drift responses in figure 6, where can be seen that for both directions, the optimized building has a significant reduction in the interstory drift for the first five stories, with moderate improvements in the sixth and seventh; nonetheless, this comes at the expense of having a bigger interstory drift in the top three stories. In practice, this means that there is a shift in the expected location of the damage; the optimized building is expected to have more damage in the top stories, as opposed to the baseline building where it is expected to take place in the intermediate stories.

Similar results were obtained for scale factors of 2.2 and 3.5, which are shown in Chapter 3. The evidence found in this stage of the thesis showed that the proposed optimization method is capable of optimizing the seismic performance RCF within minutes, with the resulting building consuming the same amounts of concrete and reinforcing steel as the initial design proposed by engineers. All things considered, the proposed method fulfills the objectives of being computationally efficient, easy to implement and effective; benefits that make it a solid candidate to be used within the design of RCF buildings. In addition, the results also validate that eigenfrequency optimization is a suitable framework for the seismic optimization of RCF.

### **1.4.3 Investigation of the method's extension of benefits using performance based earthquake engineering**

Chapters 2 and 3 of this thesis demonstrate that eigenfrequency optimization is a viable framework to formulate the seismic optimization problem and that it can be coupled with the full homogenization method to propose a computationally efficient algorithm. However, the full extent of seismic improvements from this approach and the mechanisms

by which seismic performance is improved remain unclear. Due to the method potential for practical application, this is an issue that deserves investigation. This task was conducted using performance based earthquake engineering (PBEE) and it is presented in full details in Chapter 4 of this document.

Three regular RCF buildings with 5, 10 and 15 stories are considered, as well as an irregular 6 story building. These are first designed according to the ASCE 7 standard (ASCE 2010) and the ACI 318 design code (ACI 2008), and then redesigned based on the results of the eigenfrequency optimization. The redesigned buildings satisfy all code requirements and use the same material volumes as the original design, but this material is redistributed to minimize the period. Nonlinear simulation models of the traditional and redesigned buildings are subjected to dynamic analysis that provides the input for the assessment of collapse risk and earthquake-induced losses. The structural response is quantified in terms of drift demands over the height of the building and collapse fragility curves. In addition, the expected annualized losses associated with repairing earthquake-induced damage are calculated and disaggregated based on the contributions of the buildings' structural and nonstructural components. Furthermore, the buildings' collapse modes are identified and the expected number of casualties computed.

Table 1-2. Comparison of first-mode periods  $T_n$  between traditional and optimized building designs.

<b><u>Building</u></b>	<b><u>Traditional <math>T_n</math></u></b> <b><u>(sec)</u></b>	<b><u>Optimized <math>T_n</math></u></b> <b><u>(sec)</u></b>	<b><u>% Reduction with</u></b> <b><u>optimization</u></b>
15 Story	2.28	2.14	6.1%
10 Story	1.70	1.58	7.1%
5 Story	0.95	0.88	7.4%
6 Story	0.96	0.92	4.3%

The first comparison conducted between the traditional and optimized building is the fundamental period (table 1-2), which show an average reduction of 6.2%, which by itself cannot explain the reasons behind the improvements in seismic performance described in Chapter 3.

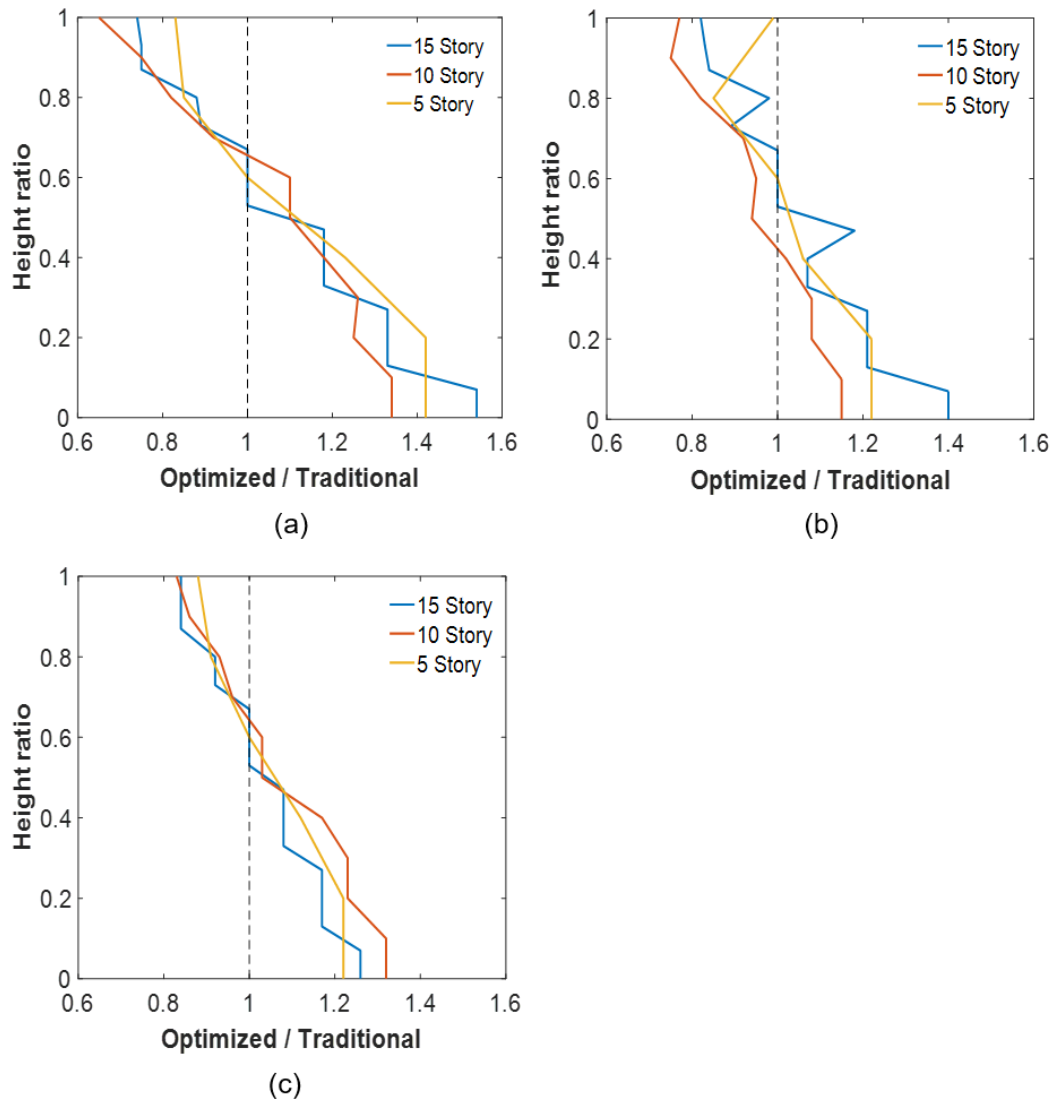


Figure 1-8. Impact of optimization on (a) column moment strength, (b) ratio of column moment to beam moment strength and (c) column shear strength over the height of the building. The x-axis reports the ratio of the optimized building's value for that parameter to that of the traditional building. The y-axis shows the distribution over height, normalized by the total height of each building.

To obtain a more comprehensive understanding of the potential implications of the changes introduced by the proposed method on the buildings' structural configuration, the column moment strength (figure 1-8a), column-to-beam moment strength ratio (figure 1-8b) and column shear strength (figure 1-8c) are computed for the 5, 10 and 15 story buildings.

In the case of the columns' moment strength (Figure 1-8a), the optimized buildings have on average 142% of that of traditional buildings at their base, with gradual decrease to a 75% average on the roof. For column shear strength and the column to beam strength ratio, the percentages of variation are respectively 127% to 87% and 125% to 84%. Though not shown in the figure, beam capacities also follow a stair-like pattern, with the optimized buildings' beams having 10% greater moment capacity at the bottom third, equal capacity in the middle and 10% lower at the top third.

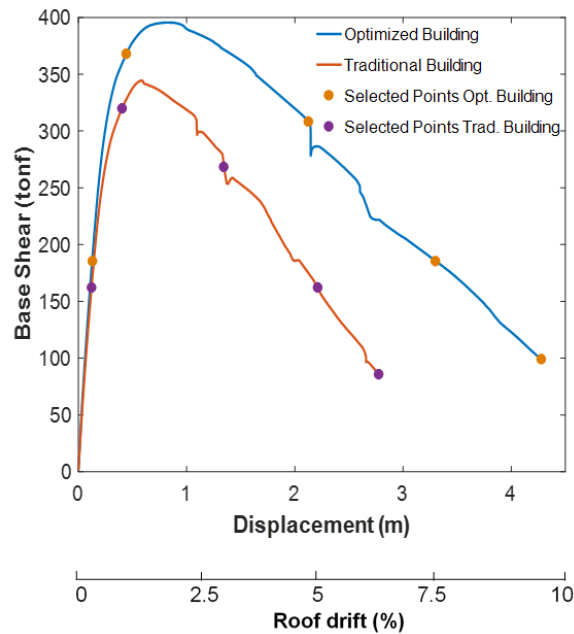


Figure 1-9. Pushover comparison of 15 story buildings.

Full details of the PBEE results are presented in Chapter 4 of this document. A brief summary of the 15 story building is presented in the following paragraphs.

Pushover results (figure 1-9) show a 15% percent of improvement in the maximum base shear withstood by the optimized building as compared to the traditional building. Besides, the post-peak slope of the optimized building that is 26% flatter than the traditional one.

The displacement profiles for the points marked in figure 1-9 is shown in figure 1-10.

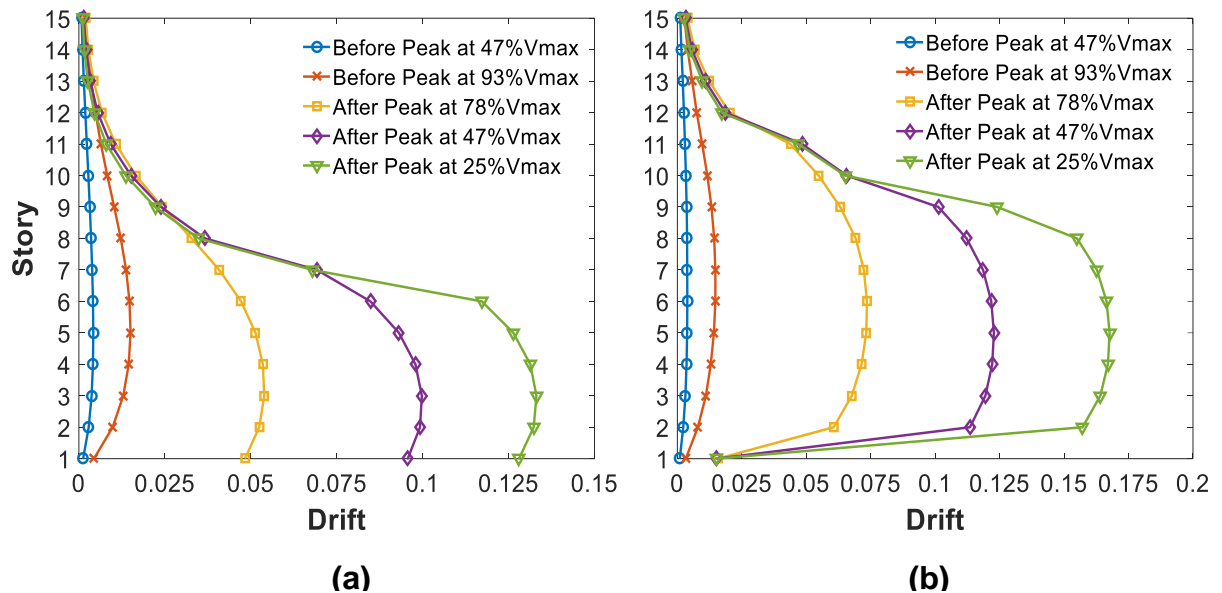


Figure 1-10. Pushover story drift distribution for the 15 story buildings: (a) traditional building and (b) optimized building. Points selected for the drift distribution plots are shown in Figure 1-9.

The behavior for the traditional building (figure 1-10a) is as expected, with largest drift values in the bottom third of the building and a sharp decline in drifts moving up in the building. This behavior is accentuated at the higher levels of displacement demand, as damage concentrates in the lower stories. The optimized building has a different behavior. To start, there are similar levels of drifts for stories 2 to 9 regardless of the level of displacement, indicating that the displacement demand and damage is spread more evenly

over the height of the building compared to the traditional building. Indeed, at all levels of displacement, 8 out of 15 stories have between 75 and 100% of the maximum story drift, compared to 6 stories having close to the maximum drift in the traditional building.

The PBEE analysis relies on nonlinear dynamic analysis to simulate the building response. For this purpose, the 44 ground motion suite of FEMA P-695 was selected (FEMA 2009) and each ground motion was scaled such that its  $Sa$  matched eight different intensity levels at  $\{0.5, 1.0, 1.5, 2.0, 2.5, 3.0, 4.5, 6.0\} Sa_D$ . Here,  $Sa_D$  for the 15 story building models denotes the spectral design acceleration at a period  $T_l = 2.2s$ , an intermediate value between the fundamental period of the traditional building (2.28s) and the optimized building (2.14s).

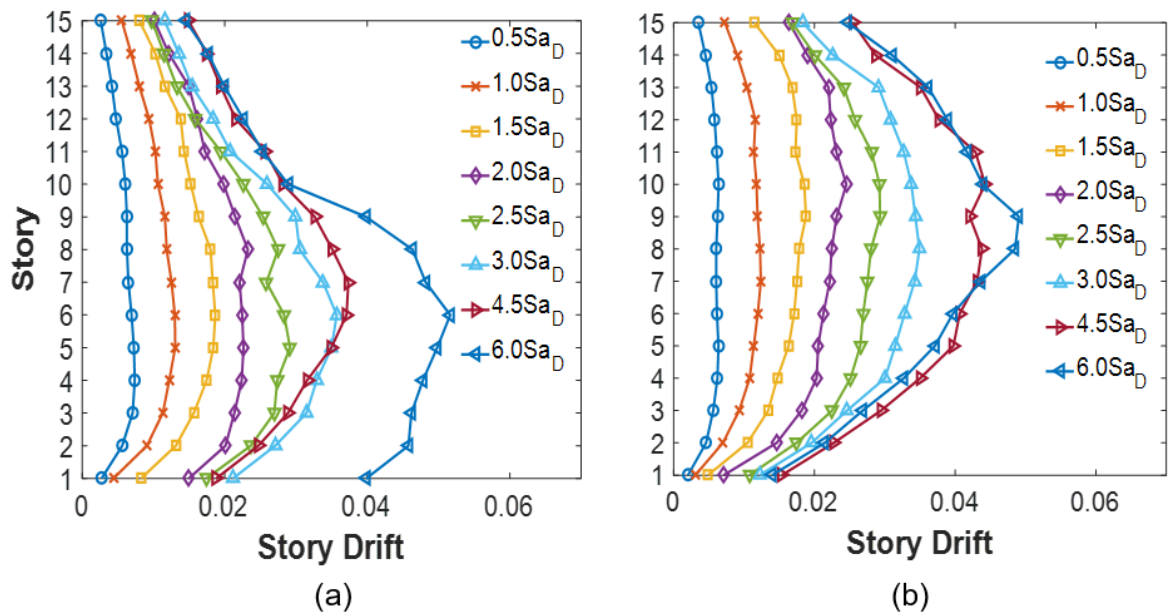


Figure 1-11. Median of maximum story drift response for the 15 story buildings: (a) traditional building, and (b) optimized building.

For those ground motions where no collapse is observed, the median of maximum drift at each story are calculated for both buildings and plotted in Figure 1-11. The behavior of

both buildings is as expected based on the pushover results, with the optimized building having a more uniform distribution of drift along its height, while in the traditional building, the drift is concentrated more in the lower stories and decreases in the uppermost stories. In addition, the story drift in the first three stories for the optimized building is notably smaller than the traditional building, which is critical because these stories have an important role in the overall structural stability.

In the dynamic analysis, collapse is considered to occur when the story drift exceeds 10% in any story of the building (Vamvatsikos and Cornell 2004). The probability of collapse is calculated at each intensity level as the ratio of the number of collapsed records divided by the total number of records (*i.e.*, 44). The results for both buildings are fitted to a lognormal distribution using the maximum likelihood method (Baker 2014) and shown in Figure 1-12.

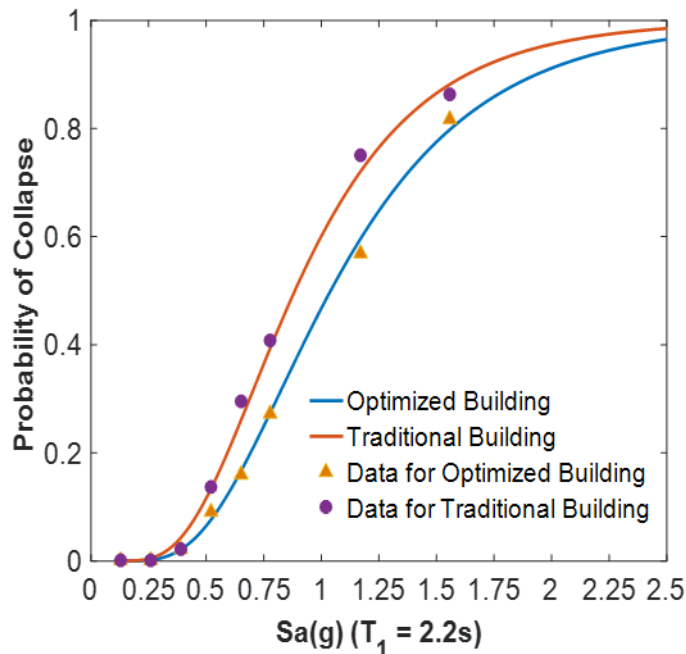


Figure 1-12. Comparison of collapse fragility functions for the 15 story buildings.

Several conclusions can be drawn about the seismic performance of optimized buildings based on the fragility results. First, for values of  $S_a$  up to  $1.5S_{aD}$  (i.e., 1.5 times the building design acceleration, which equals the maximum considered earthquake (MCE) level), the traditional and optimized buildings have similarly low probabilities of collapse. This similarity can be explained by the fact that both buildings were designed according to code regulations and they are expected to show good performance at these levels. However, as the intensity level increases, the optimized building has a significantly smaller probability of collapse than the traditional building. This reduced fragility is due to the more distributed deformations over the height of the optimized as compared to the traditional building.

For each building, the expected annual losses are calculated according to FEMA P-58 using the SP3 tool, and considering both structural and nonstructural components. This calculation considers the possible losses at each intensity level, and weighting these losses by the probability that shaking of that intensity would occur. For the optimized building, the losses are \$120,320/year and for the traditional building the losses are \$122,067/year, which for both buildings corresponds to approximately 0.38% of the building replacement cost (per year).

Although the expected annual losses are similar, the contributions of building components to the losses differ between the two buildings. Figure 1-13 shows that the main sources of losses for both buildings are the losses due to collapse, the residual drift irreparability trigger (wherein a residual drift of 1% is the median value considered to trigger an assessment that the building needs to be torn down and replaced), structural components and partition walls. However, in the traditional building, the aggregate effect of collapse

and residual drift accounts for 35% of the total loss, whereas in the optimized building, these factors contribute 27% of the losses. In contrast, losses that result from damage of structural components and partition walls represent 57% of the total loss of the traditional building, while in the optimized building their contribution to total losses is 65%.

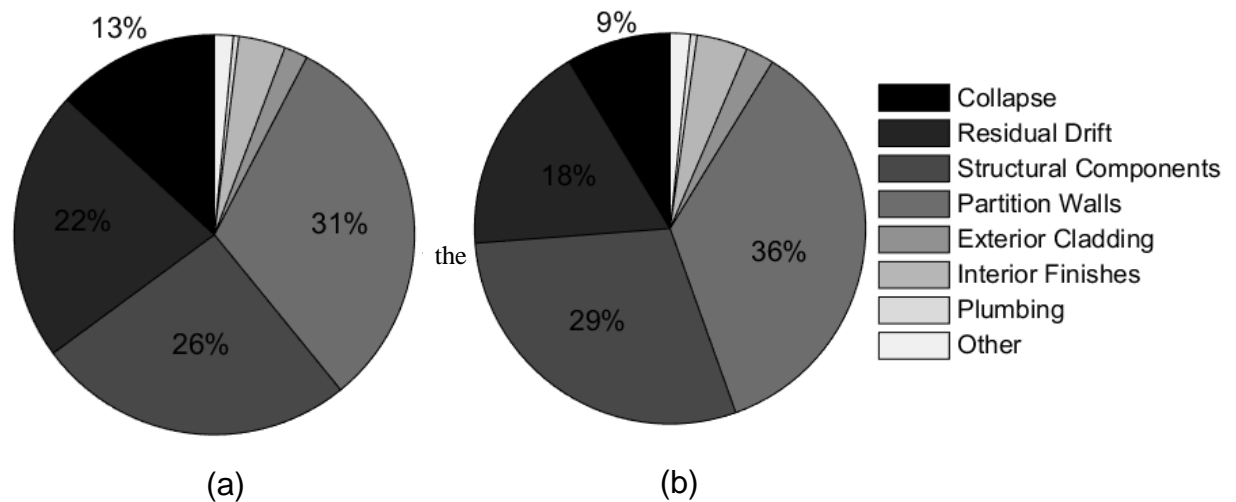


Figure 1-13. Deaggregation of losses for the 15 story buildings: (a) traditional building and (b) optimized building.

## 1.5 Conclusions and future work

This thesis proposes a method to optimize the seismic performance of reinforced concrete frames that uses eigenfrequency optimization to formulate the problem and the geometric optimization and the homogenization method as the basis of an efficient computational algorithms.

The proposed optimization method is capable of optimizing the seismic performance RCF within minutes, with the resulting building consuming the same amounts of concrete and reinforcing steel as an initial design proposed by engineers. The method fulfills the

objectives of being computationally efficient, easy to implement and effective; benefits that make it a solid candidate to be used within the design of RCF buildings. Furthermore, the results show that eigenfrequency optimization is a suitable framework for the seismic optimization of RCF.

The reasons behind the method effectiveness are that it achieves reductions of building periods of about 6% by means of redistributing material along building height. This material redistribution in turn redistributes strength in a manner that is more appropriate to withstand the seismic forces, hence optimized buildings have improved seismic performance. In particular, for the bottom third of the buildings, the column-to-beam moment strength ratios are increased on average by 21%, the moment and shear strength are increased by 32% and 23% for columns, and the moment capacity of the beams is increased by 10%. For the top third of the buildings, the column moment and shear strength is reduced by 22% and 16% respectively, while the column-to-beam moment strength ratio is decreased by 15% and the beams' moment strength is decreased by 10%.

Optimized buildings have a more uniform drift distribution along its height, compared to those of the traditional building, with important reductions in the bottom stories and larger drifts in the top stories. As a consequence, the optimized buildings are less susceptible to collapse. As a result, the expected number of fatalities is reduced from 7 to 3 and from 21 to 13 at intensity levels of 1.5 and 2.0 times the design level. However, if collapse occurs, there is a greater probability that it will happen in a larger portion of the building for the optimized building.

The method produces buildings whose expected annual losses associated with earthquake-induced damage and associated repairs are 1.4% smaller than those for traditional

buildings. Thus, the aforementioned seismic performance is achieved while maintaining the same material quantities (construction costs) and similar levels of annual seismic expected losses.

Future research on this topic can be pursued in different areas:

About eigenfrequency optimization, a continuation of this work would be investigating if it can be used for steel MRF. In addition, it would be worth investigating the application of the proposed problem formulation in three dimensions. Moreover, it is also interesting to evaluate if the problem formulation can be extended to involve more design variables without compromising the simplicity in the formulation and the computational performance. In particular, including steel reinforcement and nonlinear behavior in the problem would be a good addition for the procedure.

From an optimization perspective, this is an interesting problem because the objective function is not expensive and the search space can become very large, hence, it is worth investigating the feasibility and the computational performance of other solution techniques, such as simulated annealing or particle swarm.

From an earthquake engineering perspective, it would be interesting to evaluate how the response of the optimized buildings is sensitive to the frequency content of seismic records, and developing a software that uses the proposed method and integrates with existing structural engineering packages, giving engineers a powerful tool to improve current design practice.

## **2. EIGEFREQUENCY OPTIMIZATION WITH GEOMETRIC OPTIMIZATION FOR REINFORCED CONCRETE FRAMES**

This chapter is presented in a paper format, corresponding to the publication “Method to Improve Seismic Performance of RC Moment-Resisting Frames Using Geometric Optimization”, which is published in the Journal of Computing in Civil Engineering.

## **Method to Improve Seismic Performance of RC Moment-Resisting Frames Using Geometric Optimization**

*Abstract:* This article presents an optimization method to determine the column dimensions that maximize the fundamental frequency of a building, which translates into a highly efficient computational algorithm for approximately solving this optimization problem. A thoroughly detailed example is provided for a 10-story building whose elastic behavior is analyzed using a three-dimensional model, employing a two-dimensional fiber model to assess its inelastic performance. The results show that, compared with the classical design, which has columns of uniform depth, the maximum elastic drift is reduced by 10% and that the drift demand decreases on the lower stories of the building. In addition, the overstrength of the structure and its ductility are increased by between 10 and 30%. Similar improvements are also observed in a second example for a five-story building, showing that the method is useful at least for mid-rise buildings.

Author keywords: Structural optimization; Geometric optimization; Ductility; Overstrength; RC moment-resisting frames; Seismic performance

### **Introduction**

Structural optimization has been a very active field of research in recent decades. Nowadays, thanks to advances in computational power, as well as the development of new optimization strategies, it is possible to determine the optimal configuration of elements for many structures.

Several methodologies have been proposed for RC buildings using various approaches, for instance, optimization based on the explicit formulation of design constraints (Zou et al. 2007), as well as heuristic methods, such as genetic algorithms (GAs) (Li et al. 2010a), simulated annealing (Li et al. 2010b), and discrete gravitational search (Khatibinia et al. 2013).

Although these methodologies make use of different optimization frameworks (Fragiadakis and Lagaros 2011), they have two elements in common: their objective function consists in minimizing the cost of the structure, and the results of the optimization are the element dimensions and reinforcement layout. As a result, they also share the high computational cost and numerical issues associated with heuristic methods, and even though research has been conducted on these topics (Hoffman and Richards 2014; Zacharenaki et al. 2013), there is still room for improvement and innovation.

With this motivation and based on a robust mathematical theory (Murat and Simon 1974), this paper introduces an innovative methodology to improve the seismic performance of RC buildings. Geometric or shape optimization is now an established field in applied mathematics that has been proven useful in various engineering problems, such as, for example, airfoil design and beam optimization (Pironneau 1984) and heat diffusion (Henrot and Sokolowski 2007). In the proposed approach the idea is to maximize the fundamental frequency ( $\omega$ ) of a structure, while the material cost is indirectly considered as an optimization constraint by limiting the total volume of the structure. The physical justification of maximizing the fundamental frequency is that improving the elastic performance of the building leads to a delay in the start of the inelastic regime. An assumption about the development of this method is that the structure is sufficiently

regular, which makes it possible to introduce a surrogate model and formulate a very efficient optimization algorithm. Seismic performance is evaluated using modal spectral analysis and pushover analysis, which is considered appropriate given the regularity of the structure (Krawinkler and Seneviratna 1998). Even though seismic performance is not directly optimized, the numerical evidence provided here suggests that in some cases, increasing the first natural frequency of a building improves its seismic performance. This relationship is similar to the one found in (Herranz et al. 2012), between a good Strut-and-Tie model for designing irregular RC beams (which is evaluated in an inelastic regime), and maximizing the stiffness of the beam in its linear elastic regime through layout optimization. However, more research needs to be done to improve the understanding of the relationship between eigenfrequency optimization and seismic performance.

This paper is structured as follows. The second section, “Geometric Optimization Using a Membrane,” presents the mathematical formulation and computational algorithm for the maximization of the first eigenfrequency for the surrogate model. The next section, “Illustrative Examples,” provides a detailed application of the proposed methodology, first for a 10-story building and then for a 5-story one. The performance of the optimum buildings is compared against its non-optimized counterparts in the section titled “Structural Performance of Optimized Structure.” The final section presents the conclusions of the study and outlines directions for future research on this topic.

### **Geometric Optimization Using a Membrane**

All the buildings considered in what follows have the same floor plan, namely, a rectangular plan with depth significantly smaller than length, in order to have the first

vibration mode of the buildings containing mainly displacements in the direction of the depth of the building. The surrogate model to use consists in viewing the building in elevation as a membrane of variable thickness, then optimizing on the thickness to maximize the first eigenfrequency of the membrane and then translating this thickness into depths of the columns of the frames to be used in the building. If the building is either not regular or not slender, the proposed surrogate model is not appropriate for eigenvalue optimization. Let  $\Omega$  be a rectangular domain in the  $X - Z$  plane (Fig. 1) representing a membrane of variable thickness  $h: \Omega \rightarrow h_{\min} ; h_{\max}$ , with  $0 < h_{\min} \leq h_{\max}$  being  $b$  given values. The membrane has only displacements transversal to the  $X - Z$  plane and all points on a line perpendicular to the plane experience the same displacement, and assuming additionally that the membrane is made of homogeneous material, one finds by simplifying the linear elasticity equations under these assumptions that its stiffness is proportional to  $h$ . The thickness  $h$  could be a discontinuous function, which does not pose a problem to the optimization algorithm since the objective function can be shown to depend on  $h$  in a differentiable way.  $\Omega$  has two different boundary conditions. One is a zero displacement Dirichlet condition, which in Fig. 1 corresponds to the bottom of the membrane, representing the free boundaries of the building.

The first eigenvalue of a continuous physical system corresponds to the square of the minor natural frequency of the system (eigenfrequency), and to obtain this eigenfrequency, the Rayleigh quotient is calculated. For this the following problem on the two-dimensional membrane is solved (Fig. 1):

$$\begin{aligned}
-\operatorname{div}(h\nabla u) &= \omega^2 u & \text{in } \Omega \\
u &= 0 & \text{on } \Gamma_D \\
h\nabla u \cdot n &= 0 & \text{on } \Gamma_N,
\end{aligned} \tag{1}$$

where  $u$  is the deflection and  $\omega$  is an eigenfrequency.

To optimize on  $h$  we need to look at the variational, or weak, formulation of problem (1).

Then the space where we look for the solution is:

$$V = \{v \in H^1(\Omega); v = 0 \text{ on } \Gamma_D\}$$

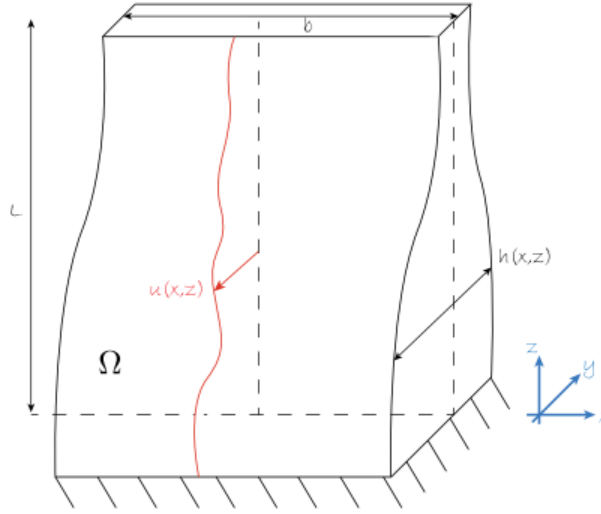


**Fig. 1.** Two-dimensional model of a membrane

where  $H^1(\Omega)$  corresponds to the space of functions defined over  $\Omega$  and over its boundary  $\Gamma_D \cup \Gamma_N$ , which are square integrable over  $\Omega$  and have first (distributional) derivatives that are also square integrable over  $\Omega$ . This is the appropriate space where one is certain that there is a unique solution to the variational formulation of problem (1).

Then the variational formulation of problem (1) becomes to look for  $u \in V$  such that

$$\int_{\Omega} h\nabla u \cdot \nabla v dx = \omega^2 \int_{\Omega} uv dx \quad \text{for all } v \in V. \tag{2}$$

Then if  $v = u$  we obtain the Rayleigh quotient

$$\omega^2 = \frac{1}{\|u\|_{L^2}^2} \int_{\Omega} h |\nabla u|^2 dx \quad (3)$$

Where

$$\|u\|_{L^2} = \sqrt{\int_{\Omega} u^2 dx}$$

Is the norm of  $u$  in the space of square integrable functions, which contains  $V$ .

The smallest eigenvalue, denoted by  $\omega_1$ , is obtained by solving

$$\omega_1^2 = J(h) = \min_{u \in V} \frac{1}{\|u\|_{L^2}^2} \int_{\Omega} h |\nabla u|^2 dx. \quad (4)$$

Denote by  $u_1$  the eigenfunction that realizes this minimum. The set of admissible thickness functions is given by

$$U_{ad} = \left\{ h : \Omega \rightarrow [h_{min}, h_{max}]; h \in L^2(\Omega); \int_{\Omega} h dx = V_0, V_0 \in \mathbb{R}^+ \right\}$$

where  $V_0 =$  given value for the volume constraint on the total volume of the material in the membrane.

Because the maximization is with respect to the thickness  $h$ , differentiating the objective function with respect to this variable and considering that  $u = u_1$ , the first eigenfunction, the evaluation of this derivative on a generic admissible perturbation  $k$  gives

$$\begin{aligned} \frac{\partial J}{\partial h}(k) = & \frac{1}{\|u_1\|_{L^2}^2} \int_{\Omega} k |\nabla u_1|^2 dx + \frac{2}{\|u_1\|_{L^2}^2} \int_{\Omega} h \nabla u_1 \cdot \nabla \frac{\partial u_1}{\partial h}(k) dx \\ & - \frac{2}{\|u_1\|_{L^2}^4} \int_{\Omega} u_1 \frac{\partial u_1}{\partial h}(k) dx \int_{\Omega} h |\nabla u_1|^2 dx. \end{aligned} \quad (5)$$

Now, using the fact that  $\frac{\partial u_1}{\partial h}(k) \in V$ , and therefore it can be used as a test function in

equation (2) for  $\omega = \omega_1$  and  $u = u_1$ , the last two terms on the right hand side of equation (5)

cancel each other. Hence, taking  $k = \frac{|\nabla u_1|^2}{\|u_1\|_{L^2}^2}$  we obtain a positive value of the derivative is

obtained and then the objective function will increase if  $h$  is perturbed infinitesimally in

this direction. Therefore, the following numerical algorithm is proposed to maximize  $\omega$ ,

based on the so-called method of perpendicular directions, meaning that it first optimizes

on  $h$  and then adjusts the eigenfunction  $u$  and eigenvalue  $\omega$  using the Arnoldi algorithm.

The idea behind the Arnoldi algorithm is to write the discretization using the finite element

method of Eq. (2) in matrix form,  $KU = \omega^2 MU$ ; then, since in the case considered  $K$  in

nonsingular, the eigenvalue problem can be written as  $K^{-1}MU = \frac{1}{\omega^2}U$ ; then, through an

orthogonalization process, it can efficiently compute the first eigenvalue  $\omega_1$  of Eq. (2).

The steps are the follows:

1. Let  $h_0$  be a given initial thickness
2. With  $h_0$  we calculate  $u_0$ , the first eigenfunction, using the Arnoldi algorithm.

3. Evaluate the objective function,  $J(h_0) = \frac{1}{\|u_0\|_{L^2}^2} \int_{\Omega} h_0 |\nabla u_0|^2 dx$ , the initial smallest eigenvalue. Call this  $J_{old}$ .
4. Calculate the direction of perturbation of  $h$ , given by  $k = \frac{|\nabla u_0|^2}{\|u_0\|_{L^2}^2}$ . Take  $t = t_0$  an initial step size.
5. Calculate the new thickness:  $h = h_0 + tk + l$ , where  $l$  is the Lagrange multiplier for the volume constraint. Choose  $l$  in such a way that  $h_{min} \leq h \leq h_{max}$  and  $\int_{\Omega} h dx = V_0$ .
6. Using  $h$  calculate  $u_0$  by the Arnoldi algorithm and evaluate  $J(h)$ . Call this  $J_{new}$ . If  $J_{new} \geq J_{old}$ , make  $J_{old} = J_{new}$ , and go to step (4). If  $J_{new} < J_{old}$  diminish the value of  $t$ . If  $t$  becomes too small, stop. If not, go to step (5).

This method is extremely efficient from a computational perspective since it generally makes one objective function evaluation per iteration, and it needs only 47 iterations to reach convergence for a 10-story building, and 43 iterations for a 5-story building, corresponding to about 30 seconds of execution time using a Desktop Computer with a Core i5 3570k and 8GB of RAM. In the next section we show that this method can also be used to optimize the dimensions of columns in regular three-dimensional frames.

## **Illustrative Examples**

### **Ten-Story Building**

To demonstrate the aforementioned procedure, we consider a 10-story moment resisting frame with 5 m spans and 3 m story height, whose plan view is shown in figure 2. To establish a baseline for comparison, this building is designed according to the Colombian Code for the Seismic Design of Structures (NSR-10 2010) for a zone of intermediate seismicity. The design results show that the design requirements of this code are fulfilled using columns with a cross section of 55cm x 75cm and a reinforcement ratio of 1.2%. Beams sections are calculated and sections of 30cm x 40cm with a top and bottom reinforcement of  $3\phi 16$  are found to satisfy the code requirements.

As a consequence of its regularity, this building can be optimized independently for both directions. A description of the optimization procedure is given next.

First, the optimization domain must be established. To optimize for the x-dimension of columns, the domain must be consistent with the elevation in the Y axis, therefore, for the building under consideration, this domain is described by rectangular shape with dimensions of 30m height and 15m width. Similarly, the optimization for the y-dimension of columns is performed using an elevation consistent with the X direction of the building, which results in a square domain with sides of 30m. As a general guideline, the width of the domain is determined based on the building plan distribution, whereas the height corresponds to the height of the building. As can be seen in Fig. 2, the building has 15m in the Y axis and 30m in the X axis, values that correspond to the width of the domain for the optimization of the x-dimension and y-dimension of columns, respectively.

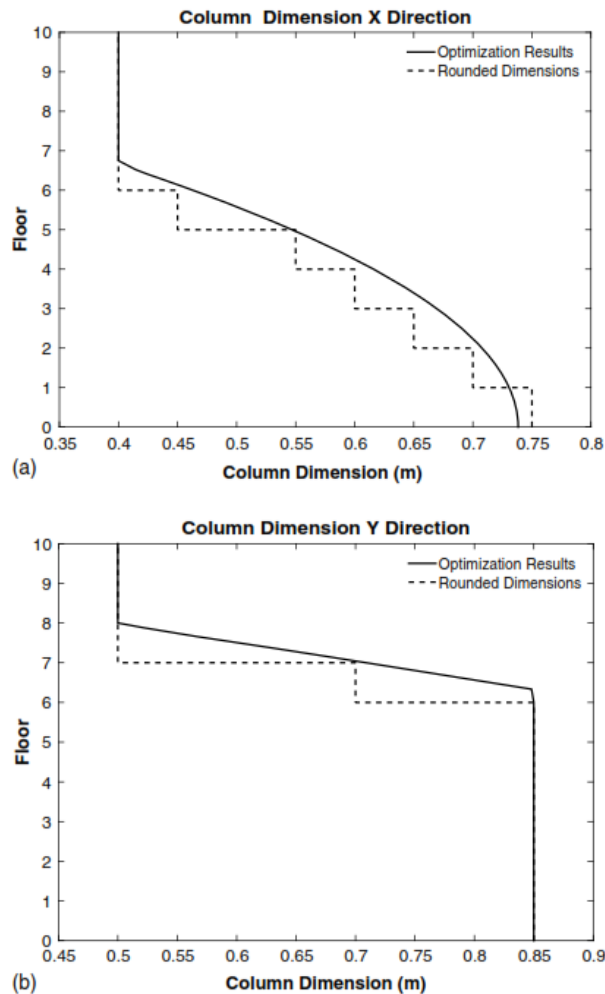


Fig. 3. Optimized and rounded column dimensions—10-story building

The second step involves setting proper values for  $[h_{\min}, h_{\max}]$ , which represent the minimum and maximum desired values for the column dimension. These values must be set for each optimization direction. Several reasonable strategies may be used for this, for instance, values suggested by past experience in structural projects, or by means of a pre-design based on approximate methods of analysis. In this example, a previous analysis suggests values around 55cm for the x-dimension and 75cm for the y-dimension, thus, a [40cm, 75cm] range is used for the former and [50cm, 85cm] for the latter.

Once  $[h_{\min} ; h_{\max}]$  are set, the same must be done with  $V_0$ . The values of  $h_{\min}$ ,  $h_{\max}$  and  $V_0$  must be chosen such that  $V_0$  lies between  $Ah_{\min}$  and  $Ah_{\max}$ , where  $A$  is the area of the membrane in plan view. Setting values outside this interval will make it impossible to achieve convergence since that would require having values lower than  $h_{\min}$  or higher than  $h_{\max}$  (depending on the case), which contradicts the previously imposed optimization constraint. For the sake of making a fair comparison, this example uses the column dimensions of the baseline structure as the basis for the calculation of  $V_0$ . In particular, for the optimization in the  $x$ -dimension, this means that  $V_0 = (0.55 \times 30 \times 30 \text{ m}) = 495 \text{ m}^3$ ; similarly, for the optimization in the  $y$ -dimension  $V_0 = 337.5 \text{ m}^3$ . It should be noted that these volumes are only for feeding the optimization method with the membrane model; they are not the actual volumes of the columns.

The third and final step is solving the optimization problem using the optimization algorithm in the previous section.

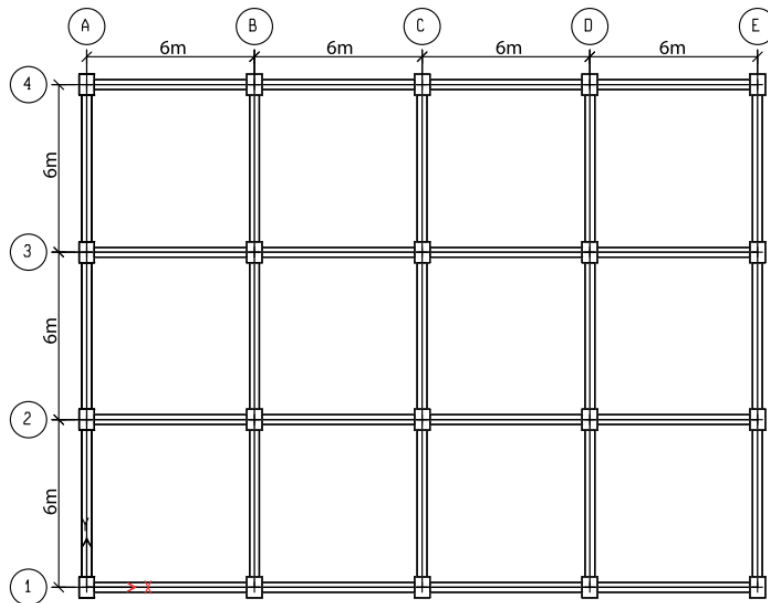


Fig. 4. Plan view of five-story building

This algorithm is implemented in FreeFem++ (Hecht 2012). As mentioned before, one of the advantages of this method is its computational efficiency; each optimization takes less than 30 seconds in a PC with a Core i5 3570k (running at stock speeds) and 8GB of RAM. The optimization results for the column dimensions are shown in Fig. 3.

Based on these results, the following observations are made:

1. The dimension profile starts at the bottom of the building with a value equal to  $h_{\max}$  and decreases until it reaches  $h_{\min}$  at the upper levels. From a seismic design perspective, this is a reasonable decision because the shear demand is higher in the lower floors and strong columns are best suited to withstand that demand.
2. Despite the latter similarity, different behaviors are observed in the profiles of the x- and y-dimensions. While the former has a gradual decrease between the first and sixth floors, the latter remains equal to its  $h_{\max}$  for the first six floors and shows a sharp decline, reaching  $h_{\min}$  at the eight floor. This kind of behavior suggests that special attention must be given to the selection of  $\frac{1}{2}h_{\min}$ ;  $h_{\max}$  in order to consider existing limitations imposed by design codes, most of which are aimed at avoiding abrupt changes in section dimensions between consecutive floors. In this particular case, however, these changes are in compliance with NSR-10 (NSR-10 2010) and therefore do not violate common design practice.
3. For construction purposes, these dimensions must be approximated to values in concordance with building practices. In this example, dimensions are rounded to the closest multiple of 5 cm, which results in columns that vary from  $75 \times 85$  cm at the base up to  $40 \times 50$  cm at Floors 8–10. These are the final dimensions of the optimization process and are used to compare against the baseline structure. The curves

showing the column dimensions before and after the rounding are shown in Fig. 3. The change induced by this rounding in the ductility is negligible, while the fundamental frequency increases from 1.468 up to 1.477, i.e., by 0.6%. These small changes are closely related to the fact that, as shown in Fig. 6, the pushover curves in both directions are barely distinguishable before and after roundup. The resulting structure has 2% lower consumption of concrete for the columns. It should be noted, however, that the optimized building requires additional in situ controls compared to the traditional building owing to the varying column dimensions.

### **Five-story Building**

As a second example, a regular five-story building is considered (see Fig. 4 for plan view) with a story height of 3 m. For this example, only the relevant parameters and results are indicated since the procedure is detailed in the previous example.

First, a baseline structure is established for the same seismic region of the previous example. Here, according to the Colombian NSR-10, columns of  $55 \times 75$  cm and beams of  $35 \times 40$  cm satisfy the code requirements. Considering these dimensions, the optimization parameters  $[h_{\min}, h_{\max}, V_0]$  for the x- and y-directions are set to  $[0.50 \text{ m}, 0.60 \text{ m}, 198 \text{ m}^3]$  and  $[0.60 \text{ m}, 0.80 \text{ m}, 202.5 \text{ m}^3]$ , respectively. After performing the optimization and rounding, the resulting dimensions are columns of  $60 \times 80$  cm for the first three stories and  $50 \times 65$  cm for the fourth and fifth stories. The change induced by this rounding in the ductility is negligible, while the fundamental frequency increases from 0.783 up to 0.791, i.e., by 1%.

### **Structural Performance of Optimized Structure**

In the two cases presented here—traditional building and optimized building—both types of building use almost the same volume of concrete for their columns (i.e., same weight), so the difference in the design shear base between the optimized and the traditional buildings is negligible.

### **Ten-Story Building**

The building with optimized column dimensions is designed according to the Colombian standard NSR-10 (NSR-10 2010). Column reinforcement ranged between 1.1 and 1.3%, and although slight differences are observed in the beams, they are kept the same as in the baseline building for the sake of an objective comparison of the effect of the optimized column dimensions. Both the baseline and the optimized buildings are modeled in three dimensions and subjected to modal analysis in ETABS v.13.1.2, using the unreduced spectrum calculated for Sincelejo (Colombia).

The results in Fig. 5 show that the maximum drift of the structures is reduced by 11%; furthermore, its location is displaced upward one story in the x-direction of the structure and two stories in the y-direction. Roof displacement is calculated and the optimized structure sees a 10.3 and 11.4% reduction compared to the baseline structure for the x- and y-directions, respectively. Further analysis of the shape of the drift shows higher stories in the optimized building having drifts larger than their corresponding counterparts in the baseline building; however, this is an expected result as a consequence of having weaker columns on these stories.

To gain a more comprehensive vision of the structural behavior, OpenSees (Mazzoni et al. 2006) is used to perform a two-dimensional pushover analysis for the typical X and Y frames of the buildings, i.e., frames corresponding to elevations designated by B and 2 in

Fig. 2. Based on these results, ductility ( $\mu$ ) and overstrength ( $\Omega_0$ ) are calculated according to the FEMA P695 (FEMA 2009) methodology.

The mathematical model of the structure is created using force-based elements with confined and unconfined concrete. To avoid localization issues, the constant fracture energy criterion (Coleman and Spacone 2001) is used, with  $G_c = 180$  N/mm, with concrete properties  $f_c = 28$  MPa,  $f_{cc} = 31$  MPa,  $e_c = 0.0019$ , and  $e_{cc} = 0.0028$ . Reinforcing steel is modeled using  $E_s = 210$  GPa,  $f_y = 420$  MPa,  $f_u = 630$  MPa, a plateau limit  $e_{sh} = 0.04$ , and an ultimate strain  $e_u = 0.14$ . P-delta effects are included, and a displacement control is used with 0.5 mm steps. Mode shapes and elastic behavior are checked and found to be consistent with the expected behavior. A uniform gravitational load of  $w_v = 3.5$  tonf/m is applied to the beams, and point loads are applied to nodes to account for the self-weight of the columns.

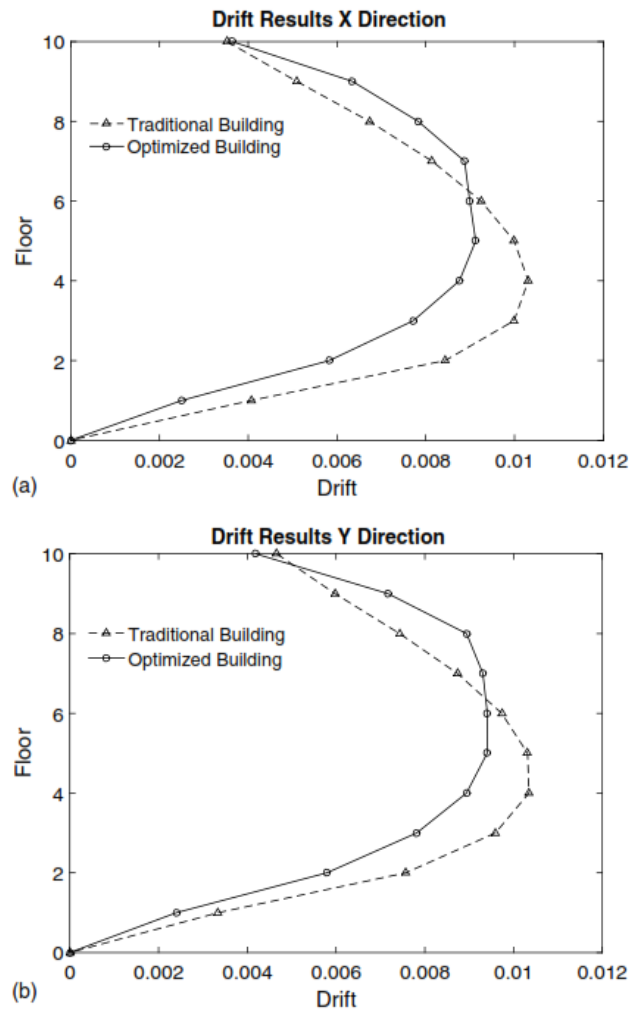
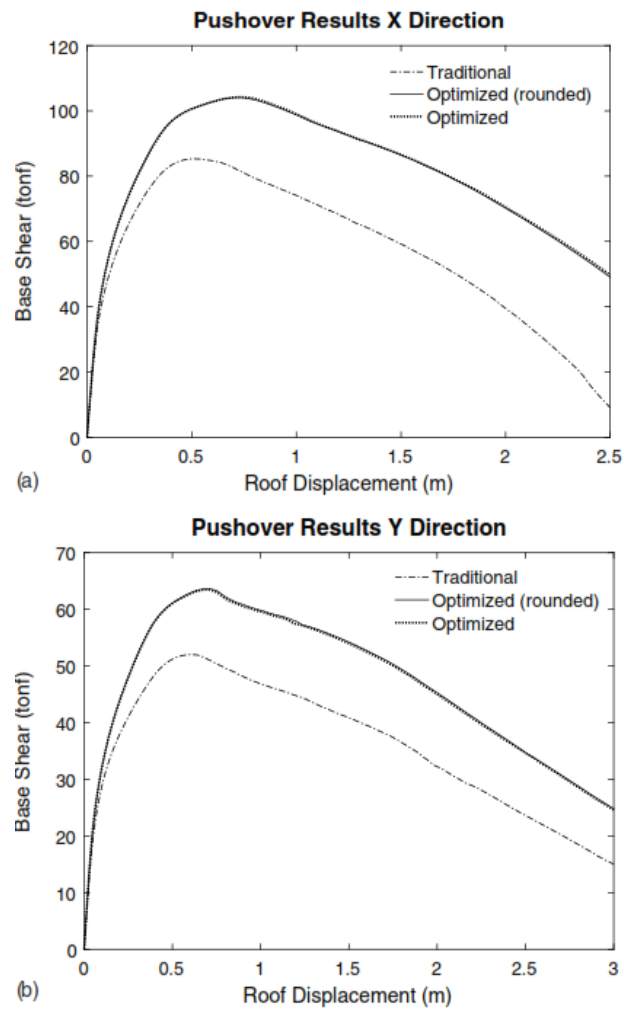


Fig. 5. Drift results—10-story building

The pushover results in Fig. 6 show that the optimized building performs significantly better than the baseline in several aspects. First of all, the slope in the elastic range is steeper for the optimized building, which means that it is more rigid than the baseline. This occurs as a direct consequence of the optimization because its goal is to maximize the first eigenvalue of the building. Second, the maximum base shear  $V_{max}$  supported by the optimized building is higher than that from the baseline. This could have an important practical implication because it suggests that the optimized building could withstand earthquakes with higher accelerations before starting to deteriorate. Third, the optimized

building has a better postpeak performance than the baseline. This can be seen in the results for the x-direction, where an approximately 8% higher (less negative) slope can be observed for the optimized building. This This behavior implies that the rate of deterioration is smaller for the optimized building, which translates into a better ability to withstand damage and the potential to resist stronger earthquakes.



**Fig. 6.** Pushover results—10-story building

This conceptual analysis is further confirmed by the overstrength and ductility calculations shown in table 1. There it can be observed that the optimized building has an overstrength that is 22.3% and 22.4% higher than the baseline structure for the X and Y directions,

respectively. Similarly, the ductility factor is 31.2% greater in the X direction and 10.2% in the Y direction.

To sum up the results, it can be said that the optimized building shows an improved behavior respect to the baseline in three key areas: elastic drift, overstrength and ductility. What is more, all these improvements come with no additional expenses associated to material costs, as the volume of the optimized building is the same as that of the baseline.

### **Five-Story Building**

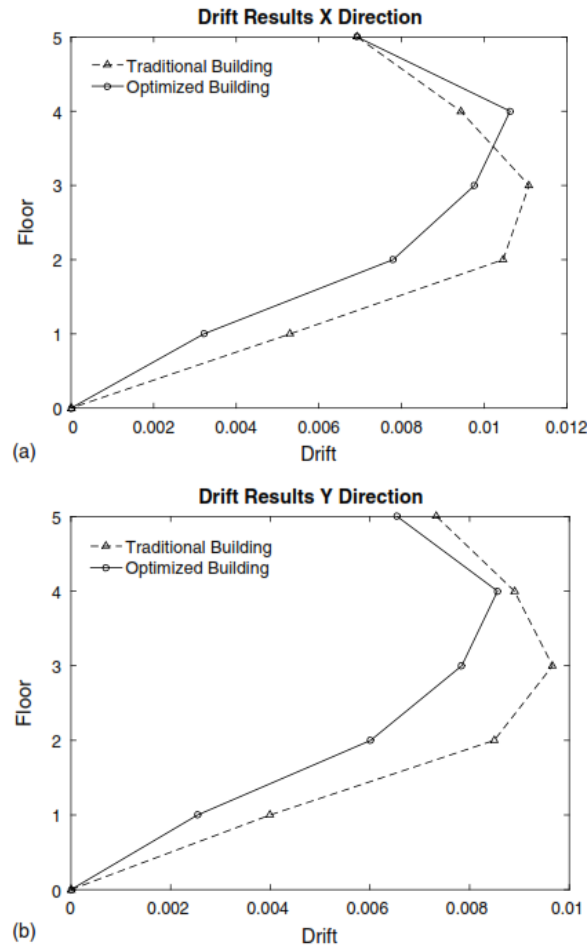
Performance for the 5-story building is analyzed using the same approach as for the 10 story. To start, we create a 3D Model in ETABS v13.1.2 and perform a Modal Spectral Analysis, whose results are shown in figure 7. Due to the fact that both buildings use almost the same volume of concrete for their columns (i.e. same weight), it must be noted that the difference in the design base shear between the optimized and the traditional building is negligible.

The results for the X direction show a reduction of the drift for the optimized building that ranges from 12% to 40% for the first three stories; nonetheless, the maximum drift only saw a reduction of 4.3% and just as in the previous example, it is displaced upwards one story. On the other hand, the Y direction shows consistent decrease in drift along the whole building, with significant improvements for the first three stories and slight benefits for the fourth and fifth stories. Roof displacement is calculated for both buildings and the optimized structure sees a reduction of 12.1% in the X direction and 17.9% in the Y direction.

**Table 1.** Pushover Results—10-Story Building

Structure	Pushover X		Pushover Y	
	$\Omega_0$	$\mu$	$\Omega_0$	$\mu$
Optimized	2.59	13.15	2.37	13.23
Traditional	2.12	10.02	1.94	12.01

Continuing with the performance evaluation, we analyze the structure using OpenSees (Mazzoni et al. 2006) with the same parameters as for the 10-Story example. The Pushover results are presented in Fig. 8 with the overstrength and ductility indicators shown in table 2.

**Fig. 7.** Drift results—five-story building

Based on these results, we see that compared to the baseline, the optimized building has 21.6% greater ductility in the X direction and 30.7% for the Y direction. Furthermore, it

has a steeper slope in the elastic range and a higher overstrength factor, likewise associated to an increase in the maximum base shear supported by the building.

**Table 2.** Pushover Results—Five-Story Building

Structure	Pushover X		Pushover Y	
	$\Omega_0$	$\mu$	$\Omega_0$	$\mu$
Optimized	2.29	10.35	2.57	15.36
Traditional	2.04	8.515	2.30	11.75

All things considered, the optimized building exhibits a better behavior than the baseline. It has lower elastic drift for both directions, greater overstrength and significantly better ductility. What is more, these improvements do not carry on any additional costs associated to materials, as the difference in concrete volume between both buildings is negligible.

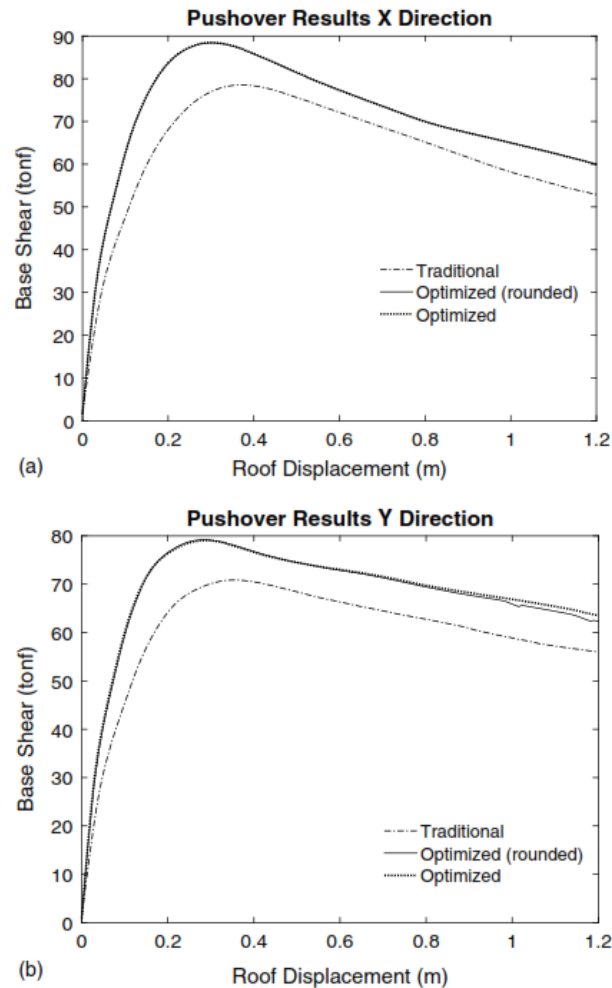


Fig. 8. Pushover results—five -story building

## CONCLUSIONS AND FUTURE WORK

A structural optimization method to determine the optimal dimensions of columns in RC Moment Resisting Frames has been proposed. The method is based on a very simplified physical model of the building, since it only considers displacements in the weaker direction of the building, which leads to the implementation of a very efficient computational algorithm, that can even be implemented using a freely available finite elements platform.

Numerical results show that, compared to a baseline building having all columns with the same dimensions, the behavior of the optimized buildings is improved between 10% and 30% in three areas: elastic drift, ductility and overstrength. These improvements are observed for buildings of

5 and 10 stories, and in both cases are achieved based on the optimization results by reducing the column dimensions with the building height. Furthermore, achieving these improvements requires no additional investment in material cost, as both buildings have the same volume of concrete. More supervision would be needed to ascertain that the correct dimensions of columns are used at the prescribed floor, nonetheless, the benefits in structural performance compensate this endeavor.

In addition to the above, an important advantage of this method comes as a result of these features; it has the potential to become a tool for practitioners, allowing them to leverage their design workflow by reducing the time spent on finding proper column dimensions.

Finally, a continuation of this work would be to include more design variables in the optimization, like column widths and beam dimensions; however, this comes with significant challenges, as it requires a more complex mathematical theory and the development of an efficient algorithm to keep the aforementioned advantages. Similarly, it is also worth to conduct a research to determine if varying the column dimension along the building height can consistently lead to improved results like the ones shown in this paper.

## **Acknowledgments**

The authors wish to thank the anonymous referees whose comments improved the presentation of the work. The first author thanks the Conicyt doctoral fellowship. The second and third authors thank the funding provided by FONDECYT Grant1090334.

### Notation

*The following symbols are used in this paper:*

$A$ = area of domain $\Omega$ ;	
$E_s$ = modulus of elasticity for reinforcing steel;	
$e_c$ = unconfined concrete compressive strain;	
$e_{cc}$ = confined concrete compressive strain;	
$e_{sh}$ = plateau limit in the constitutive relation for reinforcing steel;	
$e_u$ = ultimate strain for reinforcing steel;	$l$ = Lagrange multiplier;
$f_c$ = unconfined concrete compressive stress;	$u$ = displacement field;
$f_{cc}$ = confined concrete compressive stress;	$\mu$ = ductility;
$f_y$ = yield stress for reinforcing steel;	$V_0$ = desired material volume in $\Omega$ ;
$f_u$ = ultimate stress for reinforcing steel;	$v$ = test function;
$G_f^c$ = fracture energy;	$w_r$ = gravity load;
$h$ = membrane thickness;	$\Gamma_D$ = border with Dirichlet condition;
$h_{\min}, h_{\max}$ = minimum/maximum membrane thickness;	$\Gamma_N$ = border with Neumann condition;
$h_0$ = initial thickness;	$\Omega_0$ = overstrength (m);
$k$ = perturbation direction;	$\Omega$ = finite-element domain; and
	$\omega$ = natural frequency.

### **3. EIGENFREQUENCY OPTIMIZATION WITH FULL HOMOGENIZATION FOR REINFORCED CONCRETE FRAMES**

This chapter is presented in a paper format, corresponding to the publication “A seismic optimization procedure for RC framed buildings based on eigenfrequency optimization”, which is accepted for publication in the journal Engineering Optimization. The accepted manuscript is presented here.

## **A seismic optimization procedure for RC framed buildings based on eigenfrequency optimization**

### **Abstract**

Several seismic optimization methods have been proposed to improve the performance of RC Framed (RCF) buildings, however, they have not been widely adopted among practicing engineers because they require complex nonlinear models and are computationally expensive. This article presents a procedure to improve the seismic performance of RCF buildings based on eigenfrequency optimization, which is effective, simple to implement and efficient. The method is used to optimize a 10-story regular building, and its effectiveness is demonstrated by nonlinear time history analyses, which show important reductions in story drifts and lateral displacements when compared to a non-optimized building. A second example for an irregular 6-story building demonstrates that the method provides benefits to a wide range of RCF and supports the applicability of the proposed method.

**Keywords:** eigenfrequency optimization; homogenization; structural optimization; reinforced concrete moment frames; nonlinear time history analysis; genetic algorithms.

### **Introduction**

Reinforced concrete framed structures (RCF) are a widely used structural system in buildings across the world. These frames are designed by structural engineers following an iterative process that involves three steps (Figure 1). First, gravitational and seismic loads are evaluated following the procedures stated by design codes. Then, they calculate a set of columns and beams dimensions that satisfy the elastic drift limit imposed by the code. Finally, steel reinforcement is calculated to satisfy the codes' strength and ductility requirements. In few cases, when elements dimensions are small and they exceed the maximum allowable steel, it is necessary to adjust the columns and beams dimensions to

meet these requirements. A design is said to satisfy the code when it fulfills the drift limit and the strength and ductility requirements.

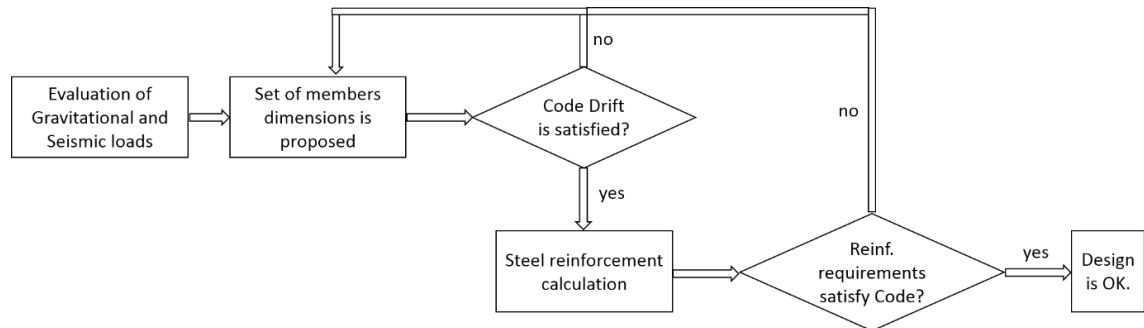


**Figure 1.** The typical design process for a reinforced concrete moment resisting frame uses an iterative process to calculate the column and beam (members) dimensions and steel reinforcement that satisfy the code provisions.

Due to the rapid pace of structural design offices, the customary practice is that a design is considered as final when it satisfies the code and conforms to what previous experience has taught. Because of this practice, most RCF buildings have suboptimal seismic performance.

To address this issue, researchers have proposed optimization methods for RCF based on different optimization frameworks (Fragiadakis & Lagaros, 2011), such as deterministic based optimization (DBO) and reliability based optimization (RBO), where the cost of the structure is considered as the objective function and the code requirements are considered as constraints. Several solution techniques have been used to solve the problem and to optimize the seismic performance. For instance, DBO have been solved with genetic algorithms (Li, Lu, & Liu, 2010) and simulated annealing (Gang Li, 2010), RBO with discrete gravitational search (Khatibinia, Salajegheh, Salajegheh, & Fadaee, 2013), DBO and RBO with evolutionary strategies (Fragiadakis & Papadrakakis, 2008),

and the implementation of particle swarm for DBO and RBO has also been discussed (Fragiadakis & Lagaros, 2011).

These methods are capable of providing good solutions to the optimization problem, however, their usage by practicing structural engineers has been scarce. This situation has occurred because of two causes: a) these methods use nonlinear structural models to evaluate the seismic performance, which are difficult to implement for the average structural engineer, and b) these methods cannot provide results within the time frames used in engineering practice. While the latter cause can be offset by increasing the computational resources, the former poses a major challenge, since the development of nonlinear structural models requires a high level of knowledge and expertise that few practitioners have.

The fact that engineers demand seismic optimization methods that are easy to implement and computationally efficient have been acknowledged by researchers, who have introduced methods with improved solution techniques (Hoffman & Richards, 2014), simplified methods for seismic evaluation (Zacharenaki et al, 2013) and where they explicitly consider code constraints (Zou et al., 2007). Although these efforts have yielded improvements in the computational cost, solving RCF seismic optimization problems still takes several hours or even days in consumer-level computers (Zacharenaki et al., 2013). More importantly, these methods still demand the development of complex nonlinear structural models and therefore, they have not captured the attention of engineers.

To meet the needs of structural engineers, this article presents an optimization procedure to improve the seismic performance of RCF buildings that uses an eigenfrequency optimization framework for the problem statement and which can be

solved using either evolutionary algorithms or the homogenization method. The physical justification of maximizing the fundamental frequency is that it improves the elastic performance of buildings, leading to a delay in the start of the inelastic behavior. This formulation brings two benefits to the proposed method: a) it does not demand complex structural models and b) it is easy to implement and computationally efficient. These benefits allow the method to work within the engineers' workflow (Figure 2) by optimizing two and three dimensional RCF buildings. The method uses the result of engineers' design and returns the set of columns and beams dimensions that satisfies the drift limit of the code, maximizes the fundamental eigenfrequency of the building and uses the same amount of concrete as the engineers' design. Based on these dimensions, the engineer finishes the design by calculating the steel reinforcement following the procedures specified by the design code that apply for his design (Figure 2). Though it would be preferable to include steel reinforcement and nonlinear behavior in the optimization, this would increase significantly the search space and would lead to a method without the benefits of ease of implementation and computational performance, which are key elements for a method to be used in practice, and are offered by the method herein proposed, which uses a problem formulation based on elastic properties of the buildings.

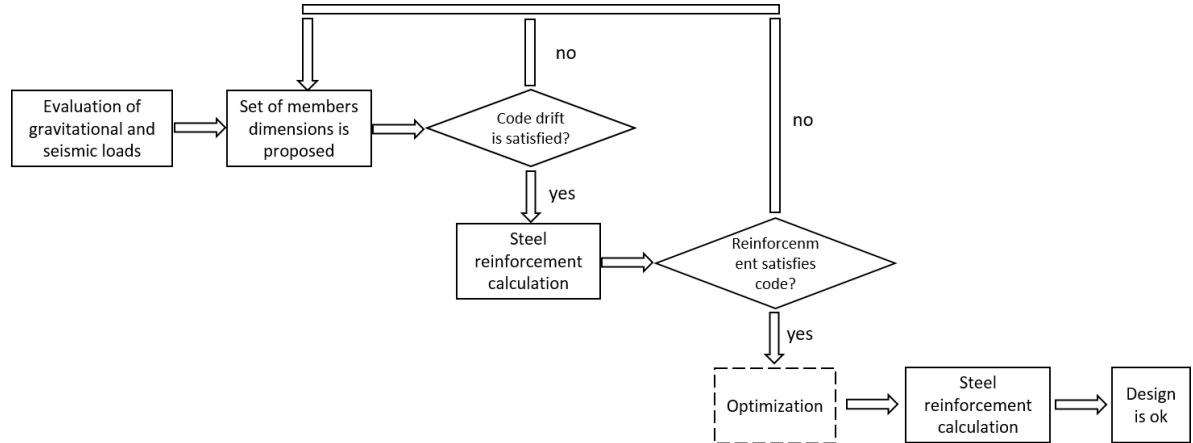


**Figure 2.** The proposed optimization method integrates within the structural design process and uses the results of the engineers design as starting point to determine a set of optimal dimensions.

In this work, the method is applied to optimize the planar frames of a three dimensional 10 story RCF building. The problem was solved in a computer with a Core i5 3570 and 8GB of RAM using the homogenization method in FreeFem++ (Hecht, 2012) in 5 minutes, and using the evolutionary algorithm Borg (Hadka & Reed, 2012) in 27 minutes. The solutions achieved by both methods use the same concrete as the building designed by the engineer and they satisfy all code requirements. After the reinforcement calculation, the tally of material quantities shows that the buildings' material consumption is the same, within building construction practices, and any differences come from the need to accommodate to those practices and not from the method.

The seismic evaluation in *OpenSees* (Mazzoni, McKenna, Scott, Fenves, & others, 2006) demonstrates that the optimized building has better seismic performance than the initial building designed by the engineer, which is evidenced by greater overstrength and ductility and smaller story displacements and interstory drifts. Seismic performance results for a second example of a six story irregular building are also presented, showing improvements in the seismic behavior. These results show that the eigenfrequency optimization procedure herein proposed can be used to improve the seismic design of RCF

buildings, and due to its computational performance and ease of implementation, it is a viable option to improve the structural engineers' workflow.

### **Eigenfrequency optimization framework for RCF**

Eigenfrequency optimization (Tsai & Cheng, 2013) describes a problem where one or more structural frequencies are optimized and it has been used for several problems in structural engineering, such as the strength maximization of RC beam column joints (Lee, Yang, & Starossek, 2012), vibration reduction in trusses (Senba et al., 2013). The authors used eigenfrequency optimization with a surrogate membrane model of RCF to optimize column dimensions, obtaining improvements in structure overstrength and ductility between 10% to 30% (Arroyo et al., 2015.).

The application of eigenfrequency optimization for RCF makes sense, because during an earthquake the response of a building is heavily dependent on the smallest natural frequencies of the structure, thus, it is reasonable to optimize these structural properties. The dominating nature of the smallest natural frequencies in the structural response has been used to develop efficient analyses procedures, such as the modal pushover analysis (A. K. Chopra et al., 2004; A. K. Chopra & Goel, 2002); moreover, several standards (ASCE 7-10; ASCE 41-06) acknowledge that the seismic behavior in structures without important torsional irregularities, is controlled by the first natural frequency, allowing the use of the equivalent lateral force procedure to evaluate the seismic demands on structural members.

In addition to optimizing a property that has a direct influence on the seismic performance of the structure, eigenfrequency optimization offers several advantages. First, the objective function is calculated based on the elastic model of the building, resulting in low

computational costs. Second, it provides easiness and flexibility in terms of the problem formulation, as it allows for a discrete statement in terms of classical structural analysis (SA), and it can also be stated in a continuous formulation based on partial differential equations (PDEs).

### *Structural analysis formulation*

The eigenfrequency optimization problem is formulated based on the stiffness ( $\mathbf{K}$ ) and mass matrix ( $\mathbf{M}$ ) of a given MRF, calculated using structural analysis theory:

$$\begin{aligned} & \text{Max} && \omega_n(\mathbf{p}) \\ & \text{subject to} && p_i \geq p_{i,\min} \\ & && V(\mathbf{p}) = V_0 \\ & && [\mathbf{K} - \omega_n^2 \mathbf{M}] \phi_n = 0 \end{aligned} \quad (1)$$

Here,  $\omega_n$  represents the n-th eigenfrequency of the structure,  $\mathbf{p}$  represents the set dimensions of beams and columns. A constraint can be imposed on each property  $p_i$  to be greater than a given value  $p_{i,\min}$ , for instance, beam height can be set to be greater than the code requirements for deflection control. In addition, a volume constraint  $V(\mathbf{p}) = V_0$  is used to set the amount of concrete. This constraint is imposed to the problem to limit the amount of material and indirectly controlling the cost of the structure, since the proposed method does not use the cost as objective function, unlike traditional RCF optimization methods. The third constraint is based on structural dynamics (Anil K. Chopra, 1995) and states that  $\omega_n$  is an eigenfrequency of the structure. The authors recommend setting the values  $p_{i,\min}$  and the value  $V_0$  using the information of a design that fulfills the design code (Figure 2); however, these parameters can also be set arbitrarily. The advantage of the

former is that the optimized dimensions will fulfill the drift limit imposed by the code, as this check is performed elastically and the optimized structure is stiffer in this regime.

Once  $\mathbf{p}$  has been determined, the reinforcement steel is obtained following design codes procedures. In practice, if the authors' recommendation is followed, engineers can modify the models in their preferred structural software and recalculate the reinforcement.

### *Formulation based on PDEs*

Eigenfrequency optimization is formulated using PDEs as follows:

$$\begin{aligned}
 & \text{Max} && \omega_n(\mathbf{p}) \\
 & \text{subject to} && \mathbf{p} \geq \mathbf{p}_{\min} \\
 & && V(\mathbf{p}) = V_0 \\
 & && -\text{div}(Ce(u)) = \omega_n^2 \mathbf{p}u \quad \text{in } \Omega \\
 & && Ce(u)n = 0 \quad \text{on } \Gamma_N \\
 & && u = 0 \quad \text{on } \Gamma_D
 \end{aligned} \tag{2}$$

Here,  $\mathbf{p}$  represents density of material, which should be greater than a function  $\mathbf{p}_{\min}$  in the domain  $\Omega$ , and  $V(\mathbf{p}) = V_0$  means that the total amount of material must be equal to a predefined volume  $V_0$ . The last three constraints mean that  $\omega_n$  is an eigenfrequency of the structure.

As a result of using the material density  $\mathbf{p}$  as the optimization variable, this formulation requires  $\mathbf{p}_{\min}$  and  $\Omega$  to be defined in terms of the lower and upper bounds of the dimensions of the structural members. Once the optimal density of material  $\mathbf{p}_{opt}$  has been obtained, it needs to be expressed as column and beam dimensions. The steel reinforcement to be used is calculated after the optimization, similarly as for the SA

formulation. Further details on how to perform these calculations are provided below in the example section.

### ***Comparison between eigenfrequency formulations***

Both formulations come with their own set of advantages and disadvantages. The main advantage of the SA over the PDE formulation lies on its more straightforward statement of the problem, where the decision variables (*i.e.* column and beam dimensions) are explicitly used. In addition to this, the SA formulation can be applied to RC and steel structures. On the other hand, the discrete character of the physical model used to evaluate the objective function and when used for evolutionary algorithms, requires that the search space be carefully defined to have a good computational performance. A description of the aforementioned evolutionary algorithms can be found in (Simon, 2013) and for its applications in engineering, see (Dasgupta & Michalewicz, 2013).

The main advantage of the PDE formulation is that it lends itself to solution methods that work with a single initial solution that is gradually improved, like the SIMP (Bendsoe & Sigmund, 2003) and the full homogenization (FH) (Tartar, 2009) methods, offering higher computational efficiency and the associated possibility of having a larger search space. The tradeoffs are that the mathematical representation of the decision variables requires a conversion into member dimensions and that their implementation require a good understanding of the finite element method, hence it is more complex than the SA formulation, though not as complex as existing optimization methods that need nonlinear models of the building.

### **Numerical implementation**

#### ***Formulation based on SA***

The SA formulation has a very straightforward implementation when used with numerical software like Matlab. It requires writing a function whose inputs are the columns and beams dimensions and its outputs are the desired eigenfrequencies. This can be done for either two or three dimensional problems. This function only requires knowledge of structural analysis that is taught in most universities. This represents an advantage compared to the PDE formulation, and specially against existing optimization methods that need the development of nonlinear models.

Once the function is written, an appropriate solver must be used to find a solution. In this article, a state of the art multiobjective optimization algorithm, Borg (Hadka & Reed, 2012), is used as a solver. An example function written in Matlab that works with this algorithm for a 15 story building is provided (Arroyo, 2015).

### ***Formulation based on PDE***

The PDE formulation requires solving the problem using the finite element method according to problem (1). In this formulation, an optimization domain  $\Omega$  must be defined based on the maximum desired dimensions for beams and columns. In this domain, the columns and beams dimensions are expressed as a material density  $\rho$ , therefore, the minimum dimensions are expressed as  $\rho_{\min}$ . As previously discussed, this formulation allows to use efficient optimization techniques, however, it is more complex to implement than the SA formulation.

In this article, the full homogenization (FH) method is used as a solution technique for this approach. For the sake of completeness, a description of the mathematical basis of the FH method for a two dimensional case is presented in the following subsection. A more complete description of the method can be found in (Allaire, 2002) and, more

specifically, for eigenfrequency optimization in (Allaire et al., 2001). Being this a first study on eigenfrequency optimization for RCF based on FH, this work focuses only on the first eigenfrequency, and the solution method presented herein accounts for this fact. Readers not interested in the mathematical details can skip this subsection and proceed directly to the algorithm described in 3.2.2. In this work, this algorithm is coded in FreeFem++ (Hecht, 2012).

### *Mathematical model*

Let  $\Omega \subset \mathbb{R}^2$  be a bounded open set in  $\mathbb{R}^2$ . In  $\Omega$  we have two linearly elastic materials with Hooke's laws  $A$  and  $B$ . Let  $\epsilon$  be a positive real number,  $\epsilon \approx 0$ , such that  $A = \epsilon B$ . Therefore,  $A$  is the Hooke law of a very flexible material, and in the limit when  $\epsilon \rightarrow 0$ , it imitates void. Let  $\chi \in L^\infty(\Omega; \{0,1\})$  be a characteristic function of the most rigid material, i.e.,  $\chi(x) = 1$  if material  $B$  is present at  $x$ , and  $\chi(x) = 0$  otherwise.

The heterogeneous Hooke's law in  $\Omega$  is

$$C(x) = (1 - \chi(x))A + \chi(x)B.$$

The heterogeneous density in  $\Omega$  is

$$\rho(x) = (1 - \chi(x))\rho_A + \chi(x)\rho_B,$$

where  $\rho_A, \rho_B > 0$  are the densities of the materials.

The boundary  $\partial\Omega$  is divided in two disjoint parts  $\Gamma_D$  and  $\Gamma_N$  supporting respectively Dirichlet boundary condition (zero displacement) and Neumann boundary condition (zero traction). The vibration frequencies  $\omega$  of the heterogeneous domain  $\Omega$ , filled by  $A$  and  $B$ , are the square roots of the eigenvalues of the following problem:

$$\begin{aligned}
-\operatorname{div}(Ce(u)) &= \omega^2 \rho u && \text{in } \Omega \\
Ce(u)n &= 0 && \text{on } \Gamma_N \\
u &= 0 && \text{on } \Gamma_D
\end{aligned} \tag{3}$$

where  $u \in H^1(\Omega)^2$  is the displacement field, and  $e(u) = \frac{1}{2}(\nabla u + \nabla^T u)$  is the infinitesimal strain tensor. As is well known, problem (3) admits a countable family of positive eigenvalues.

$$0 < \omega_1^2 \leq \omega_2^2 \leq \dots \leq \omega_k^2 \rightarrow +\infty$$

In this work we want to maximize the first eigenvalue, which is given by the following formula

$$\omega_1^2 = \min_{u \in \mathcal{H}} \frac{\int_{\Omega} Ce(u) : e(u) dx}{\int_{\Omega} \rho |u|^2 dx},$$

where  $\mathcal{H} = \{u \in H^1(\Omega)^2 \mid u = 0 \text{ on } \Gamma_D\}$ .

We want to find the best arrangement of  $A$  and  $B$  in  $\Omega$  that maximizes  $\omega_1^2$ . If  $\rho_A = \rho_B$  and there is no volume constraint on the amount being used of each material, the problem has a trivial solution, that is to fill  $\Omega$  only with the most rigid material, namely, that with elasticity tensor  $B$ . Therefore, we add a constraint on the volume being used of that material, say  $V_0$ , and introduce a Lagrange multiplier  $l \in \mathbb{R}$  for such constraint. Then the optimization problem becomes

$$\sup_{\chi \in L^\infty(\Omega; \{0,1\})} \left\{ \omega_1^2 + l \left( \int_{\Omega} \chi(x) dx - V_0 \right) \right\} \tag{4}$$

We want to find a sequence of characteristic functions  $\chi_n$  that maximizes (4). However, it is known that this problem admits no optimal solution. Hence, one needs to enlarge the class of admissible designs by allowing fine mixtures of the two materials on a scale which is much smaller than the mesh used for the actual computation. However, the set of all Hooke's laws that can be created is not known. Fortunately in the case of eigenfrequency optimization, the optimal microstructure is known to be among the subset of sequential laminates (Allaire, 2002). This process of enlarging the set of admissible designs in order to get a well-posed problem is called relaxation. The derivation of the relaxed formulation was done by the pioneering work of Murat and Tartar (Murat & Tartar, 1997), which is briefly sketched for the sake of completeness.

Let  $\chi_n \in L^\infty(\Omega; \{0,1\})$  be a maximizing sequence for (4). We want to pass to the limit in (4) and compute its maximal value. The sequence  $\chi_n$  is bounded in  $L^\infty(\Omega; \{0,1\})$ , therefore one can extract a subsequence, still denoted by  $\chi_n$ , such that it converges in  $L^\infty(\Omega)$  weak- $\star$  to  $\theta$ . The limit  $\theta$  is, in general, a density, i.e., it belongs to  $L^\infty(\Omega; [0,1])$ . According to the theory of H-convergence (Murat & Tartar, 1997), a subsequence of  $C_n = (1 - \chi_n(x))A + \chi_n(x)B$  H-converges to a homogenized Hooke's law  $C^*$  as  $n \rightarrow \infty$ . As a consequence the eigenvalue  $(\omega_1^n)^2$  and its corresponding normalized eigenfunction  $u_1^n$ , solutions to

$$\begin{aligned} -\operatorname{div}(C_n e(u)) &= (\omega_1^n)^2 \rho_n u && \text{in } \Omega \\ C_n e(u)n &= 0 && \text{on } \Gamma_N \\ u &= 0 && \text{on } \Gamma_D \end{aligned} \tag{5}$$

satisfy  $\lim_{n \rightarrow \infty} \omega_1^n = \omega_1$ , and the sequence of eigenfunctions  $u_1^n$  converges weakly in  $H^1(\Omega)^2$

and strongly in  $L^2(\Omega)^2$  to a limit eigenfunction  $u_1$  such that

$$\begin{aligned} -\operatorname{div}(C^* e(u_1)) &= \omega_1^2 \bar{\rho} u_1 && \text{in } \Omega \\ C^* e(u_1) n &= 0 && \text{on } \Gamma_N \\ u_1 &= 0 && \text{on } \Gamma_D \end{aligned} \quad (6)$$

with  $\bar{\rho}(x)$ , the weak limit of the sequence  $\rho_n$ , *i.e.*,

$$\bar{\rho}(x) = (1 - \theta(x))\rho_A + \theta(x)\rho_B.$$

In turn  $C^*$  belongs to  $\mathcal{G}_\theta$ , defined as

$$\mathcal{G}_\theta = \left\{ \text{H-limits of } C_n = (1 - \chi_n)A + \chi_n B \mid \chi_n \rightharpoonup \theta \right\}$$

Thanks to the work of Murat and Tartar (Murat & Tartar, 1997), we can find the optimal Hooke's law  $C^*$  in the subset  $L_\theta$  of sequential laminates obtained by laminating  $B$  around a core of  $A$  in proportion  $\theta$  and  $1 - \theta$ , respectively.

Thus, we define a relaxed objective functional by

$$\max_{\theta \in L^\infty(\Omega; [0,1])} \max_{C^* \in L_\theta} \left\{ \omega_1^2(\theta, C^*) + l \left( \int_\Omega \theta(x) dx - V_0 \right) \right\} \quad (7)$$

The new material is built by laminating, in a very fine scale, a proportion  $\theta_1$  of  $B$  with a proportion  $1 - \theta_1$  of  $A$  in one direction, say  $e^1$ , and then the resultant tensor  $A^1$  is laminated again, at a scale coarser than the previous one but still finer than the macroscale, in a direction  $e^2$ , and in proportion  $\theta_2$  with one of the initial materials, say  $A$ , and obtain  $C^*$ , the Hooke's law of a rank 2 laminate. Figure 3 illustrates this procedure.

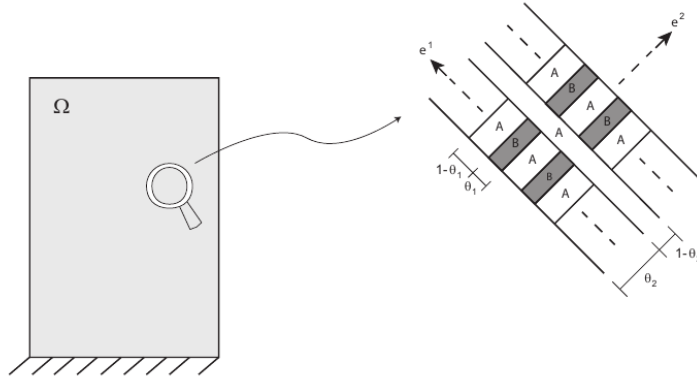


**Figure 3.** Homogenized rank 2 laminated material

The effective Hooke's law  $C^*$  is obtained from equation (2.68) in (Allaire et al., 2001)

$$C^* = B + (1 - \theta) \left( (A - B)^{-1} + \theta (m_1 f_B(e^1) + m_2 f_B(e^2)) \right)^{-1} \quad (8)$$

Where  $\theta = \theta_1 \theta_2$  is the total proportion of material  $B$ , the unit vectors  $e^1, e^2$  are the lamination directions, the real numbers  $0 \leq m_1, m_2 \leq 1$  such that  $m_1 + m_2 = 1$ , are the lamination parameters, and  $f_B(e^i)$  is a positive non-definite fourth-order tensor defined for any symmetric matrix  $\xi$  by the following quadratic form

$$f_B(e^i) \xi : \xi = \frac{1}{\mu} |\xi e^i|^2 - K (\xi e^i \cdot e^i)^2,$$

where  $K = \frac{\mu + \lambda}{\mu(2\mu + \lambda)}$  and  $\mu, \lambda$  are the Lamé parameters of material  $B$ .

By means of theorem (4.1.46) in (Allaire, 2002), in the case when the first eigenvalue is simple we can find the globally optimal lamination parameters and lamination directions in order to maximize our objective function.

If the eigenvalues of the stress tensor  $\sigma = C^* e(u_1)$  are denoted  $\sigma_1$  and  $\sigma_2$ , they are given by

$$\sigma_1 = \frac{1}{2} \left( \sigma_{11} + \sigma_{22} + \sqrt{(\sigma_{11} - \sigma_{22})^2 + 4\sigma_{12}^2} \right),$$

$$\sigma_2 = \frac{1}{2} \left( \sigma_{11} + \sigma_{22} - \sqrt{(\sigma_{11} - \sigma_{22})^2 + 4\sigma_{12}^2} \right)$$

The lamination parameters are

$$m_1 = \frac{|\sigma_2|}{|\sigma_1| + |\sigma_2|} \quad \text{and} \quad m_2 = \frac{|\sigma_1|}{|\sigma_1| + |\sigma_2|},$$

therefore the intermediate proportions are:

$$\theta_1 = \frac{|\sigma_1| + \theta |\sigma_2|}{|\sigma_1| + |\sigma_2|} \quad \theta_2 = \frac{\theta (|\sigma_1| + |\sigma_2|)}{|\sigma_1| + \theta |\sigma_2|}.$$

The lamination directions are chosen as the eigenvectors of  $\sigma$ . Then

$$e^1 = \begin{pmatrix} \frac{\sigma_{12}}{\sqrt{\sigma_{12}^2 + (\sigma_1 - \sigma_{11})^2 + \delta^2}} \\ \frac{\sigma_1 - \sigma_{11}}{\sqrt{\sigma_{12}^2 + (\sigma_1 - \sigma_{11})^2 + \delta^2}} \end{pmatrix} \quad e^2 = \begin{pmatrix} e_y^1 \\ -e_x^1 \end{pmatrix},$$

where  $\delta = \varepsilon 10^{-6}$  is introduced to avoid numerical problems.

The optimal density of rigid material is chosen by:

$$\theta = \max \left\{ \theta_{min}, \min \left\{ 1, \sqrt{\frac{g^*(\sigma)}{l \int_{\Omega} \bar{\rho} |u|^2}} \right\} \right\} \quad (9)$$

where:

- $\theta_{min}$  = lower limit for material density.  
 $g^*(\sigma) = \frac{2\mu + \lambda}{4\mu(\mu + \lambda)} (|\sigma_1| + |\sigma_2|)^2$   
 $l$  = lagrange multiplier for the volume constraint of the rigid material  
 $\bar{\rho} = \theta_p B + (1 - \theta_p) A$   
 $\theta_p$  = optimal density of rigid material obtained in the previous iteration  
 $u$  = first eigenfunction obtained in the previous iteration.

### *Computational algorithm*

The previous subsection shows the formulas necessary to implement a computational algorithm. The algorithm is constructed as follows:

- (1). Initialization of the design parameters  $(\theta_0, C_0^*)$ .  $\theta_0$  can be set to  $V_0$ .
- (2). Iteration until convergence, for  $k \geq 0$ :
  - a) Compute the first eigenfunction  $u_1^k$  with the previous design parameters  $(\theta_k, C_k^*)$ , and calculate the stress field  $\sigma_k$ .
  - b) Update the design variables  $(\theta_{k+1}, C_{k+1}^*)$  by using the stress  $\sigma_k$  in the explicit optimality formulas (8) and (9). Convergence can be monitored using norm of  $u_1^k - u_1^{k-1}$ . Also, a limit can be imposed to the maximum number of iterations.

To optimize 3D buildings, this algorithm is applied to frames in each building direction X and Y independently, because it is expected that for structures without important irregularities, the first mode in each direction is not significantly affected by the first mode in the perpendicular direction.

### **Example application: optimization of a 10 story building**

In order to demonstrate that the proposed method can produce better designs than the current engineering practice, we consider a 10 story building whose plan view is shown in Figure 4. The building has four moment resisting frames in the X direction and seven in the Y direction, it is completely regular, its total height is 30 m and has a 12 cm slab. Concrete and reinforcement steel are considered to satisfy the standard strength requirements 4000 psi and A615Gr60. Following the procedure depicted in Figure 1, and since the proposed method is aimed to be used within engineering practice, a preliminary step is to design this building for residential purposes, according to the ASCE 7 and the ACI 318 for the state of California (37.38°N, 121.88°W) using ETABS v13.1.2 (Habibullah, 1997), which will be used to demonstrate that the proposed method (Figure 2) produces buildings with superior seismic performance than those designed by traditional engineering practice (Figure 1). The design results are columns with a cross section of 55cm x 75cm and a reinforcement ratio of 1.18%, with beam sections of 35cm x 40cm with a top and bottom reinforcement ratios of 0.93% and 0.70%. These column and beam dimensions are used as the base for the optimization algorithm, as illustrated in Figure 2.

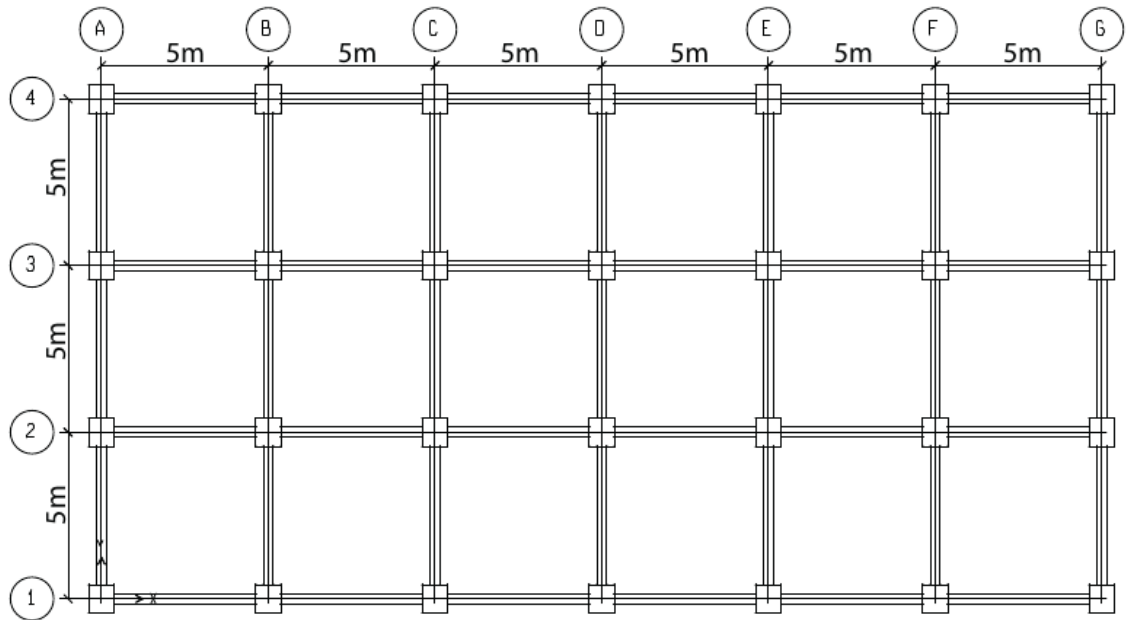


**Figure 4.** The 10 story building to be optimized has 5m spans in both directions, with four frames in the X direction and seven in the Y direction.

In this example, the optimization is performed using two dimensional frames, one representative of the X direction and the other of the Y direction. The minimum and maximum dimensions for the optimization algorithm are defined based on the design results. Columns sections will be allowed to vary between 52.5cmx60cm to 80cmx85cm. For beams, the height will vary between 35cm to 50cm and the width will be fixed in the design value, since this property has a smaller influence in seismic performance than the other optimization variables.

The optimized building is constrained to have the same volume as the designed building, allowing to elaborate a direct comparison since both buildings will have the same costs of concrete. Although the reinforcing steel is not constrained, it is expected that the optimized building will use a similar amount, given that it will have the same volume of concrete. Comparisons with other optimization methods are not presented here because they do not accomplish the goal of being implementation-friendly for practitioners;

however, we acknowledge that once they are implemented, and given enough computational resources, they might provide more effective solutions, since they optimize the reinforcing steel.

### *Numerical results*

The proposed building is optimized according to the SA and the PDE formulations presented in this article. For the SA formulation, this was accomplished following the process described in section 3.1, writing a Matlab function and using it as input for the Borg MOEA (Hadka & Reed, 2012), which is a state of the art multiobjective optimization algorithm that combines epsilon-dominance, randomized restarts and autoadaptive multioperator recombination. As previously discussed, this is a very straightforward implementation that only demands knowledge of structural analysis. The PDE formulation is written in FreeFem++, but it requires a more detailed discussion, which is presented in the following paragraphs.

The first step is to define the optimization domain  $\Omega$ . We begin by establishing a centerline consistent with the elevation view of a typical moment resisting frame in this direction, i.e., those in axis 1 to 4. After that, we set the maximum dimensions for columns and beams, which are used to define the domain borders. In this case, 80cm is chosen for the maximum column dimension in the X direction, and 50cm for the beam height. An easy way to visualize  $\Omega$  is as an elevation view of the building formwork. The second step is to define the value of  $V_0$ . Taking into account that  $\Omega$  is a bidimensional domain,  $V_0$  is defined as a fraction of the area of  $\Omega$ . For this example, we calculate  $V_0$  as the area

occupied by the corresponding view of the elements in the baseline building, which corresponds to a 76% of  $\Omega$ .

The third step involves defining the minimum density of material  $\theta_{min}$  based on the minimum column and beam dimensions.  $\theta_{min}$  is calculated as the ratio between the minimum and maximum dimensions, which gives a uniform value  $\theta_{min} = 0.65$  for this example. We did not impose a constraint for the relative stiffness between stories, since the optimal solutions found are always with decreasing stiffness in height, therefore, avoiding having a lower story being softer than a higher one.

To perform the optimization in the Y direction we follow the same steps. First we calculate  $V_0$  as the 85% of the domain and, finally, based on the minimum dimension for columns and beams we obtain  $\theta_{min} = 0.7$ . In this formulation, the optimized dimensions are obtained after converting the material density into column and beam dimensions. Hence, the mass and stiffness are strictly positive at each point in  $\Omega$ , making the mass and stiffness matrices to be positive definite.

The resulting dimensions from both formulations are rounded to multiples of 5cm to accommodate with construction practices, providing the same final result for columns and beams dimensions, shown in Table 1.

**Table 1.** Dimensions for 10-story buildings (all dimensions are given in cm)

	OPTIMIZED BUILDING				TRADITIONAL BUILDING	
	COLUMNS		BEAMS		COLUMNS	BEAMS
Story	Inner	Outer	X Dir	Y Dir	Both	Both
10	50x60	50x60	35x35	35x35	55x75	35x40
9	55x65	55x65	35x35	35x35	55x75	35x40
8	55x70	55x70	35x40	35x40	55x75	35x40

7	60x70	55x70	35x40	35x40	55x75	35x40
6	60x75	55x75	35x40	35x40	55x75	35x40
5	60x75	55x75	35x40	35x40	55x75	35x40
4	65x80	60x80	35x45	35x45	55x75	35x40
3	70x80	65x80	35x45	35x50	55x75	35x40
2	70x80	70x80	35x45	35x50	55x75	35x40
1	70x85	70x80	35x45	35x45	55x75	35x40

Based on the rounded dimensions calculated for both directions and following the procedure of Figure 2, the reinforcing steel for the optimized building is calculated in ETABS v13.1.2. The results indicate that the elements of the optimized building use the same reinforcement ratios as their traditional counterparts. The calculation of materials consumption shows that the baseline building uses 1201.5 m<sup>3</sup> of concrete and 68758 kg of longitudinal reinforcing steel. The optimized building respectively uses 1231.94 m<sup>3</sup> and 69217 kg, values that are 2.5% and 0.67% higher than the baseline building, but they are within the error margin of construction practices and are the result of the roundup process required to accommodate to them. The buildings' total weight is 2770.33 ton for the traditional building and 2840.38 ton for the optimized one.

A close examination of the optimization results shows that the dimensions of structural members in the bottom third of the building are increased compared to the baseline building, with columns having about 25% greater cross sectional area and beams being 5 cm taller. These dimensions are gradually reduced with the building height up to the top floor, where columns are approximately 25% smaller than in the baseline building, and beam height is decreased by 5cm.

### *Computational efficiency*

An important remark about the proposed optimization algorithm is its numerical efficiency. Running in a desktop with an Intel Core i5 4460 at 3.2GHz and 8GB of RAM, it takes 5 minutes to run the optimization for both directions with the homogenization method and 27 minutes using Borg (with an  $\varepsilon = 0.01$  for the building frequency), times that are fast enough for engineering practice. Although not presented here, the proposed method was also used to optimize a 5 story and a 15 story buildings, with computational times of 3 and 8 minutes for the homogenization method and 13 and 40 minutes for evolutionary algorithms (Borg). The Matlab code of the objective function for the 15 story building can be freely downloaded (<http://bit.ly/23am22r>) and used with any genetic algorithm solver. As mentioned before, the easy implementation and computational efficiency of the method come with a tradeoff on its effectiveness, since the reinforcing steel is calculated by the engineer following the design codes.

These computational times compare favorably to other methods reported in literature, where the computational time for optimizing in two dimensions may range, depending on the seismic evaluation method, between 12 hours and 1.5 weeks for a bidimensional 3 story building on a Core 2 Duo (Zacharenaki et al., 2013). The reason for those long computational times is that this optimization method uses nonlinear models to evaluate the seismic performance of the building; what does not occur in the proposed method that takes advantage of the influence of the eigenfrequency in the structural response and optimizes directly this property.

To sum up, the proposed method brings a combination of computational performance and easiness of implementation, providing a viable practical alternative for the design of RCF building that is not compromised by its tradeoff on effectiveness.

### ***Structural performance of optimized building***

As previously stated, the proposed optimization approach works with the hypothesis that optimizing the eigenfrequency brings benefits to the structural performance, and although previous research (Arroyo et al., 2015.; Lee et al., 2012; Senba et al., 2013) supports this idea, in this section we proceed to demonstrate that this hypothesis holds by comparing the seismic performance of the optimized building with the baseline.

Since the method ensures better seismic performance only in the elastic range, in order to have a comprehensive vision of the structural behavior, *OpenSees* (Mazzoni et al., 2006) is used to perform a 2D Pushover Analysis for the typical X and Y frames of the buildings, i.e. frames corresponding to elevations designated by B and 2 in figure 4. Beams and columns are modeled using fiber elements with rebar, confined and unconfined concrete, with 5 integration points. To avoid localization issues, the Constant Fracture Energy Criterion (Coleman & Spacone, 2001) is used with  $G_f^c = 180N/mm$  and with concrete properties  $f_c = 28MPa$ ,  $f_{cc} = 33.6MPa$ ,  $e_c = 0.0019$ , in the modified Kent-Scott-Park model. Reinforcing steel is modeled using a bilinear relation, with  $E_s = 210GPa$ ,  $f_y = 420MPa$ ,  $f_u = 630MPa$ , and an ultimate strain  $e_u = 0.14$ . The foundation is modeled as rigid, and gravity loads for the model are calculated based on the expected loads and using the combination  $1.05D+0.25L$ . P-Delta effects are included with gravity loads calculated based on the tributary area of the beams. Rayleigh damping is applied to the structure with 3% damping in the first and third modes. Masses were

assigned in nodes based on the tributary areas and the elements self-mass. Displacement control is used in the Pushover using 0.5mm steps.

Based on the Pushover results, ductility ( $\mu$ ) and overstrength ( $\Omega_0$ ) are calculated according to the FEMA P695 (FEMA 2009). We also perform a Nonlinear Time History Analysis for the two buildings using both components of the 22 ground motion suite of the FEMA P695 (table 2), normalized and anchored according to chapter A-8 in FEMA P695 (FEMA 2009) such that the median of the spectral acceleration set matches the spectral acceleration of the  $D_{max}$  spectrum (see Figure A-1 in FEMA 2009) at the fundamental period of the buildings.

**Table 2.** Summary of earthquake information. Taken from FEMA P-695

ID	M	Year	Name
1	6.7	1994	Northridge
2	6.7	1994	Northridge
3	7.1	1999	Duzce, Turkey
4	7.1	1999	Hector Mine
5	6.5	1979	Imperial Valley, Delta
6	6.5	1979	Imperial Valley, El Centro
7	6.9	1995	Kobe, Japan, Nishi-Akashi
8	6.9	1995	Kobe, Japan, Shin-Osaka
9	7.5	1999	Kocaeli, Turkey, Duzce
10	7.5	1999	Kocaeli, Turkey, Arcelik
11	7.3	1992	Landers
12	7.3	1992	Landers
13	6.9	1989	Loma Prieta, Capitola
14	6.9	1989	Loma Prieta, Gilroy
15	7.4	1990	Manjil, Iran
16	6.5	1987	Superstition Hills, El Centro
17	6.5	1987	Superstition Hills, Poe Road
18	7	1992	Cape Mendocino
19	7.6	1999	Chi-Chi, Taiwan, CHY101
20	7.6	1999	Chi-Chi, Taiwan, TCU045
21	6.6	1971	San Fernando
22	6.5	1976	Friuli, Italy

After this process, the suite was run at three different scale factors, 1.0, 2.2 and 3.5 and the displacement and interstory drift were recorded for each story of the building. For each scale factor we calculate the median of the maximum values taken from each record of the

GM suite, for each story of the building and each demand parameter, i.e., displacement and drift.

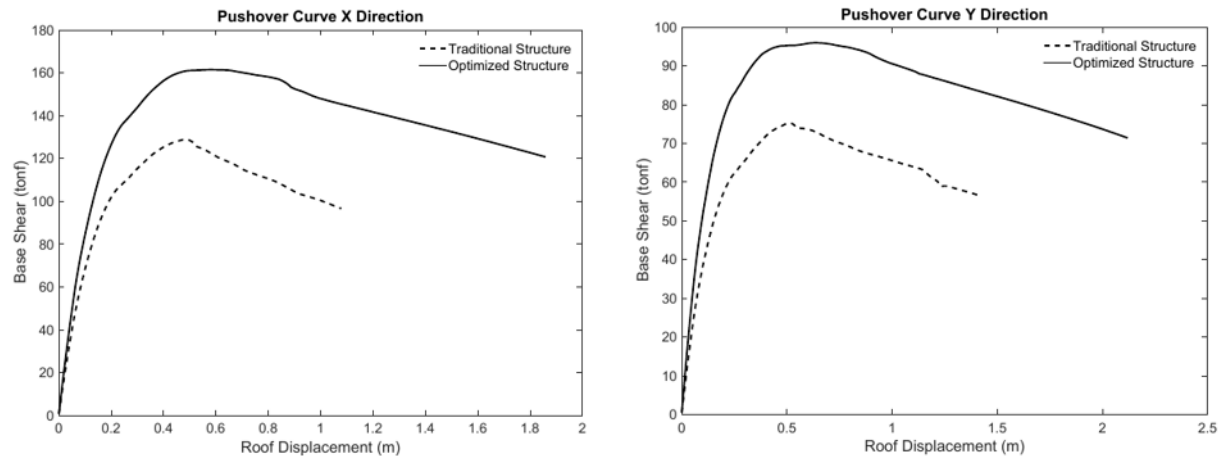


**Figure 5.** The pushover results show that the optimized structure supports a larger base shear and has a smaller post peak slope than the original structure.

Pushover Results for the X and Y directions are shown in figure 5 and they show that the optimized building performs significantly better than the baseline in several aspects:

- The slope in the elastic range is steeper for the optimized building, which means that it is more rigid than the traditional. This comes as a direct consequence of the optimization, as its goal is maximizing the first eigenvalue of the building.
- The maximum base shear  $V_{max}$  supported by the optimized building is higher than the one from the baseline. This could have an important practical implication, as it suggests that the optimized building could withstand earthquakes with higher accelerations before starting to deteriorate.
- The optimized building has a better post-peak performance than the baseline.

This analysis is further confirmed by calculating the overstrength and ductility as shown in Table 2, where it can be observed that the optimized building has an overstrength that is 23.8% and 27.9% higher than the baseline building for the X and Y direction, respectively. On the other hand, the ductility factor sees a notable improvement, as it is 81.9% greater in the X direction and 98.2% in the Y direction.

**Table 3. Overstrenght and Ductility for the 10 story buildings**

Structure	Pushover X		Pushover Y	
	$\Omega_0$	$\mu$	$\Omega_0$	$\mu$
Optimized	4.00	11.50	3.58	14.07
Traditional	3.23	6.33	2.80	7.1

The performance improvement shown in the Pushover is verified using Nonlinear Time History Analysis. We start by looking at the displacement response for a scale factor of 1.0 in figure 6, where it can be appreciated that the median displacement of the optimized building is smaller than the baseline, in a range that varies from 45% for the first floor in the X direction, down to 10% for the tenth floor in the Y direction.

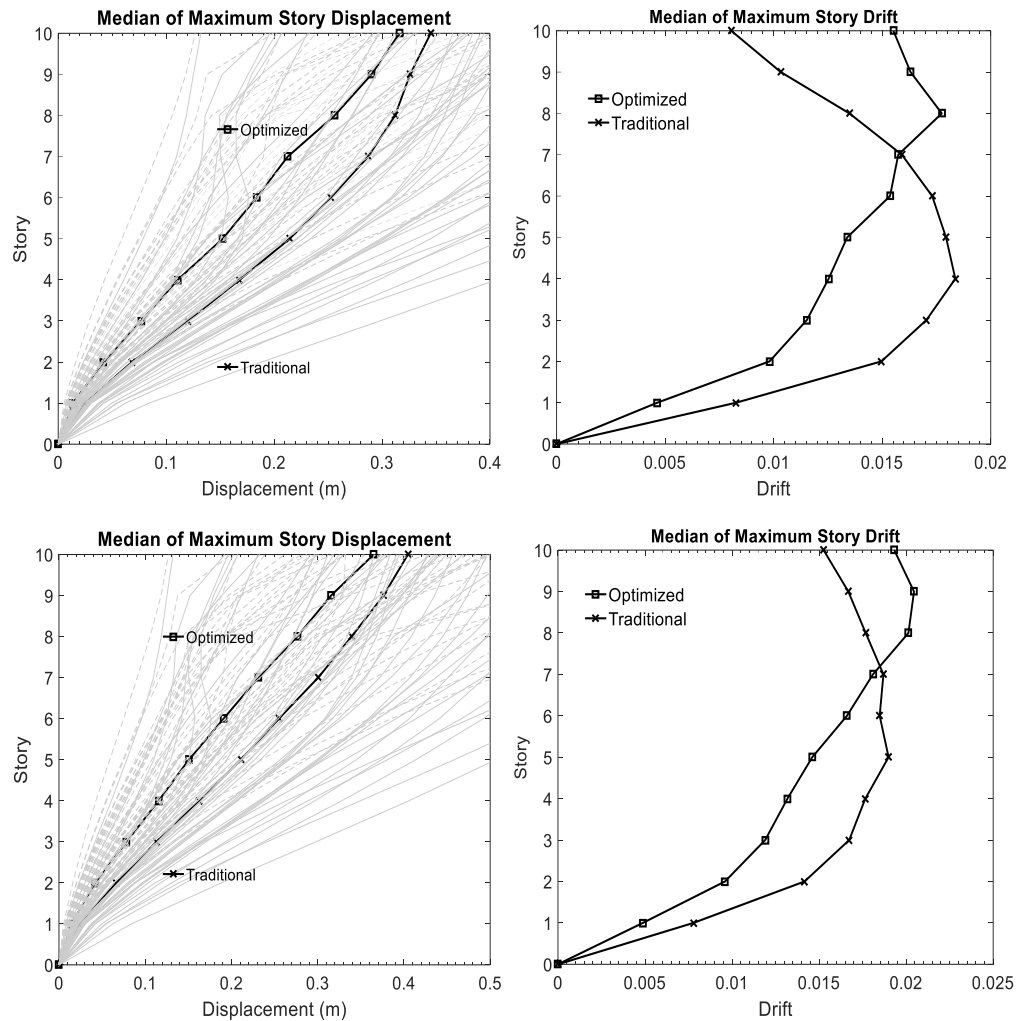


**Figure 6.** The displacement and drift responses for a scale factor of 1.0 are smaller for the optimized building, especially in the bottom stories. Top: X direction. Bottom: Y direction. Dotted and continuous gray lines represent individual ground motion results for the optimized and traditional buildings, respectively.

The behavior of the structures is further clarified by examining the drift responses in figure 6, where can be seen that for both directions, the optimized building has a significant reduction in the interstory drift for the first five stories, with moderate improvements in the sixth and seventh; nonetheless, this comes at the expense of having a bigger interstory drift in the top three stories. In practice, this means that there is a shift in

the expected location of the damage; the optimized building is expected to have more damage in the top stories, as opposed to the baseline building where it is expected to take place in the intermediate stories.

When we increase the scale factor to 2.2 we start to see some differences between the performance in the X and the Y directions, as shown in figure 7. In the X direction the behavior is similar to the previous one for a scale factor of 1.0, with the optimized building having smaller displacement along the building, and a notable reduction in the interstory drift for the first half of the building that comes at the expense of having larger drifts in the upper stories. On the other hand, the performance in the Y direction shows notable differences in displacements, especially in the bottom stories, where we observe reductions that go up to 60% for the first story. Similarly, we see that there are significant reductions for the optimized building in the interstory drift for the first seven stories, and even though the interstory drift in stories 8 to 10 is larger than in the baseline, these differences are significantly smaller than the ones seen downwards in the building.

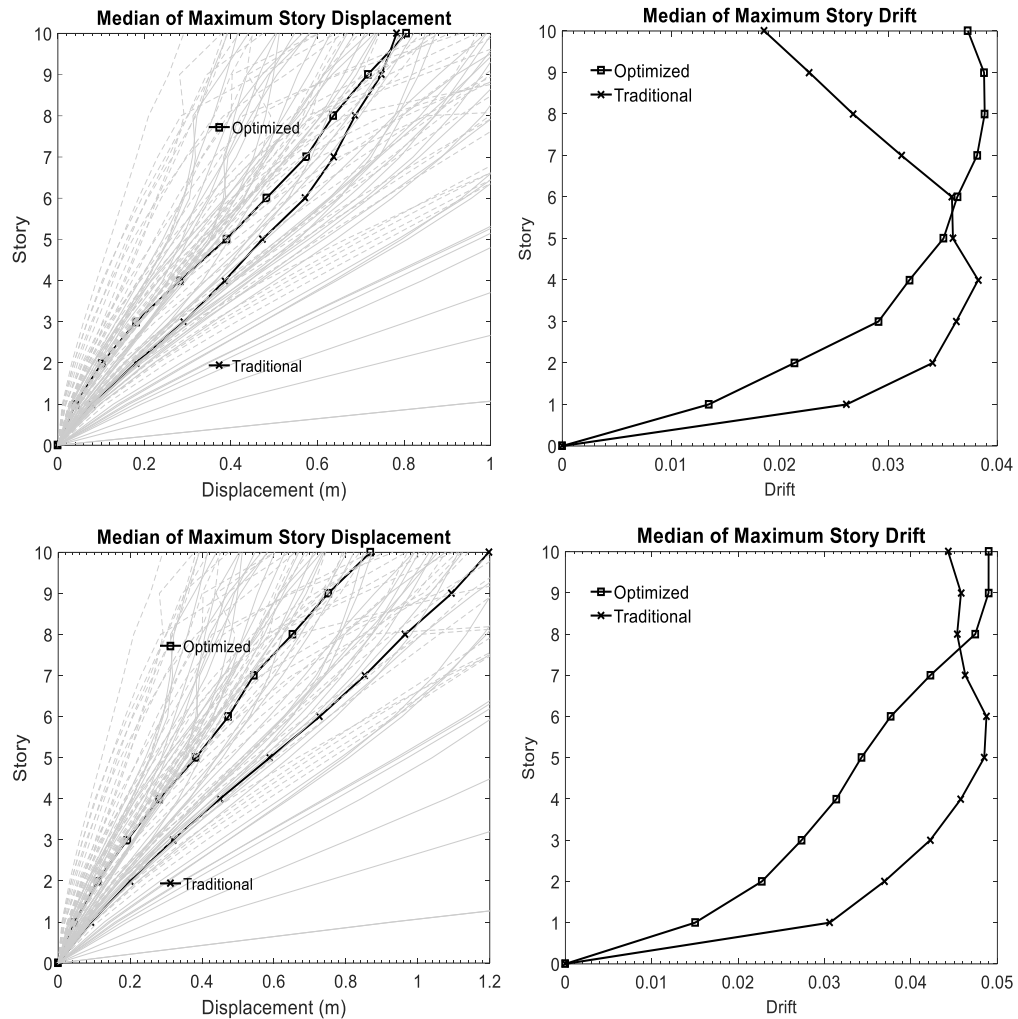


**Figure 7.** The displacement and drift responses for a scale factor of 2.2 are smaller for the optimized building, especially in the bottom stories. Top: X direction. Bottom: Y direction. Dotted and continuous gray lines represent individual ground motion results for the optimized and traditional buildings, respectively.

It is important to note that the observed changes in the structural performance are worthy tradeoffs for a building, as it is preferable to have damage in upper floors than have it in the bottom of the building, as the latter can compromise the structural stability and it is more prone to cause undesirable consequences.

Finally, when we increase the scale factor to 3.5 in figure 8, the differences between the two buildings become even clearer, especially in the bottom stories. For the X

direction, we observe in figure 8 that there are notorious differences in displacements for all stories, all of them favoring the performance of the optimized building. It can be appreciated that the first four stories in the baseline structure have interstory drifts close to 10%; in the meantime, in the optimized building, all these stories have interstory drifts smaller than 6%, with the first floor having almost a third of its baseline counterpart.

The displacements in the Y direction of the optimized building are greatly reduced compared to its baseline. For instance, the displacement of the first floor is more than ten times smaller for the optimized building than for the baseline building; what is more, if we look at the roof displacement, we observe that for the baseline building it is greater than 3.0m, while for the optimized building, it is close to 1.5m.

The difference in structural performance for the Y direction is further confirmed by examination of the drifts in the right side of figure 8, where it is seen that for each floor, the interstory drift of the optimized structure is smaller than its baseline counterpart. In addition to this, we observe that the first five floors in the traditional building have an interstory drift around 20%, meanwhile in the optimized building, this value goes from 3.5% in the first floor, up to 5.5% in the fifth.

To sum up the results, the Pushover results show that when compared to the baseline building, the optimized building has greater overstrength and a significantly increased ductility. As expected from the Pushover result, the seismic performance during an earthquake is better in the optimized structure, what is further proved by the NLTHA, whose results show that the optimum structure is more capable to withstand the demand caused by the selected ground motion suite for different scale factors.

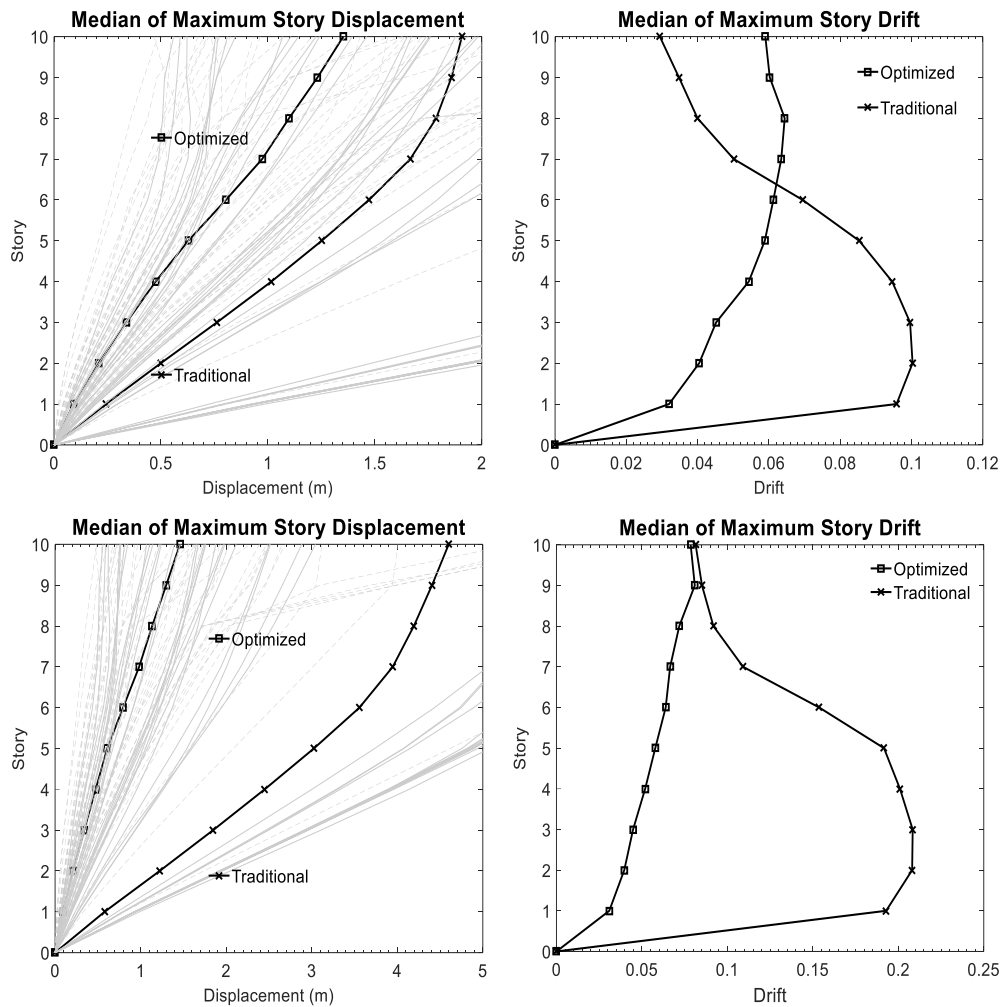


**Figure 8.** The displacement and drift responses for a scale factor of 3.5 are significantly smaller for the optimized building, especially in the bottom stories. Top: X direction. Bottom: Y direction. Dotted and continuous gray lines represent individual ground motion results for the optimized and traditional buildings, respectively.

### *Application for an irregular building*

To further illustrate the effectiveness of the proposed optimization method, an irregular 6 story building is considered, whose plan view is shown in Figure 9a. The building is designed for a seismic zone with  $S_a = 0.55g$ . The optimization is carried on independently for each frame in each direction of the building, and the reinforcement for the optimized dimensions is determined using a three dimensional model in ETABS v13.2.1. No further details are given to keep the length of the article at a reasonable level.

The traditional and optimized buildings are analyzed using three dimensional models in *OpenSees* with the previously described material models and parameters, and the Pushover results for the X and Y direction (Figure 9b and 9c) show that there are improvements in the building performance for both directions.

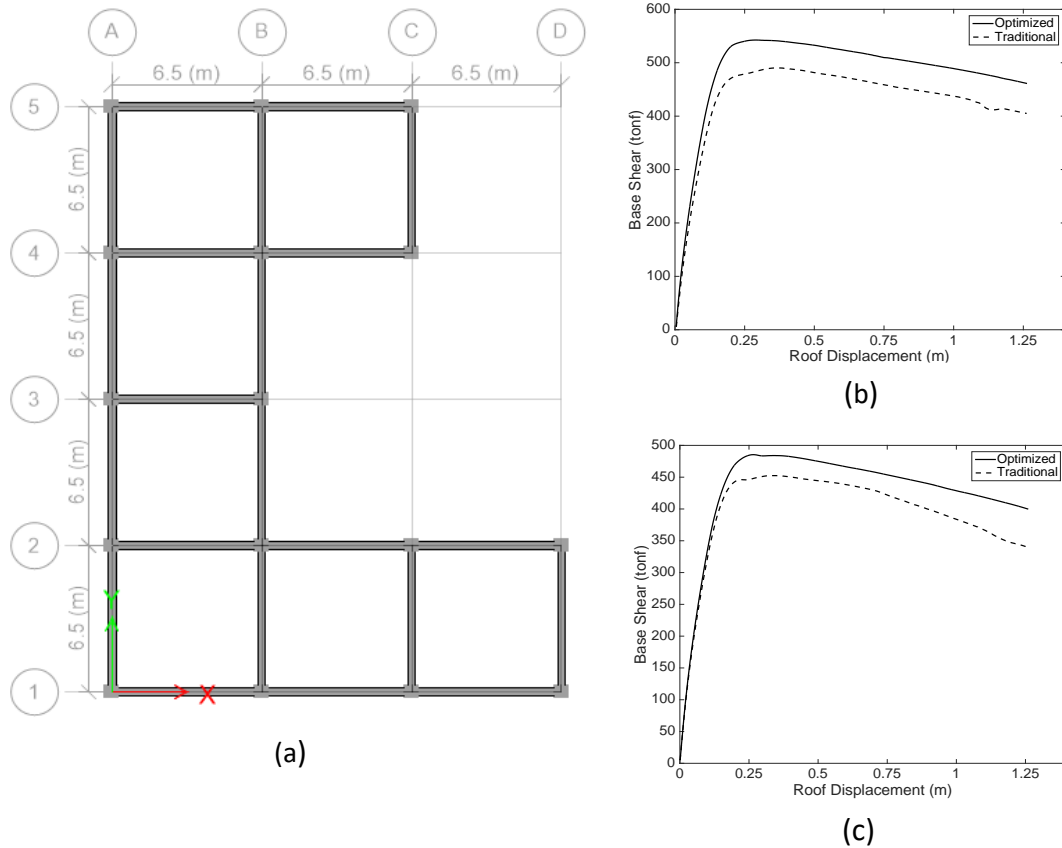


**Figure 9.** The proposed method is used to optimize a six story irregular building (a), with pushovers in the X direction (b) and Y direction (c) showing improvements in the overstrength and ductility.

Due to its computational cost, we did not evaluate the seismic performance of this building using incremental dynamic analysis, but given the improvement in the pushover results, we expect the building to show similar improvements in the nonlinear dynamic analyses. This example shows that the method can be used for irregular buildings,

for which is possible to optimize the seismic performance by means of the bidimensional optimization of their individual frames.

### **Conclusions and perspectives**

The results from this research allow drawing several conclusions:

The proposed optimization method is capable of optimizing the seismic performance RCF within minutes, with the resulting building consuming the same amounts of concrete and reinforcing steel as the initial design proposed by engineers. The seismic performance results obtained in OpenSees for the 10 story building considered herein show improvements in several aspects. The pushover analyses indicate that the optimized building has 23.9% greater overstrength and 81.7% greater ductility. The results of incremental dynamic analyses show that the story drifts and displacements are reduced in the bottom stories. These reductions became larger as the scale factor was increased, suggesting that buildings optimized using the proposed method may have lower collapse fragility. The pushover results for a 6 story irregular building demonstrate that the method can be used in general for RCF. Besides the benefits of being computationally fast and effective, the provided Matlab code demonstrates that the proposed method can be easily implemented; with the potential to improve the structural engineers' workflow.

In terms of the solution techniques, genetic algorithms and the homogenization method are appropriate within the proposed method, however they differ in terms of the computational efficiency and the simplicity of its formulation. For the example considered, the homogenization method solved the problem in 5 minutes, less than one fifth of the computational time using genetic algorithms. On the other hand, the problem formulation

using genetic algorithms is straightforward and only requires knowledge of structural analysis, while the homogenization method requires a good understanding of the finite elements method. For a quick implementation, the genetic algorithm implementation is preferable; however, the computational performance of the homogenization method may offset its more complex formulation when the reductions in computational time for several models are aggregated.

All things considered, the proposed method fulfills the objectives of being computationally efficient, easy to implement and effective; benefits that make it a solid candidate to be used within the design of RCF buildings. In addition, the results show that eigenfrequency optimization is a suitable framework for the seismic optimization of RCF.

Future research on this topic can be pursued in different areas:

About eigenfrequency optimization, a continuation of this work would be investigating if it can be used for steel MRF. In addition, it would be worth investigating the application of the proposed problem formulation in three dimensions. Moreover, it is also interesting to evaluate if the problem formulation can be extended to involve more design variables without compromising the simplicity in the formulation and the computational performance. In particular, including steel reinforcement and nonlinear behavior in the problem would be a good addition for the procedure.

From an optimization perspective, this is an interesting problem because the objective function is not expensive and the search space can become very large, hence, it is worth investigating the feasibility and the computational performance of other solution techniques, such as simulated annealing or particle swarm.

From an earthquake engineering perspective, it would be interesting to evaluate how the response of the optimized buildings is sensitive to the frequency content of seismic records, and developing a software that uses the proposed method and integrates with existing structural engineering packages, giving engineers a powerful tool to improve current design practice.

### Acknowledgements

The corresponding author wishes to acknowledge the Chilean Government and CONICYT for granting his Ph.D. scholarship in the framework of the program Doctorado Nacional Para Extranjeros.

### REFERENCES

- Administration, U. S. F. E. M. (2009). *Quantification of Building Seismic Performance Factors, FEMA P695/ June 2009*.
- Allaire, G. (2002). *Shape optimization by the homogenization method*. Springer.
- Allaire, G., Aubry, S., & Jouve, F. (2001). Eigenfrequency optimization in optimal design. *Computer Methods in Applied Mechanics and Engineering*, 190(28), 3565–3579. [http://doi.org/10.1016/S0045-7825\(00\)00284-X](http://doi.org/10.1016/S0045-7825(00)00284-X)
- American Concrete Institute (ACI Committee 318). (2011). Building Code Requirements for Structural Concrete (ACI 318-11) and Commentary (318R-11). American Concrete Institute Farmington Hills, MI.
- American Society of Civil Engineers. (2013). *Minimum Design Loads for Buildings and Other Structures*. American Society of Civil Engineers.
- American Society of Civil Engineers, Reston, Virginia. (2006). Seismic Rehabilitation of Existing Buildings (ASCE/SEI 41-06).
- Arroyo, O. (2015). Eigenfrequency formulation example of a 15 story building. Retrieved from <https://drive.google.com/file/d/0B6xQxHwiWx-QdHg4al9VNjh2Mnc/view?usp=sharing>
- Arroyo, O., Prieto, V., & Gutiérrez, S. (n.d.). Method to Improve Seismic Performance of RC Moment-Resisting Frames Using Geometric Optimization. *Journal of Computing in Civil Engineering*, 0(0), 04015046. [http://doi.org/10.1061/\(ASCE\)CP.1943-5487.0000529](http://doi.org/10.1061/(ASCE)CP.1943-5487.0000529)
- Bendsoe, M. P., & Sigmund, O. (2003). *Topology optimization: theory, methods and applications*. Springer Science & Business Media.
- Chopra, A. K. (1995). *Dynamics of structures* (Vol. 3). Prentice Hall New Jersey.
- Chopra, A. K., & Goel, R. K. (2002). A modal pushover analysis procedure for estimating seismic demands for buildings. *Earthquake Engineering & Structural Dynamics*, 31(3), 561–582. <http://doi.org/10.1002/eqe.144>

- Chopra, A. K., Goel, R. K., & Chintanapakdee, C. (2004). Evaluation of a modified MPA procedure assuming higher modes as elastic to estimate seismic demands. *Earthquake Spectra*, 20(3), 757–778. <http://doi.org/10.1193/1.1775237>
- Coleman, J., & Spacone, E. (2001). Localization issues in force-based frame elements. *Journal of Structural Engineering*, 127(11), 1257–1265.
- Dasgupta, D., & Michalewicz, Z. (2013). *Evolutionary Algorithms in Engineering Applications*. Springer Science & Business Media.
- Fragiadakis, M., & Lagaros, N. D. (2011). An overview to structural seismic design optimisation frameworks. *Computers & Structures*, 89(11), 1155–1165.
- Fragiadakis, M., & Papadrakakis, M. (2008). Performance-based optimum seismic design of reinforced concrete structures. *Earthquake Engineering & Structural Dynamics*, 37(6), 825–844. <http://doi.org/10.1002/eqe.786>
- Gang Li, H. L. (2010). A hybrid simulated annealing and optimality criteria method for optimum design of RC buildings. *Structural Engineering and Mechanics*, 35(1). <http://doi.org/10.12989/sem.2010.35.1.019>
- Habibullah, A. (1997). ETABS-Three Dimensional Analysis of Building Systems, Users Manual. *Computers and Structures Inc., Berkeley, California*.
- Hadka, D., & Reed, P. (2012). Borg: An Auto-Adaptive Many-Objective Evolutionary Computing Framework. *Evolutionary Computation*, 21(2), 231–259. [http://doi.org/10.1162/EVCO\\_a\\_00075](http://doi.org/10.1162/EVCO_a_00075)
- Hecht, F. (2012). New development in freefem++. *Journal of Numerical Mathematics*, 20(3-4), 251–266.
- Hoffman, E. W., & Richards, P. W. (2014). Efficiently Implementing Genetic Optimization with Nonlinear Response History Analysis of Taller Buildings. *Journal of Structural Engineering*, 140(8).
- Khatibinia, M., Salajegheh, E., Salajegheh, J., & Fadaee, M. (2013). Reliability-based design optimization of reinforced concrete structures including soil–structure interaction using a discrete gravitational search algorithm and a proposed metamodel. *Engineering Optimization*, 45(10), 1147–1165.
- Lee, D.-K., Yang, C.-J., & Starossek, U. (2012). Topology design of optimizing material arrangements of beam-to-column connection frames with maximal stiffness. *Scientia Iranica*, 19(4), 1025–1032. <http://doi.org/10.1016/j.scient.2012.06.004>
- Li, G., Lu, H., & Liu, X. (2010). A hybrid genetic algorithm and optimality criteria method for optimum design of RC tall buildings under multi-load cases. *The Structural Design of Tall and Special Buildings*, 19(6), 656–678. <http://doi.org/10.1002/tal.505>
- Mazzoni, S., McKenna, F., Scott, M. H., Fenves, G. L., & others. (2006). OpenSees command language manual. *Pacific Earthquake Engineering Research (PEER) Center*.
- Murat, F., & Tartar, L. (1997). Calculus of variations and homogenization. In *Topics in the mathematical modelling of composite materials* (pp. 139–173). Springer.
- Senba, A., Oka, K., Takahama, M., & Furuya, H. (2013). Vibration reduction by natural frequency optimization for manipulation of a variable geometry truss. *Structural and Multidisciplinary Optimization*, 48(5), 939–954. <http://doi.org/10.1007/s00158-013-0933-6>
- Simon, D. (2013). *Evolutionary Optimization Algorithms*. John Wiley & Sons.

- Tartar, L. (2009). *The general theory of homogenization: a personalized introduction* (Vol. 7). Springer.
- Tsai, T. D., & Cheng, C. C. (2013). Structural design for desired eigenfrequencies and mode shapes using topology optimization. *Structural and Multidisciplinary Optimization*, 47(5), 673–686.
- Zacharenaki, A. E., Fragiadakis, M., & Papadrakakis, M. (2013). Reliability-based optimum seismic design of structures using simplified performance estimation methods. *Engineering Structures*, 52, 707–717.
- Zou, X., Chan, C., Li, G., & Wang, Q. (2007). Multiobjective optimization for performance-based design of reinforced concrete frames. *Journal of Structural Engineering*, 133(10), 1462–1474.

#### **4. EVALUATION OF THE IMPACT OF EIGENFREQUENCY OPTIMIZATION USING PERFORMANCE BASED EARTHQUAKE ENGINEERING**

This chapter is presented in a paper format, corresponding to the publication “A PBEE evaluation of a seismic design method for reinforced concrete frames based on eigenfrequency optimization”, which is under review at the time of elaborating this document. The submitted manuscript is presented here.

## **A PBEE evaluation of a seismic design method based on eigenfrequency optimization**

### **Abstract**

Reinforced concrete frames (RCF) are a widely used structural system, whose design is based on drift, strength and ductility requirements given by design codes. Recently an eigenfrequency optimization method has been proposed, which minimizes the fundamental period of RCF structures, which has potential to be a practical tool to improve the seismic performance of RCF. In this work we use performance based earthquake engineering (PBEE) to assess the effectiveness of the design method. The findings show that the method is effective for low to median rise buildings, because it produces distributions of strength and stiffness more suitable to withstand seismic forces, specifically with stronger columns, beams and ratio of column to beams at the base of the building. Consequently, optimized buildings have reduced drifts at lower stories, smaller collapse risk and lesser expected casualties. These improvements come despite material volumes that are the same as traditionally-designed structures and seismic economic losses that are virtually identical.

### **1. Introduction**

Reinforced concrete frames (RCF) are a widely used structural system around the world, especially in developing countries, due to the system's relatively low cost compared to other alternatives. Indeed, reports from the World Housing Encyclopedia show that these structures account for about 75% of the building stock in Turkey (WHE Report 64), 60% in Colombia (WHE Report 11) and 80% in Mexico (WHE Report 115). Reflecting this ubiquity, there has been significant research effort to develop methods to improve RCF seismic design procedures beyond the code minimum (e.g. Zou, et al. 2007; Li & Liu, 2010; Li et al. 2010; Khatibinia et al. 2013; Bai et al. 2016; Arroyo et al. 2016; Hajirasouliha et al. 2012; Arroyo and Gutiérrez 2016).

Among these methods, Arroyo et al. (2016) and Arroyo and Gutiérrez (2016) propose a design procedure based on eigenfrequency optimization. This approach uses a topology problem formulation that minimizes the frame's fundamental period. The optimization

procedure is easy to implement and can be used to obtain - within minutes - RCF designs with improved overstrength (comparison of lateral strength relative to the design strength requirement) and deformation capacity (Arroyo et al. 2016). This method uses an iterative procedure to select member sizes subject to constraints in the total volume of material used and the equilibrium conditions. However, the full extent of seismic improvements from this approach and the mechanisms by which seismic performance is improved remain unclear, especially since it is potentially at odds with studies suggesting worse seismic performance of shorter period buildings. These issues deserve a thorough investigation due to the potential for practical application of eigenfrequency-based design methods.

This paper uses performance-based earthquake engineering (PBEE) to investigate the reach of the seismic improvements and evaluate the effectiveness of the eigenfrequency optimization method presented in Arroyo and Gutiérrez (2016). For this purpose, three regular RCF buildings with 5, 10 and 15 stories are considered, as well as a 6 story building with an asymmetric plan configuration. The buildings are first designed according to the ASCE 7 standard (ASCE 2010) and the ACI 318 design code (ACI 2008), and then redesigned based on the results of the eigenfrequency optimization. The redesigned buildings still satisfy all code requirements and use the same material volumes as the original design, but this material is redistributed to minimize the period. To investigate the extent of the method effectiveness, nonlinear simulation models of the traditional and redesigned buildings are subjected to dynamic analysis that provides the input for the assessment of collapse risk and earthquake-induced losses. The structural response is quantified in terms of drift demands over the height of the building and collapse fragility curves. In addition, the expected annualized losses associated with repairing earthquake-induced damage are calculated and disaggregated based on the contributions of the buildings' structural and nonstructural components. Furthermore, the buildings' collapse modes are identified and the expected number of casualties computed. In addition, the paper addresses how period minimization introduces changes in the configuration of buildings, which translate into better seismic performance. Design characteristics investigated include column-to-beam strength ratios and column shear and moment capacities over the height of the building.

## 2. Seismic design and optimization of case study buildings

### 2.1. Case study buildings

Four RCF buildings are considered in this study. Three of them are regular buildings with 5, 10 and 15 stories; the fourth building has 6 stories with an irregular plan configuration. The buildings' structural system consists of moment-resisting space frames, wherein multiple frame lines are designed to resist lateral loads in each direction. Story heights are 3m. Framing layouts are presented in Table 1 for the regular buildings and in Figure 1 for the irregular building. The regular buildings are designed for a California location (37.38°N, 122.26°W) with soil type D conditions and Seismic Design Category D ( $S_a(1s) = 0.945g$ ). The irregular building is designed for a moderate seismicity zone with ( $S_a(1s) = 0.27g$ ).

**Table 1.** Regular (rectangular) building geometries in plan.

<u>Building</u>	<u>Number of bays in X Direction</u>	<u>Number of bays in Y Direction</u>
5 Story	4@6m	3@6m
10 Story	6@5m	3@5m
15 Story	4@7.5m	4@7.5m

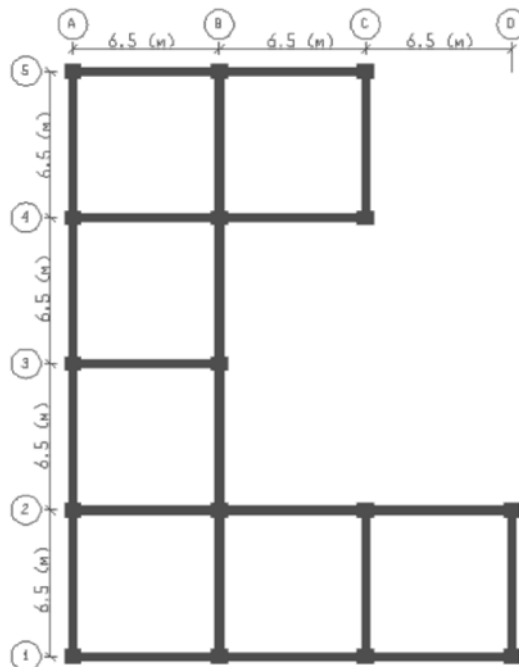


**Figure 1.** Plan view of irregular six story building.

## 2.2 Traditional designs

The buildings are first designed according to U.S. seismic codes; these buildings are referred to as the “traditional buildings”. The traditional buildings are designed using three-dimensional models in ETABS v13.1.2 (Habibullah 1997), using response spectrum analysis according to current seismic design codes (ASCE 2010), (IBC 2015). The building floor systems are designed with a 7 cm slab with joists in the X direction. The buildings are designed for the office live load requirements of ASCE 7-10 (ASCE 2010), but since there is only a small difference in the live loads between office and residential occupancies, the same building designs are later used to represent both condominium and office structures. The dimensions of columns and beams are assumed to be uniform over the height of the building to represent typical design and construction practice of countries like Colombia and Peru and elsewhere, where this practice is customary to facilitate construction. The member dimensions and steel reinforcement for the four buildings in this study are summarized in Table 2. These designs satisfy all code-required forces, drift limits, capacity design principles (strong column weak beam, etc.), and detailing requirements.

**Table 2.** Traditional design of columns, beams, and joists (dimensions given in cm). For beams,  $\rho$  and  $\rho'$  represent the bottom and top beam reinforcement ratios.

<b><u>Building</u></b>	<b><u>Columns</u></b>	<b><u>Beams</u></b>	<b><u>Joist</u></b>
5 Story	50x60, $\rho = 1.2\%$	35x45, $\rho = 0.6\%$ , $\rho' = 1.2\%$	12x38
10 Story	55x75, $\rho = 1.1\%$	30x40, $\rho = 0.8\%$ , $\rho' = 1.6\%$	12x32
15 Story	90x90, $\rho = 1.5\%$	40x60, $\rho = 0.5\%$ , $\rho' = 0.9\%$	15x52
6 Story	60x70, $\rho = 1.2\%$	35x45, $\rho = 0.6\%$ , $\rho' = 1.2\%$	15x38

## 2.3 Optimized designs

The building designs are improved using the eigenfrequency optimization method from Arroyo and Gutiérrez (2016); these designs are referred to here as the “optimized buildings”. In all cases, the optimized buildings are constrained to use the same amount of concrete as the traditional buildings, and they use the same steel reinforcement ratios. In

order to accommodate to construction practices, the members' dimensions are rounded to multiples of 5 cm and steel ratios design uses standard ASTM rebar sizes. This process leads to minor differences in concrete and steel consumption (less than 3%) between the traditional and redesigned buildings, which can be considered within the margin of error in construction practice.

The method is used to determine the dimensions of structural members minimizes the buildings' fundamental periods, achieving an average reduction of 6.2%, as shown in Table 3. Table 4 shows the impact of the redesign for the 15 story building, producing dimensions that are larger in the bottom floors, and gradually reduced along the building height. The optimization results of the other buildings give similar results.

**Table 3.** Comparison of first-mode periods  $T_n$  between traditional and optimized building designs.

<b><u>Building</u></b>	<b><u>Traditional <math>T_n</math></u></b> <b><u>(sec)</u></b>	<b><u>Optimized <math>T_n</math></u></b> <b><u>(sec)</u></b>	<b><u>% Reduction with</u></b> <b><u>optimization</u></b>
15 Story	2.28	2.14	6.1%
10 Story	1.70	1.58	7.1%
5 Story	0.95	0.88	7.4%
6 Story	0.96	0.92	4.3%

**Table 4.** Dimensions for 15 story buildings (all dimensions are given in cm). Columns are square, so the number reported quantifies each dimension. For the beam, just beam depth is reported.

	<b><u>Optimized building</u></b>			<b><u>Traditional building</u></b>	
	<b><u>Columns</u></b>		<b><u>Beams</u></b>	<b><u>Columns</u></b>	<b><u>Beams</u></b>
Story	Inner	Outer	Both	Both	Both
13-15	80	80	55	90	60
12	85	80	55	90	60
11	85	80	60	90	60
8-10	90	85	60	90	60
7	95	85	65	90	60
6	95	90	65	90	60
5	95	95	65	90	60
2-4	100	100	65	90	60
1	105	100	65	90	60

While the period reductions obtained as a result of the optimization are small, the changes in member dimensions suggest that period minimization has a significant impact

in the building behavior during a seismic event. To provide a more comprehensive understanding of the potential implications of these changes on the seismic performance, Figure 2 shows how the design changes between the traditional and optimized building over the height of the building, considering column moment strength (Figure 2a), column-to-beam moment strength ratio (Figure 2b) and column shear strength (Figure 2c).

Figure 2 shows a clear trend for these three design characteristics, wherein in each case the ratio between the capacity of the optimized building and the traditional buildings is higher than 1.0 at the base of each building, and decreases gradually to a value lower than 1.0 at the top of the building. In the case of the columns' moment capacity (Figure 2a), the optimized buildings have on average 142% of that of traditional buildings at their base, with gradual decrease to a 75% average on the roof. For column shear strength and the column to beam strength ratio, the percentages of variation are respectively 127% to 87% and 125% to 84%. Though not shown in the figure, beam capacities also follow a stair-like pattern, with the optimized buildings' beams having 10% greater moment capacity at the bottom third, equal capacity in the middle and 10% lower at the top third.

As Figure 2 shows, minimizing the period using the eigenfrequency method is a mean of achieving a redistribution of strength and ductility along buildings' height with potential to improve the seismic performance. These changes to buildings' strength suggest that the optimized buildings should be capable to withstand larger moment and shear forces in the bottom stories. In addition, because of the 21% larger ratio of columns to beam strengths in the bottom of the optimized buildings, there is a higher probability that structural failures will occur in beams, which is a preferable mode for the system-level stability, potentially delaying structural collapse. Nevertheless, member strengths are reduced for stories at the top third of the buildings. However, the nature of seismic demands in buildings suggests that these reductions will not likely negatively affect the seismic performance. Even with the reduction at the top of the building, the designs still satisfy code requirements.

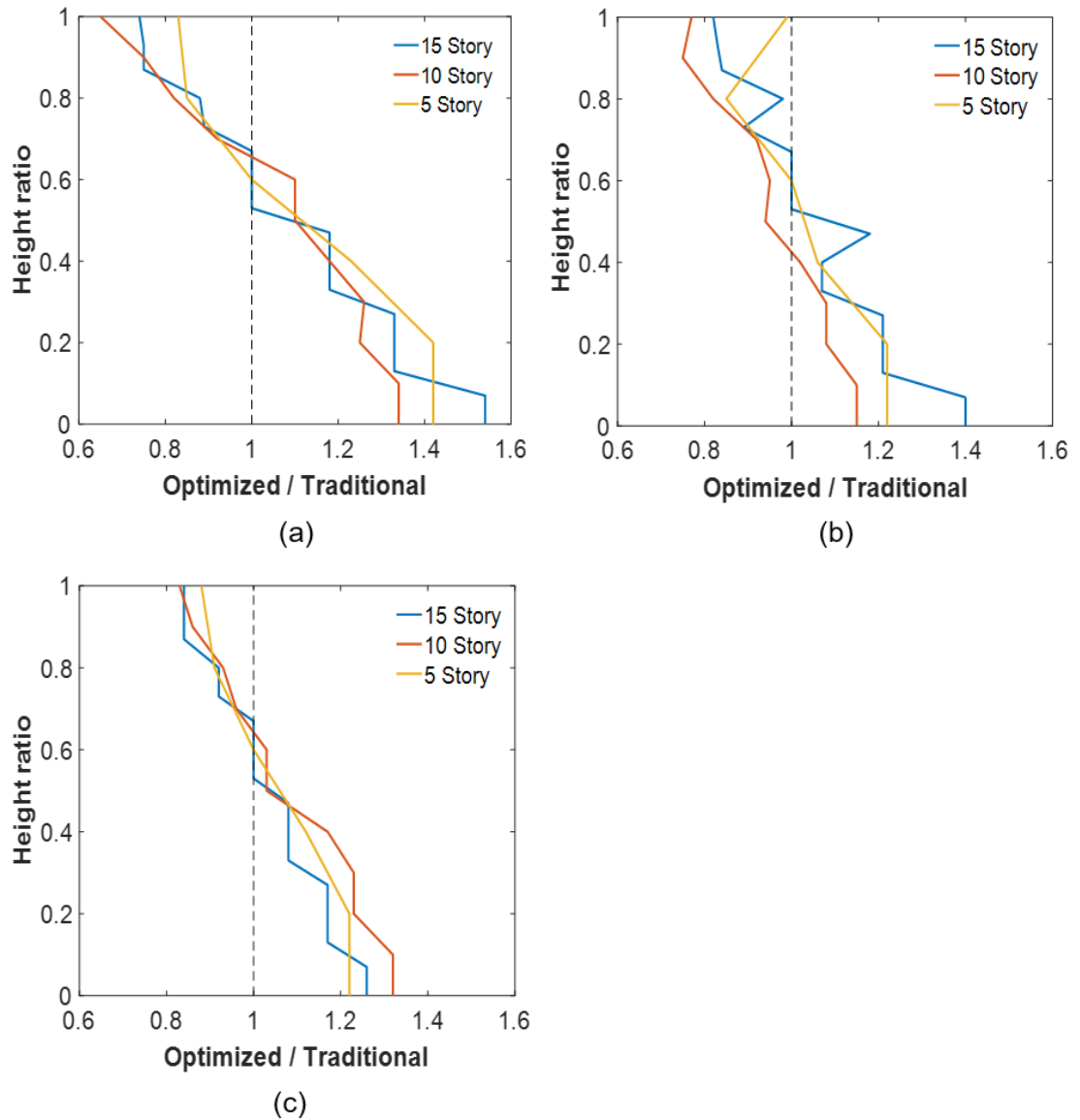


**Figure 2.** Impact of optimization on (a) column moment strength, (b) ratio of column moment to beam moment strength and (c) column shear strength over the height of the building. The x-axis reports the ratio of the optimized building's value for that parameter to that of the traditional building. The y-axis shows the distribution over height, normalized by the total height of each building.

### 3. Performance-based seismic assessment of traditional and optimized buildings

In this section, the optimized and traditional buildings are evaluated using PBEE, analyzing their collapse risks and earthquake-induced losses.

### 3.1. Methodology

PBEE is a framework for the probabilistic seismic performance assessment of buildings, where uncertainties are explicitly considered and the performance is expressed based on possible consequences (Porter 2003; Günay and Mosalam 2013). These consequences are evaluated in terms of human losses (death and serious injuries), direct economic losses (building repair and/or replacement costs) and indirect losses (repair time and unsafe placarding) that result from building damage during an earthquake. The PBEE framework has seen several applications related to RC buildings by the authors and others (*e.g.*, Haselton et al. 2011; Liel et al. 2011; Ramirez et al. 2012; Tesfamariam et al. 2013; Tesfamariam et al. 2014). Here, we apply PBEE through the FEMA P-58 methodology (FEMA 2012), which integrates many of the research developments in PBEE over the last 10 years to provide a standardized set of tools (*e.g.*, fragility functions, population models, etc.) necessary to conduct PBEE assessments for different types of buildings subject to earthquake-induced ground shaking.

In this study, the seismic performance of the traditional and the optimized buildings is compared in terms of the collapse risk, expected annual loss and the expected number of casualties. This constitutes a time-based assessment, wherein evaluate the building performance over time, taking into consideration all possible earthquakes and intensities and their annual frequencies of exceedance. These calculations are carried out for each building considering: i) office/commercial and ii) residential occupancies. The performance evaluation is carried out using the results of the nonlinear time history analysis at different intensity levels, with the aid of the software SP3, a web tool developed by the Haselton-Baker Risk Group (“SP3 | Seismic Performance Prediction Program by Haselton Baker Risk Group” 2015), which takes the FEMA P-58 methods, fragility and population model library as its foundation.

Structural analysis models are created for the traditional and optimized buildings to gather the information required to perform the PBEE evaluation. These models are created in the *OpenSees* (Mazzoni et al. 2006) software platform and consist of 2D planar frame models in each of the orthogonal direction for each building. (A 3D model created for the irregular 6 story building is discussed later). Beam and columns are modeled using fiber

elements with fibers of rebar, confined and unconfined concrete, with 5 integration points. To avoid localization issues, the Constant Fracture Energy Criterion (Coleman and Spacone 2001) is used with  $G_f^c = 180 \text{ N/mm}$  and with concrete properties  $f_c = 28 \text{ MPa}$ ,  $f_{cc} = 33.6 \text{ MPa}$ ,  $e_c = 0.0019$  in the modified Kent-Scott-Park model for concrete. Reinforcing steel is modeled using a bilinear relation, and  $E_s = 210 \text{ GPa}$ ,  $f_y = 420 \text{ MPa}$ ,  $f_u = 630 \text{ MPa}$  and an ultimate strain  $e_u = 0.14$ . The foundation is modeled as rigid, and gravity loads for the model are calculated based on the expected loads and using the combination  $1.05D + 0.25L$ . P-Delta effects are included. Rayleigh damping is applied to the structure with 3% damping in the first and third modes.

Here, full details are presented for the 15 story buildings, while a summary of results is presented for the other three case study buildings.

### *3.2. Results for the 15 story building*

#### *3.2.1 Pushover results*

First, pushover results are presented in Figure 3, showing a 15% percent of improvement in the maximum base shear withstood by the optimized building as compared to the traditional building. In addition, the pushover also reveals a post-peak slope of the optimized building that is approximately 26% flatter than the traditional structure, suggesting the potential for improved behavior under more intense shaking.

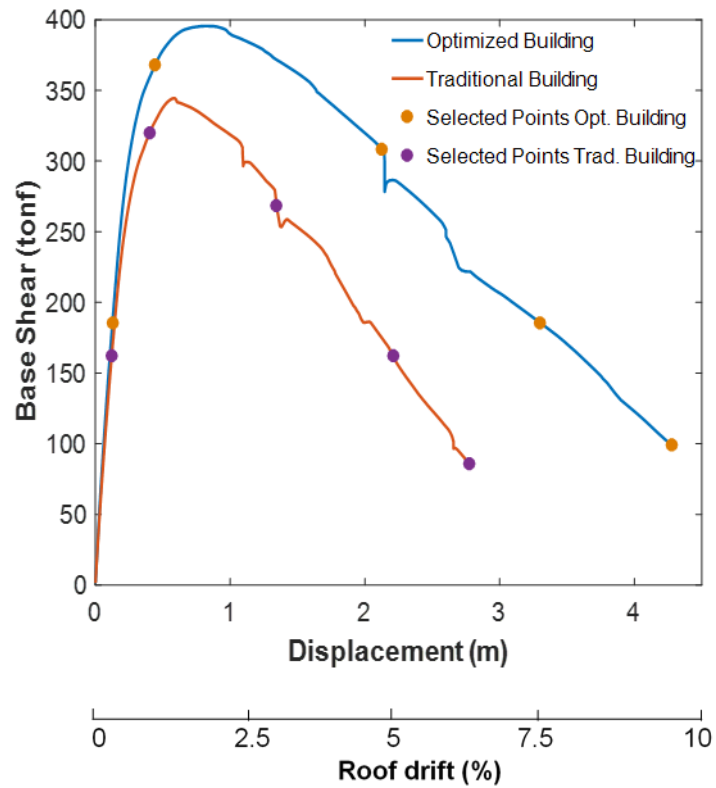


**Figure 3.** Pushover comparison of 15 story buildings.

The behavior of the structures during the pushover is further examined by selecting five points (shown in Figure 3) and examining the displacement profile in the building at each point, as provided in

Figure 4. The behavior for the traditional building (Figure 4a) is as expected, with the largest drift values in the bottom third of the building and a sharp decline in drifts moving up in the building. This behavior is accentuated at the higher levels of displacement demand, as damage occurs and concentrates in the lower stories.

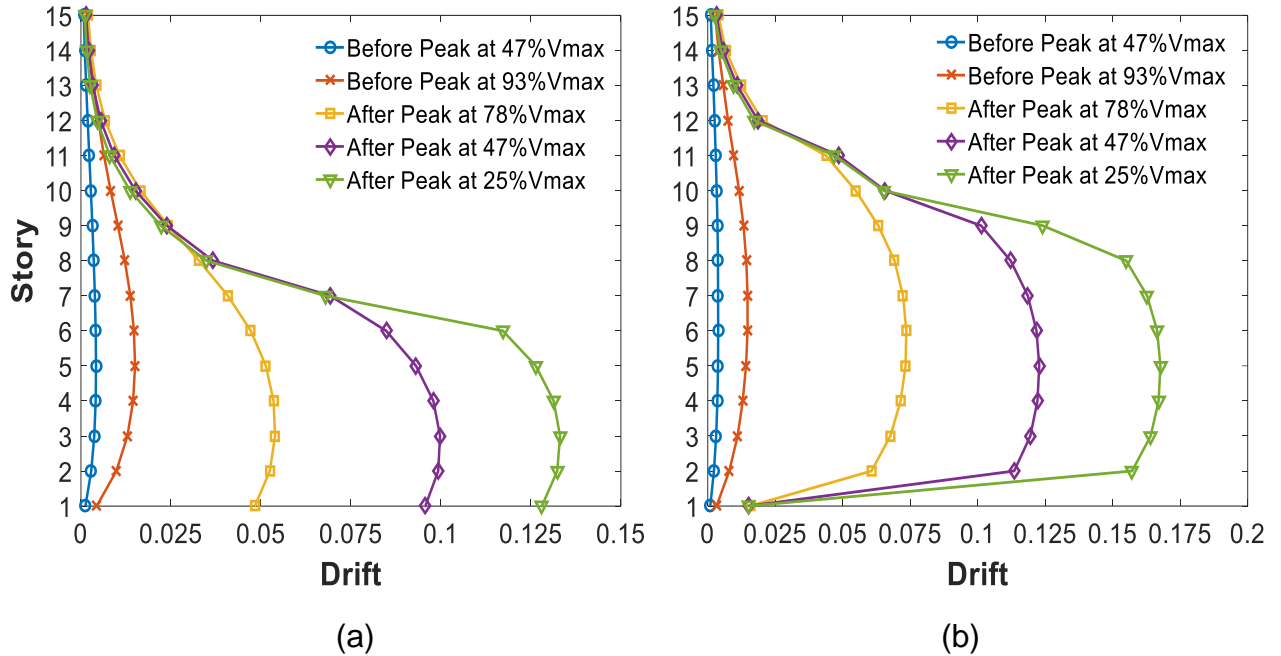


**Figure 4.** Pushover story drift distribution for the 15 story buildings: (a) traditional building and (b) optimized building. Points selected for the drift distribution plots are shown in Figure 3.

The results for the optimized building (Figure 4b) reveal different behavior. To start, there are similar levels of drifts for stories 2 to 9 regardless of the level of displacement, indicating that the displacement demand and damage is spread more evenly over the height of the building compared to the traditional building. Indeed, at all levels of displacement, 8 out of 15 stories have between 75 and 100% of the maximum story drift, compared to 6 stories having close to the maximum drift in the traditional building. These observations suggest a hypothesis that the optimized building may be capable of withstanding greater levels of displacement because the damage is distributed in a greater portion of the structure.

### 3.2.2 Dynamic structural response

The performance evaluation relies on nonlinear dynamic analysis to simulate the building response. In this approach, a set of selected ground motions are scaled and applied to the structure at multiple stripes of ground shaking intensity intensity. For this purpose, the 44 ground motion suite of FEMA P-695 was selected (FEMA 2009) and each ground

motion was scaled such that its  $Sa$  matched eight different intensity levels at  $\{0.5, 1.0, 1.5, 2.0, 2.5, 3.0, 4.5, 6.0\} Sa_D$ . Here,  $Sa_D$  for the 15 story building models denotes the spectral design acceleration at a period  $T_l = 2.2s$ , an intermediate value between the fundamental period of the traditional building (2.28s) and the optimized building (2.14s). From the analysis results, the median value of key structural responses, namely story drifts, floor accelerations, and residual drifts, are calculated together with measurements of record-to-record variability to obtain the probability distributions at each intensity level. These engineering demand parameters are chosen because they are good predictors of damage and consequences (Ramirez et al. 2012).

For those ground motions where no collapse is observed, the median of maximum drift at each story are calculated for both buildings and plotted in Figure 5. Figure 5 shows that the behavior of both buildings is as expected based on the pushover results, with the optimized building having a more uniform distribution of drift along its height, while in the traditional building, the drift is concentrated more in the lower stories and decreases in the uppermost stories. In addition, the story drift in the first three stories for the optimized building is notably smaller than the traditional building, which is critical because these stories have an important role in the overall structural stability. (Note that for the highest intensity level, many of the records caused collapse, so there were fewer data points used in the computation and the trends reflect the scarcity of data in this range.)

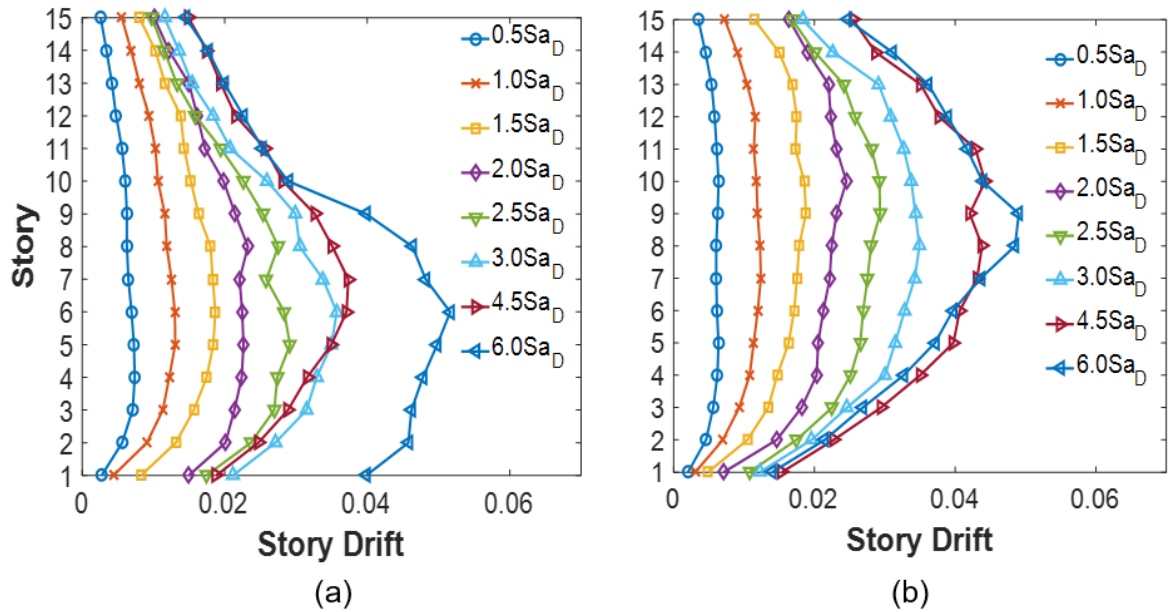


**Figure 5.** Median of maximum story drift response for the 15 story buildings: (a) traditional building, and (b) optimized building.

### 3.2.3 Collapse fragilities

A collapse fragility function expresses the probability of building collapse as a function of ground motion intensity. Collapse fragilities are typically described by a lognormal distribution that is defined by a median value and dispersion. In the dynamic analysis, collapse is considered to occur when the story drift exceeds 10% in any story of the building (Vamvatsikos and Cornell 2004). The probability of collapse is calculated at each intensity level as the ratio of the number of collapsed records divided by the total number of records (*i.e.*, 44). The results for both buildings are fitted to a lognormal distribution using the maximum likelihood method (Baker 2014) and shown in Figure 6.

From the collapse fragility results, several conclusions can be drawn. First, for values of  $Sa$  up to  $1.5Sa_D$  (*i.e.*, 1.5 times the building design acceleration, which equals the maximum considered earthquake (*MCE*) level), the traditional and optimized buildings have similarly low probabilities of collapse. This similarity can be explained by the fact that both buildings were designed according to code regulations and they are expected to show good performance at these levels. However, as the intensity level increases, the optimized building has a significantly smaller probability of collapse than the traditional

building. This reduced fragility is due to the more distributed deformations over the height of the optimized as compared to the traditional building.

### 3.2.4 Loss estimation

Loss estimation requires the development of a performance model, which constitutes an inventory of all the building assets at risk during an earthquake. These include structural and nonstructural components. In FEMA P-58, components are classified into fragility groups which consist of all components that have similar construction characteristics and vulnerability to damage induced by ground motions (FEMA 2012). Those components within a fragility group are further categorized into performance groups on the basis of the relevant earthquake demands (*e.g.*, story drift, floor acceleration). For instance, RC beams in special moment frames can be classified as a fragility group (Charette and Marshall 1999) that is associated with demands quantified in terms of the story drift. These beams would be further separated into performance groups at each story and in each direction.

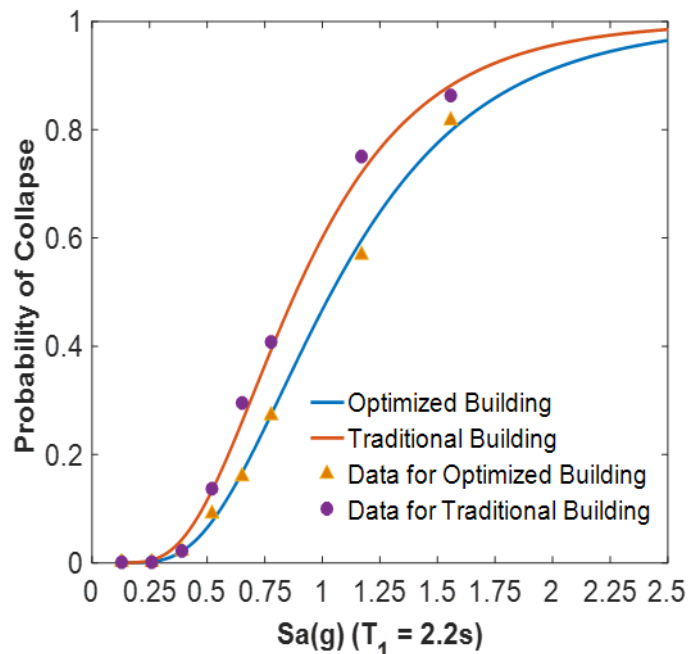


**Figure 6.** Comparison of collapse fragility functions for the 15 story buildings.

The fragility of each group is quantified by defining the median and dispersion of the engineering demands necessary to cause different damage and repair states for various

types of components. FEMA P-58 (FEMA 2012) compiles these parameters to define over 700 fragility groups for both structural and nonstructural components. For example, fragility curves are provided for RC beams, defining the probability of exceeding particular damage states (*e.g.*, spalling of concrete cover, core concrete crushing), as a function of story drift.

In this study, expected annual losses are calculated according to FEMA P-58 using the SP3 tool, and considering both structural (*i.e.*, beams and columns) and nonstructural (*e.g.* wall partitions, plumbing, paint, etc.) components. This calculation considers the losses possible at each intensity level, and weighting these losses by the probability that shaking of that intensity would occur. For the optimized building, the losses are \$120,320/year and for the traditional building the losses are \$122,067/year, which for both buildings corresponds to approximately 0.38% of the building replacement cost (per year). These values are similar to those reported by Ramirez et al. (2012) for code-conforming RC MRF between 0.5% and 1.2%.

Although the expected annual losses are similar, the contributions of building components to the losses differ between the two buildings. Figure 7 shows that the main sources of losses for both buildings are the losses due to collapse, the residual drift irreparability trigger (wherein a residual drift of 1% is the median value considered to trigger an assessment that the building needs to be torn down and replaced), structural components and partition walls. However, in the traditional building, the aggregate effect of collapse and residual drift accounts for 35% of the total loss, whereas in the optimized building, these factors contribute 27% of the losses. In contrast, losses that result from damage of structural components and partition walls represent 57% of the total loss of the traditional building, while in the optimized building their contribution to total losses is 65%. This difference is explained by the more uniform distribution of the interstory drift in the optimized building, which results in an overall greater number of components being damaged, but, at the same time, a reduced susceptibility to collapse.

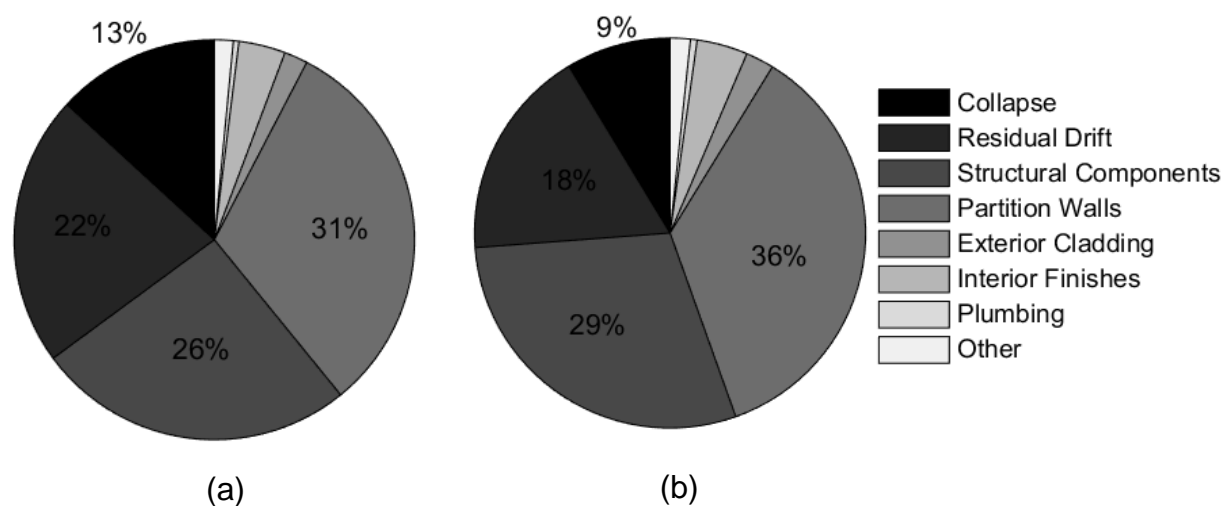


**Figure 7.** Deaggregation of losses for the 15 story buildings: (a) traditional building and (b) optimized building.

### 3.2.5 Collapse modes and casualty estimation

Population models are used as the basis for casualty estimation. They describe the number of people inside the building, and also consider the distribution of people within the building and its variability during the time of the day and different days of the year. Models for common occupancies, *e.g.* office, residential, etc., are included as part of the FEMA P-58 report, building on previous research (*e.g.*, Coburn et al. 1992; Mitrani-Reiser 2007).

Casualties depend not only on the building population, but also the expected collapse modes of the building, which are obtained here from nonlinear dynamic analysis. For records causing collapse, collapse is identified as taking place in those stories having either more than 10% drift in that story, or greater than 80% of the maximum observed story drift in the building. For the 15 story buildings, results are grouped in three collapse modes: those with fewer than 6 collapsed stories, between 6 and 10 stories collapsed, and greater than 10 stories. The fraction of the floor area collapsed is calculated based on all records collapsing in a particular mode, taking the median fraction of floor area collapsed for that record set. The results for the three collapse modes are shown in Table 3. Mode 1 (collapse in fewer than six stories) has a significantly higher probability of occurrence for the

traditional building, while Modes 2 and 3 are more likely to occur for the optimized one. Modes 2 and 3 involve failure of larger portions of the structure, as expected based on the results from pushover and dynamic analyses.

**Table 5.** Collapse modes for the 15 story buildings

<u>Mode of collapse</u>	<u>Fraction of floor area collapsed</u>	<u>Mode probability</u>	
		<u>Traditional</u>	<u>Optimized</u>
1 (6 or fewer stories collapsed)	0.27	0.50	0.36
2 (6 to 10 stories collapsed)	0.53	0.43	0.51
3 (more than 10 stories collapsed)	0.80	0.07	0.13

Based on these collapse modes, the expected number of casualties is calculated considering two different occupancies: a) the building used as an office and b) the building used as a residential multi-unit condominium structure. The results, summarized in Table 4, provide a clear indication that the optimized building better safeguards human life, as it has a significantly lower number of expected casualties for both occupancy cases. Moreover, the percent difference is larger for the smaller intensity levels, *i.e.* those with a larger probability of occurrence, and which are more relevant from a practical perspective.

**Table 6.** Casualty estimates for the 15 story buildings

<u>IM level</u>	<u>Office occupancy Fatalities</u>		<u>Residential occupancy Fatalities</u>	
	<u>Trad</u>	<u>Opt</u>	<u>Trad</u>	<u>Opt</u>
$0.5S_{aD}$	0	0	0	0
$1.0S_{aD}$	1	0	1	0
$1.5S_{aD}$	3	2	7	3
$2.0S_{aD}$	10	6	21	13
$2.5S_{aD}$	17	12	37	27
$3.0S_{aD}$	26	20	54	43
$4.5S_{aD}$	42	39	92	85
$6.0S_{aD}$	49	51	106	109

### 3.3. Results for the 5 and the 10 story buildings

The optimization of the 5 story and the 10 story buildings had similar impacts on the design to those observed for the 15 story building (Figure 2 and Table 3). As a result, the observed seismic responses for the 5 story and the 10 story buildings are similar to that of the 15-story building. Figure 8 shows the collapse fragility functions for both buildings, which exhibit a similar trend to that shown in Figure 6.

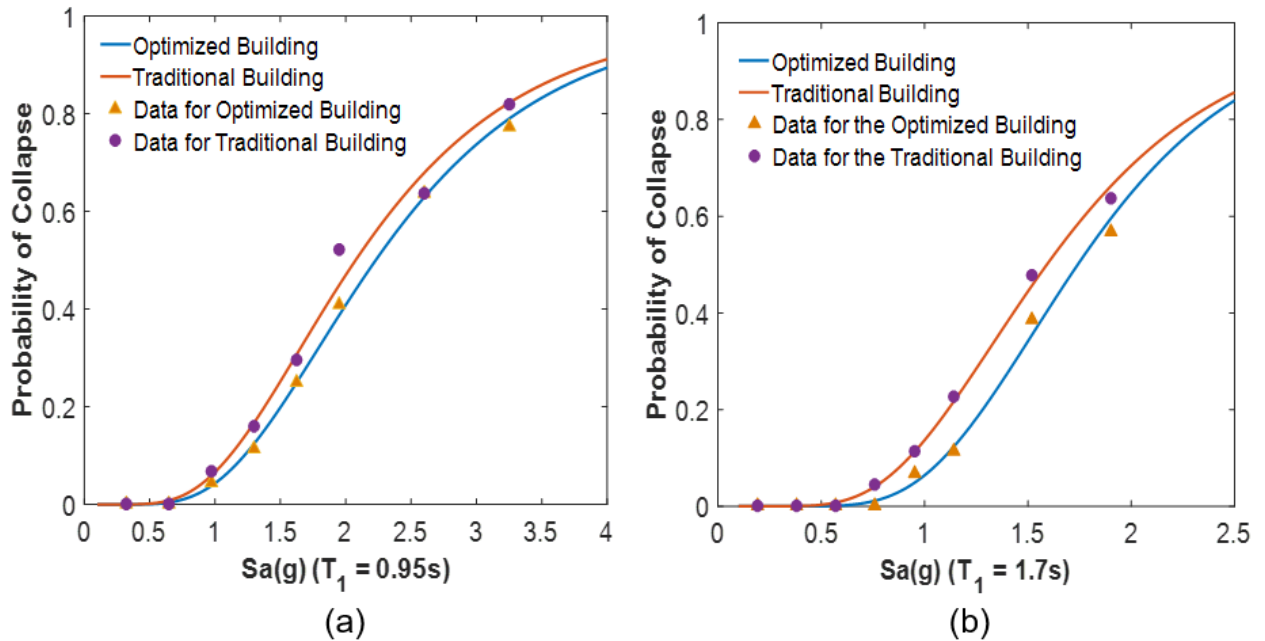


**Figure 8.** Collapse fragility curves for (a) the 5 story and (b) the 10 story buildings.

The dynamic response of non-collapsed records is presented in Figure 9 for the 5 story buildings and in Figure 10 for the 10 story buildings. (The performance is shown for the Y direction for the 5 story buildings and in the X direction for the 10 story buildings. Although both X and Y directions were considered during the analysis, only one is shown to illustrate that the behavior has a similar trend that was observed for the 15 story buildings.) In both cases, the optimized buildings have significantly smaller drifts in the bottom third of the building than its traditional counterparts, which explains why these buildings show better (less fragile) collapse performance. In addition, as observed previously, the optimized buildings have a more uniform distribution of drift along their height, and bigger drifts in the topmost stories.

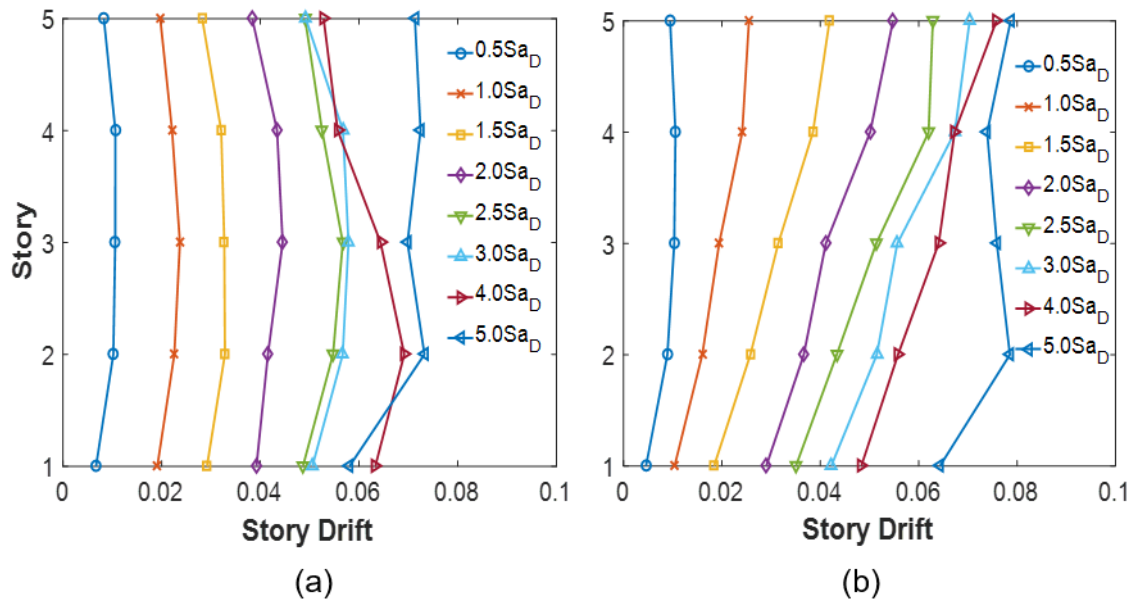


**Figure 9.** Median of maximum story drift response for Y direction in the 5 story buildings: (a) traditional building, (b) optimized building.

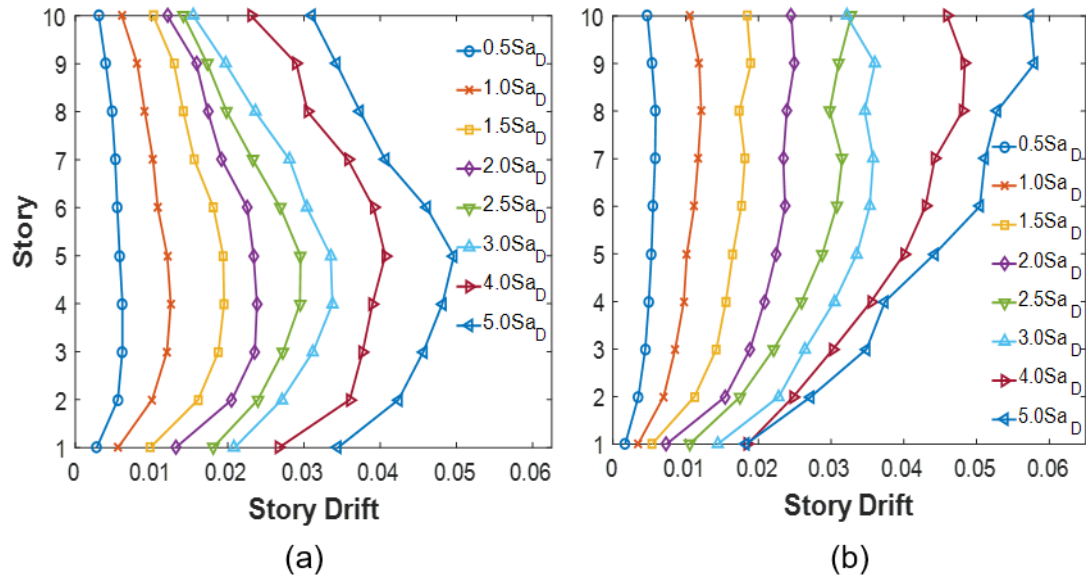


**Figure 10.** Median of maximum story drift response for X direction in the 10 story buildings: (a) traditional building, (b) optimized building.

As a result of the aforementioned similarities in seismic response to the optimized 15-story building, the optimized 5 story and 10 story buildings have similar benefits in their performance relative to the traditional building of the same height. The authors also performed casualty and loss estimates for these buildings (both traditional and optimized),

confirming the findings for the 15 story buildings; these results are not presented here for reasons of brevity.

### 3.4. Results for the irregular building

Due to the irregular plan configuration of this building, its seismic performance is evaluated in *OpenSees* by a pushover analysis applied to three dimensional models of the buildings in two directions, as presented in Figure 11. Pushover results show that the optimized building is capable of withstanding a larger base shear than the traditional building in both directions; in addition, it has a better post peak behavior, especially in the Y direction, where the post peak slope shows slower deterioration compared to the traditional building.

Although we have not evaluated the performance of this building in the complete PBEE framework, the improvement in pushover performance is similar to that seen in regular buildings (Figure 2) so we expect the building to show similar improvements in collapse capacity, casualties and losses as observed in the comparison of the traditional and optimized regular buildings. This example shows that the eigenfrequency optimization approach brings benefits to irregular buildings, even when its frames are optimized independently and only first fundamental eigenfrequency is considered in the optimization.

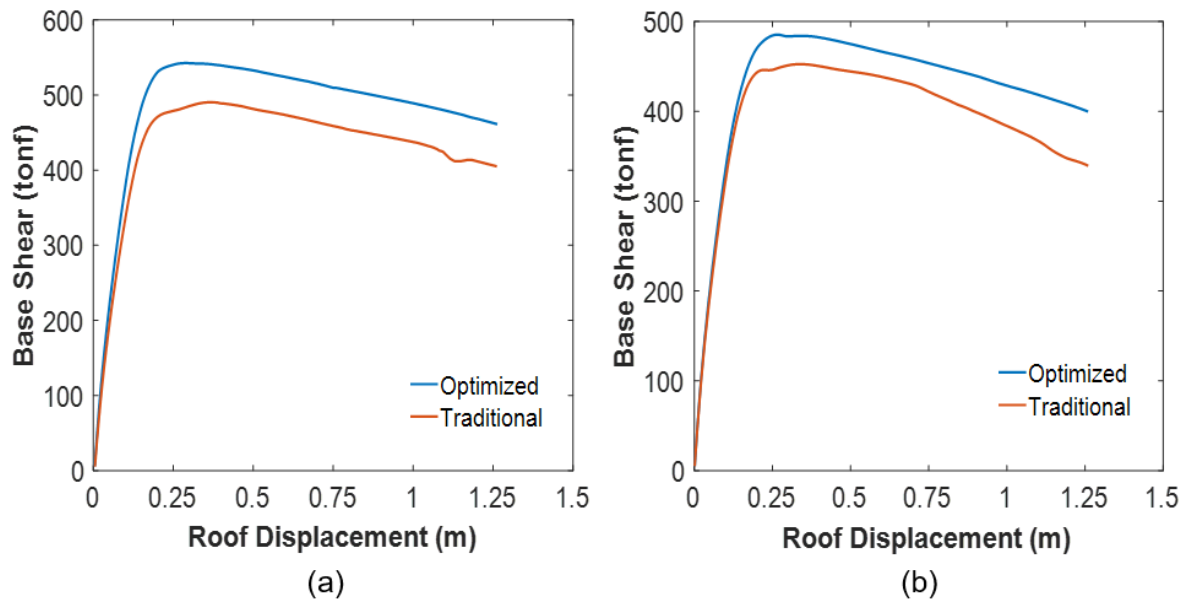


**Figure 11.** Pushover results for a C-shaped irregular building in: (a) X Direction, and (b) Y Direction.

#### 4. Conclusions and perspectives

This paper evaluates a seismic design procedure for RC MRF which is based on minimization of the first-mode period (maximizes the eigenfrequency) subject to material constraints and seismic code requirements. This article applied PBEE to four buildings to investigate the causes and extent of seismic improvements that result from applying the eigenfrequency optimization method introduced in Arroyo and Gutiérrez (2016). The results reveal a number of advantages of the optimized designed buildings compared to the traditional buildings:

- (1) This design procedure achieves reductions of building periods of about 6% by means of redistributing material along building height. This material redistribution in turn redistributes strength in a manner that is more appropriate to withstand the seismic forces, hence optimized buildings have improved seismic performance. In particular, for the bottom third of the buildings, the column-to-beam moment strength ratios are increased on average by 21%, the moment and shear strength are increased by 32% and 23% for columns, and the moment capacity of the beams is increased by 10%. For the top third of the buildings, the column moment and shear strength is reduced by 22% and 16% respectively, while the column-to-beam moment strength ratio is decreased by 15% and the beams' moment strength is decreased by 10%.
- (2) Buildings subject to the design procedure experience a more uniform drift distribution along its height, compared to those of the traditional building, with important reductions in the bottom stories and larger drifts in the top stories.
- (3) As a consequence, the optimized buildings are less susceptible to collapse. As a result, the expected number of fatalities is reduced from 7 to 3 and from 21 to 13 at intensity levels of 1.5 and 2.0 times the design level. However, if collapse occurs,

there is a greater probability that it will happen in a larger portion of the building for the optimized building.

- (4) The method produces buildings whose expected annual losses associated with earthquake-induced damage and associated repairs are 1.4% smaller than those for traditional buildings, *i.e.* almost identical. Thus, the aforementioned seismic performance is achieved while maintaining the same material quantities (construction costs) and similar levels of annual seismic expected losses. However, the components contributing to the loss differ. In the optimized building, the contribution of structural components and partition walls is 65%, and annual losses associated to collapse and residual drift have a 27% participation. In contrast, for the traditional building these participations are 57% and 35%, respectively.

These results show that a design approach based on period minimization can produce important impacts on seismic design and performance by increasing stiffness – and strength – at the lower stories, particularly in columns, and distributing damage more uniformly over the height of the building. These benefits are achieved even though the differences in period between the traditional and optimized designs are modest.

## References

ACI Committee, American Concrete Institute, & International Organization for Standardization. 2008. Building code requirements for structural concrete (ACI 318-08) and commentary. American Concrete Institute.

American Society of Civil Engineers (ASCE). 2010. Minimum Design Loads for Buildings and Other Structures (ASCE 7-10). Standards. American Society of Civil Engineers.

American Society of Civil Engineers, Reston, Virginia. 2006. Seismic Rehabilitation of Existing Buildings (ASCE/SEI 41-06).

Arroyo, Orlando, Prieto, Víctor, and Gutiérrez, Sergio. 2016. "Method to Improve Seismic Performance of RC Moment-Resisting Frames Using Geometric Optimization." *Journal of Computing in Civil Engineering* 30 (3).

Arroyo, Orlando and Gutiérrez, Sergio. 2016. "A seismic optimization procedure for RC framed buildings based on eigenfrequency optimization". Accepted, to appear in *Engineering Optimization*.

Bai, J., Jin, S., Zhang, C., & Ou, J. 2016. "Seismic optimization design for uniform damage of reinforced concrete moment-resisting frames using consecutive modal pushover analysis". *Advances in Structural Engineering*.

Baker, Jack W. 2014. "Efficient Analytical Fragility Function Fitting Using Dynamic Structural Analysis." *Earthquake Spectra* 31 (1): 579–599.

Charette, R. P., and H. E. Marshall. 1999. "UNIFORMAT II Elemental Classification for Building Specifications, Cost Estimating, and Cost Analysis." NISTIR 6389. NIST.

Coburn, A. W., R. J. S. Spence, and A. Pomonis. 1992. "Factors Determining Human Casualty Levels in Earthquakes: Mortality Prediction in Building Collapse." In *Proceedings of the Tenth World Conference on Earthquake Engineering*, 10:5989–94.

Coleman, J, and Enrico Spacone. 2001. "Localization Issues in Force-Based Frame Elements." *Journal of Structural Engineering* 127 (11): 1257–65.

Federal Emergency Management Agency (FEMA). 2012. "Next Generation Methodology for Seismic Performance Assessment of Buildings, Prepared by the Applied Technology Council for the Federal Emergency Management Agency, Report No. FEMA P-58."

Federal Emergency Management Agency (FEMA). 2009. "Quantification of Building Seismic Performance Factors".

Günay, Selim, and Khalid M. Mosalam. 2013. "Peer Performance-Based Earthquake Engineering Methodology, Revisited." *Journal of Earthquake Engineering* 17 (6): 829–58.

Habibullah, Ashraf. 1997. "ETABS-Three Dimensional Analysis of Building Systems, Users Manual." Computers and Structures Inc., Berkeley, California.

Hajirasouliha, I., Asadi, P., & Pilakoutas, K. 2012. "An efficient performance-based seismic design method for reinforced concrete frames". *Earthquake Engineering & Structural Dynamics*, 41(4), 663-679.

Haselton, Curt B., Abbie B. Liel, Gregory G. Deierlein, Brian Dean, and Jason Chou. 2011. "Seismic Collapse Safety of Reinforced Concrete Buildings. I: Assessment of Ductile Moment Frames." *Journal of Structural Engineering* 137 (4): 481–491.

Hoffman, Eric W, and Paul W Richards. 2014. "Efficiently Implementing Genetic Optimization with Nonlinear Response History Analysis of Taller Buildings." *Journal of Structural Engineering* 140 (8).

International Code Council. 2015. *International Building Code*. Published by ICC (distributed by Cengage Learning), USA.

Khatibinia, M, E Salajegheh, J Salajegheh, and MJ Fadaee. 2013. "Reliability-Based Design Optimization of Reinforced Concrete Structures Including Soil–structure Interaction Using a Discrete Gravitational Search Algorithm and a Proposed Metamodel." *Engineering Optimization* 45 (10): 1147–1165.

Liel, Abbie B., Curt B. Haselton, and Gregory G. Deierlein. 2011. "Seismic Collapse Safety of Reinforced Concrete Buildings. II: Comparative Assessment of Nonductile and Ductile Moment Frames." *Journal of Structural Engineering* 137 (4): 492–502.

Li, Gang, Haiyan Lu, and Xiang Liu. 2010. "A Hybrid Genetic Algorithm and Optimality Criteria Method for Optimum Design of RC Tall Buildings under Multi-Load Cases." *The Structural Design of Tall and Special Buildings* 19 (6): 656–78.

Li, and X. Liu. 2010. "A Hybrid Simulated Annealing and Optimality Criteria Method for Optimum Design of RC Buildings." *Structural Engineering and Mechanics* 35 (1): 19–35.

Mazzoni, Silvia, Frank McKenna, Michael H Scott, Gregory L Fenves, and others. 2006. "OpenSees Command Language Manual." Pacific Earthquake Engineering Research (PEER) Center.

Mitrani-Reiser, Judith. 2007. "An Ounce of Prevention: Probabilistic Loss Estimation for Performance-Based Earthquake Engineering." PhD, California Institute of Technology. <http://resolver.caltech.edu/CaltechETD:etd-05282007-233606>.

Porter, Keith A. 2003. "An Overview of PEER's Performance-Based Earthquake Engineering Methodology." In *Proceedings of Ninth International Conference on Applications of Statistics and Probability in Civil Engineering*.

Ramirez, C. M., A. B. Liel, J. Mitrani-Reiser, C. B. Haselton, A. D. Spear, J. Steiner, G. G. Deierlein, and E. Miranda. 2012. "Expected Earthquake Damage and Repair Costs in Reinforced Concrete Frame Buildings." *Earthquake Engineering & Structural Dynamics* 41 (11): 1455–75.

"SP3 | Seismic Performance Prediction Program by Haselton Baker Risk Group." 2015. Seismic Performance Prediction Program. Accessed June 8. <http://www.hbrisk.com/>.

Tesfamariam, Solomon, Katsuichiro Goda, and Goutam Mondal. 2014. "Seismic Vulnerability of RC Frame with Unreinforced Masonry Infill Due to Mainshock-Aftershock Earthquake Sequences." *Earthquake Spectra*, January.

Tesfamariam, S., M. Sánchez-Silva, and P. Rajeev. 2013. "Effect of Topology Irregularities and Construction Quality on Life-Cycle Cost of Reinforced Concrete Buildings." *Journal of Earthquake Engineering* 17 (4): 590–610.

Vamvatsikos, Dimitrios, and C. Allin Cornell. 2004. "Applied Incremental Dynamic Analysis." *Earthquake Spectra* 20 (2): 523–53.

World housing encyclopedia report No. 11. Consulted online August 1 on <http://db.world-housing.net/building/11>

World housing encyclopedia report No. 64. Consulted online August 1 on <http://db.world-housing.net/building/64>

World housing encyclopedia report No. 115. Consulted online August 1 on <http://db.world-housing.net/building/115>

Zou, XK, CM Chan, G Li, and Q Wang. 2007. "Multiobjective Optimization for Performance-Based Design of Reinforced Concrete Frames." *Journal of Structural Engineering* 133 (10): 1462–1474.